

Method/basis set dependence of NICS values among metallic nano-clusters and hydrocarbons

*Zahra Badri, Cina Foroutan-Nejad, Parviz Rashidi-Ranjbar**

School of Chemistry, College of Science, University of Tehran, Tehran, Iran.

Fax: +98 21 6649 5291

Tel: +98 21 6111 3301

ranjbar@khayam.ut.ac.ir

* To whom correspondence should be addressed

Table S-1. NICS values at center, 1 Å and 2 Å above the ring plane of Li_3^+ at different levels of theory; out-of-plane values are denoted by italic font, page S-18.

Table S-2. NICS values at center, 1 Å and 2 Å above the ring plane of Cu_3^+ at different levels of theory; out-of-plane values are denoted by italic font, page S-18.

Table S-3. NICS values at center, 1 Å and 2 Å above the ring plane of Ag_3^+ at different levels of theory; out-of-plane values are denoted by italic font, page S-19.

Table S-4. NICS values at center, 1 Å and 2 Å above the ring plane of Au_3^+ at different levels of theory; out-of-plane values are denoted by italic font, page S-19.

Table S-5. NICS values at center, 1 Å and 2 Å above the ring plane of Sc_3^- at different levels of theory; out-of-plane values are denoted by italic font, page S-20.

Table S-6. NICS values at center, 1 Å and 2 Å above the ring plane of Y_3^- at different levels of theory; out-of-plane values are denoted by italic font, page S-20.

Table S-7. NICS values at center, 1 Å and 2 Å above the ring plane of La_3^- at different levels of theory; out-of-plane values are denoted by italic font, page S-21.

Table S-8. NICS values at center, 1 Å and 2 Å above the ring plane of Al_4^{2-} at different levels of theory; out-of-plane values are denoted by italic font, page S-21.

Table S-9. NICS values at center, 1 Å and 2 Å above the ring plane of Ga_4^{2-} at different levels of theory; out-of-plane values are denoted by italic font, page S-22.

Table S-10. NICS values at center, 1 Å and 2 Å above the ring plane of Cu_4^{2-} at different levels of theory; out-of-plane values are denoted by italic font, page S-23.

Table S-11. NICS values at center, 1 Å and 2 Å above the ring plane of Ag_4^{2-} at different levels of theory; out-of-plane values are denoted by italic font, page S-24.

Table S-12. NICS values at center, 1 Å and 2 Å above the ring plane of Au_4^{2-} at different levels of theory; out-of-plane values are denoted by italic font, page S-24.

Table S-13. Δ NICS values (The differences between NICS values at the optimized geometries and those computed at the fixed geometries of Def2-QZVPP) at center and 1 Å above the ring plane of Li_3^+ at different levels of theory, page 25.

Table S-14. Δ NICS values (The differences between NICS values at the optimized geometries and those computed at the fixed geometries of Aug-cc-pVQZ) at center and 1 Å above the ring plane of Cu_3^+ at different levels of theory, page S-25.

Table S-15. Δ NICS values (The differences between NICS values at the optimized geometries and those computed at the fixed geometries of Def2-QZVPP) at center and 1Å above the ring plane of Ag_3^+ at different levels of theory, page S-25.

Table S-16. Δ NICS values (The differences between NICS values at the optimized geometries and those computed at the fixed geometries of Def2-QZVPP) at center and 1Å above the ring plane of Au_3^+ at different levels of theory, page S-26.

Table S-17. Δ NICS values (The differences between NICS values at the optimized geometries and those computed at the fixed geometries of Aug-cc-pVQZ) at center and 1Å above the ring plane of Sc_3^- at different levels of theory, page S-26.

Table S-18. Δ NICS values (The differences between NICS values at the optimized geometries and those computed at the fixed geometries of Def2-QZVPP) at center and 1Å above the ring plane of Y_3^- at different levels of theory, page S-26.

Table S-19. Δ NICS values (The differences between NICS values at the optimized geometries and those computed at the fixed geometries of Def2-QZVPP) at center and 1Å above the ring plane of La_3^- at different levels of theory, page S-26.

Table S-20. Δ NICS values (The differences between NICS values at the optimized geometries and those computed at the fixed geometries of Def2-QZVPP) at center and 1Å above the ring plane of Al_4^{2-} at different levels of theory, page S-27.

Table S-21. Δ NICS values (The differences between NICS values at the optimized geometries and those computed at the fixed geometries of Def2-QZVPP) at center and 1Å above the ring plane of Ga_4^{2-} at different levels of theory, page S-27.

Table S-22. Δ NICS values (The differences between NICS values at the optimized geometries and those computed at the fixed geometries of Def2-QZVPP) at center and 1Å above the ring plane of Cu_4^{2-} at different levels of theory, page S-27.

Table S-23. Δ NICS values (The differences between NICS values at the optimized geometries and those computed at the fixed geometries of Def2-QZVPP) at center and 1Å above the ring plane of Ag_4^{2-} at different levels of theory, page S-28.

Table S-24. Δ NICS values (The differences between NICS values at the optimized geometries and those computed at the fixed geometries of Def2-QZVPP) at center and 1Å above the ring plane of Au_4^{2-} at different levels of theory, page S-28.

Table S-25. Δ BL values (The differences between bond lengths of the cluster at the optimized geometries and those computed at Def2-QZVPP) of Li_3^+ at different levels of theory, page S-29.

Table S-26. Δ NICS values (The differences between bond lengths of the cluster at the optimized geometries and those computed at Aug-cc-pVQZ) of Cu_3^+ at different levels of theory, page S-29.

Table S-27. Δ NICS values (The differences between bond lengths of the cluster at the optimized geometries and those computed at Def2-QZVPP) of Ag_3^+ at different levels of theory, page S-29.

Table S-28. Δ NICS values (The differences between bond lengths of the cluster at the optimized geometries and those computed at Def2-QZVPP) of Au_3^+ at different levels of theory, page S-29.

Table S-29. Δ NICS values (The differences between bond lengths of the cluster at the optimized geometries and those computed at Aug-cc-pVQZ) of Sc_3^- at different levels of theory, page S-30.

Table S-30. Δ NICS values (The differences between bond lengths of the cluster at the optimized geometries and those computed at Def2-QZVPP) of Y_3^- at different levels of theory, page S-30.

Table S-31. Δ NICS values (The differences between bond lengths of the cluster at the optimized geometries and those computed at Def2-QZVPP) of La_3^- at different levels of theory, page S-30.

Table S-32. Δ NICS values (The differences between bond lengths of the cluster at the optimized geometries and those computed at Def2-QZVPP) of Al_4^{2-} at different levels of theory, page S-30.

Table S-33. Δ NICS values (The differences between bond lengths of the cluster at the optimized geometries and those computed at Def2-QZVPP) of Ga_4^{2-} at different levels of theory, page S-31.

Table S-34. Δ NICS values (The differences between bond lengths of the cluster at the optimized geometries and those computed at Def2-QZVPP) of Cu_4^{2-} at different levels of theory, page S-31.

Table S-35. Δ NICS values (The differences between bond lengths of the cluster at the optimized geometries and those computed at Def2-QZVPP) of Ag_4^{2-} at different levels of theory, page S-31.

Table 36. Δ NICS values (The differences between bond lengths of the cluster at the optimized geometries and those computed at Def2-QZVPP) of Au_4^{2-} at different levels of theory, page S-32.

Figure S-1A. NICS (0) values of $C_3H_3^+$ at different levels of theory. Numbers 1 to 13 on the horizontal axis denote different basis sets which are employed for optimization and computation of NICS values, (1) 6-31G, (2) 6-31G(d), (3) 6-31G(d,p), (4) 6-31+G(d), (5) 6-31+G(d,p), (6) 6-31++G(d,p), (7) 6-311++G(d,p), (8) 6-311++G(2df,2pd), (9) 6-311++G(3df,3pd), (10) cc-pVDZ, (11) cc-pVTZ, (12) aug-cc-pVDZ, (13) aug-cc-pVTZ, page S-33.

Figure S-1B. NICS (1) values of $C_3H_3^+$ at different levels of theory. Numbers 1 to 13 on the horizontal axis denote different basis sets which are employed for optimization and computation of NICS values, (1) 6-31G, (2) 6-31G(d), (3) 6-31G(d,p), (4) 6-31+G(d), (5) 6-31+G(d,p), (6) 6-31++G(d,p), (7) 6-311++G(d,p), (8) 6-311++G(2df,2pd), (9) 6-311++G(3df,3pd), (10) cc-pVDZ, (11) cc-pVTZ, (12) aug-cc-pVDZ, (13) aug-cc-pVTZ, page S-33.

Figure S-2A. NICS (0) values of $C_3H_3^-$ at different levels of theory. Numbers 1 to 13 on the horizontal axis denote different basis sets which are employed for optimization and computation of NICS values, (1) 6-31G, (2) 6-31G(d), (3) 6-31G(d,p), (4) 6-31+G(d), (5) 6-31+G(d,p), (6) 6-31++G(d,p), (7) 6-311++G(d,p), (8) 6-311++G(2df,2pd), (9) 6-311++G(3df,3pd), (10) cc-pVDZ, (11) cc-pVTZ, (12) aug-cc-pVDZ, (13) aug-cc-pVTZ, page S-34.

Figure S-2B. NICS (1) values of $C_3H_3^-$ at different levels of theory. Numbers 1 to 13 on the horizontal axis denote different basis sets which are employed for optimization and computation of NICS values, (1) 6-31G, (2) 6-31G(d), (3) 6-31G(d,p), (4) 6-31+G(d), (5) 6-31+G(d,p), (6) 6-31++G(d,p), (7) 6-311++G(d,p), (8) 6-311++G(2df,2pd), (9) 6-311++G(3df,3pd), (10) cc-pVDZ, (11) cc-pVTZ, (12) aug-cc-pVDZ, (13) aug-cc-pVTZ, page S-34.

Figure S-3A. NICS (0) values of $C_4H_4^{2+}$ at different levels of theory. Numbers 1 to 13 on the horizontal axis denote different basis sets which are employed for optimization and computation of NICS values, (1) 6-31G, (2) 6-31G(d), (3) 6-31G(d,p), (4) 6-31+G(d), (5) 6-31+G(d,p), (6) 6-31++G(d,p), (7) 6-311++G(d,p), (8) 6-311++G(2df,2pd), (9) 6-311++G(3df,3pd), (10) cc-pVDZ, (11) cc-pVTZ, (12) aug-cc-pVDZ, (13) aug-cc-pVTZ, page S-35.

Figure S-3B. NICS (1) values of $C_4H_4^{2+}$ at different levels of theory. Numbers 1 to 13 on the horizontal axis denote different basis sets which are employed for optimization and computation of NICS values, (1) 6-31G, (2) 6-31G(d), (3) 6-31G(d,p), (4) 6-31+G(d), (5) 6-31+G(d,p), (6) 6-31++G(d,p), (7) 6-311++G(d,p), (8) 6-311++G(2df,2pd), (9) 6-311++G(3df,3pd), (10) cc-pVDZ, (11) cc-pVTZ, (12) aug-cc-pVDZ, (13) aug-cc-pVTZ, page S-35.

Figure S-4A. NICS (0) values of C_4H_4 at different levels of theory. Numbers 1 to 13 on the horizontal axis denote different basis sets which are employed for optimization and

computation of NICS values, (1) 6-31G, (2) 6-31G(d), (3) 6-31G(d,p), (4) 6-31+G(d), (5) 6-31+G(d,p), (6) 6-31++G(d,p), (7) 6-311++G(d,p), (8) 6-311++G(2df,2pd), (9) 6-311++G(3df,3pd), (10) cc-pVDZ, (11) cc-pVTZ, (12) aug-cc-pVDZ, (13) aug-cc-pVTZ, page S-36.

Figure S-4B. NICS (1) values of C_4H_4 at different levels of theory. Numbers 1 to 13 on the horizontal axis denote different basis sets which are employed for optimization and computation of NICS values, (1) 6-31G, (2) 6-31G(d), (3) 6-31G(d,p), (4) 6-31+G(d), (5) 6-31+G(d,p), (6) 6-31++G(d,p), (7) 6-311++G(d,p), (8) 6-311++G(2df,2pd), (9) 6-311++G(3df,3pd), (10) cc-pVDZ, (11) cc-pVTZ, (12) aug-cc-pVDZ, (13) aug-cc-pVTZ, page S-36.

Figure S-5A. NICS (0) values of $C_5H_5^+$ at different levels of theory. Numbers 1 to 13 on the horizontal axis denote different basis sets which are employed for optimization and computation of NICS values, (1) 6-31G, (2) 6-31G(d), (3) 6-31G(d,p), (4) 6-31+G(d), (5) 6-31+G(d,p), (6) 6-31++G(d,p), (7) 6-311++G(d,p), (8) 6-311++G(2df,2pd), (9) 6-311++G(3df,3pd), (10) cc-pVDZ, (11) cc-pVTZ, (12) aug-cc-pVDZ, (13) aug-cc-pVTZ, page S-37.

Figure S-5B. NICS (1) values of $C_5H_5^+$ at different levels of theory. Numbers 1 to 13 on the horizontal axis denote different basis sets which are employed for optimization and computation of NICS values, (1) 6-31G, (2) 6-31G(d), (3) 6-31G(d,p), (4) 6-31+G(d), (5) 6-31+G(d,p), (6) 6-31++G(d,p), (7) 6-311++G(d,p), (8) 6-311++G(2df,2pd), (9) 6-311++G(3df,3pd), (10) cc-pVDZ, (11) cc-pVTZ, (12) aug-cc-pVDZ, (13) aug-cc-pVTZ, page S-37.

Figure S-6A. NICS (0) values of $C_5H_5^-$ at different levels of theory. Numbers 1 to 13 on the horizontal axis denote different basis sets which are employed for optimization and computation of NICS values, (1) 6-31G, (2) 6-31G(d), (3) 6-31G(d,p), (4) 6-31+G(d), (5) 6-31+G(d,p), (6) 6-31++G(d,p), (7) 6-311++G(d,p), (8) 6-311++G(2df,2pd), (9) 6-311++G(3df,3pd), (10) cc-pVDZ, (11) cc-pVTZ, (12) aug-cc-pVDZ, (13) aug-cc-pVTZ, page S-38.

Figure S-6B. NICS (1) values of $C_5H_5^-$ at different levels of theory. Numbers 1 to 13 on the horizontal axis denote different basis sets which are employed for optimization and computation of NICS values, (1) 6-31G, (2) 6-31G(d), (3) 6-31G(d,p), (4) 6-31+G(d), (5) 6-31+G(d,p), (6) 6-31++G(d,p), (7) 6-311++G(d,p), (8) 6-311++G(2df,2pd), (9) 6-311++G(3df,3pd), (10) cc-pVDZ, (11) cc-pVTZ, (12) aug-cc-pVDZ, (13) aug-cc-pVTZ, page S-38.

Figure S-7A. NICS (0) values of C_6H_6 at different levels of theory. Numbers 1 to 13 on the horizontal axis denote different basis sets which are employed for optimization and computation of NICS values, (1) 6-31G, (2) 6-31G(d), (3) 6-31G(d,p), (4) 6-31+G(d), (5) 6-31+G(d,p), (6) 6-31++G(d,p), (7) 6-311++G(d,p), (8) 6-311++G(2df,2pd), (9) 6-

311++G(3df,3pd), (10) cc-pVDZ, (11) cc-pVTZ, (12) aug-cc-pVDZ, (13) aug-cc-pVTZ, page S-39.

Figure S-7B. NICS (1) values of C_6H_6 at different levels of theory. Numbers 1 to 13 on the horizontal axis denote different basis sets which are employed for optimization and computation of NICS values, (1) 6-31G, (2) 6-31G(d), (3) 6-31G(d,p), (4) 6-31+G(d), (5) 6-31+G(d,p), (6) 6-31++G(d,p), (7) 6-311++G(d,p), (8) 6-311++G(2df,2pd), (9) 6-311++G(3df,3pd), (10) cc-pVDZ, (11) cc-pVTZ, (12) aug-cc-pVDZ, (13) aug-cc-pVTZ, page S-39.

Figure S-8A. NICS (0) values of $C_7H_7^+$ at different levels of theory. Numbers 1 to 13 on the horizontal axis denote different basis sets which are employed for optimization and computation of NICS values, (1) 6-31G, (2) 6-31G(d), (3) 6-31G(d,p), (4) 6-31+G(d), (5) 6-31+G(d,p), (6) 6-31++G(d,p), (7) 6-311++G(d,p), (8) 6-311++G(2df,2pd), (9) 6-311++G(3df,3pd), (10) cc-pVDZ, (11) cc-pVTZ, (12) aug-cc-pVDZ, (13) aug-cc-pVTZ, page S-40.

Figure S-8B. NICS (1) values of $C_7H_7^+$ at different levels of theory. Numbers 1 to 13 on the horizontal axis denote different basis sets which are employed for optimization and computation of NICS values, (1) 6-31G, (2) 6-31G(d), (3) 6-31G(d,p), (4) 6-31+G(d), (5) 6-31+G(d,p), (6) 6-31++G(d,p), (7) 6-311++G(d,p), (8) 6-311++G(2df,2pd), (9) 6-311++G(3df,3pd), (10) cc-pVDZ, (11) cc-pVTZ, (12) aug-cc-pVDZ, (13) aug-cc-pVTZ, page S-40.

Figure S-9A. NICS (0) values of $C_8H_8^{2+}$ at different levels of theory. Numbers 1 to 13 on the horizontal axis denote different basis sets which are employed for optimization and computation of NICS values, (1) 6-31G, (2) 6-31G(d), (3) 6-31G(d,p), (4) 6-31+G(d), (5) 6-31+G(d,p), (6) 6-31++G(d,p), (7) 6-311++G(d,p), (8) 6-311++G(2df,2pd), (9) 6-311++G(3df,3pd), (10) cc-pVDZ, (11) cc-pVTZ, (12) aug-cc-pVDZ, (13) aug-cc-pVTZ, page S-41.

Figure S-9B. NICS (1) values of $C_8H_8^{2+}$ at different levels of theory. Numbers 1 to 13 on the horizontal axis denote different basis sets which are employed for optimization and computation of NICS values, (1) 6-31G, (2) 6-31G(d), (3) 6-31G(d,p), (4) 6-31+G(d), (5) 6-31+G(d,p), (6) 6-31++G(d,p), (7) 6-311++G(d,p), (8) 6-311++G(2df,2pd), (9) 6-311++G(3df,3pd), (10) cc-pVDZ, (11) cc-pVTZ, (12) aug-cc-pVDZ, (13) aug-cc-pVTZ, page S-41.

Figure S-10A. NICS (0) values of $C_8H_8^{2-}$ at different levels of theory. Numbers 1 to 13 on the horizontal axis denote different basis sets which are employed for optimization and computation of NICS values, (1) 6-31G, (2) 6-31G(d), (3) 6-31G(d,p), (4) 6-31+G(d), (5) 6-31+G(d,p), (6) 6-31++G(d,p), (7) 6-311++G(d,p), (8) 6-311++G(2df,2pd), (9) 6-311++G(3df,3pd), (10) cc-pVDZ, (11) cc-pVTZ, (12) aug-cc-pVDZ, (13) aug-cc-pVTZ, page S-42.

Figure S-10B. NICS (1) values of $C_8H_8^{2-}$ at different levels of theory. Numbers 1 to 13 on the horizontal axis denote different basis sets which are employed for optimization and computation of NICS values, (1) 6-31G, (2) 6-31G(d), (3) 6-31G(d,p), (4) 6-31+G(d), (5) 6-31+G(d,p), (6) 6-31++G(d,p), (7) 6-311++G(d,p), (8) 6-311++G(2df,2pd), (9) 6-311++G(3df,3pd), (10) cc-pVDZ, (11) cc-pVTZ, (12) aug-cc-pVDZ, (13) aug-cc-pVTZ, page S-42.

Figure S-11A. NICS (0) values of $C_9H_9^-$ at different levels of theory. Numbers 1 to 13 on the horizontal axis denote different basis sets which are employed for optimization and computation of NICS values, (1) 6-31G, (2) 6-31G(d), (3) 6-31G(d,p), (4) 6-31+G(d), (5) 6-31+G(d,p), (6) 6-31++G(d,p), (7) 6-311++G(d,p), (8) 6-311++G(2df,2pd), (9) 6-311++G(3df,3pd), (10) cc-pVDZ, (11) cc-pVTZ, (12) aug-cc-pVDZ, (13) aug-cc-pVTZ, page S-43.

Figure S-11B. NICS (1) values of $C_9H_9^-$ at different levels of theory. Numbers 1 to 13 on the horizontal axis denote different basis sets which are employed for optimization and computation of NICS values, (1) 6-31G, (2) 6-31G(d), (3) 6-31G(d,p), (4) 6-31+G(d), (5) 6-31+G(d,p), (6) 6-31++G(d,p), (7) 6-311++G(d,p), (8) 6-311++G(2df,2pd), (9) 6-311++G(3df,3pd), (10) cc-pVDZ, (11) cc-pVTZ, (12) aug-cc-pVDZ, (13) aug-cc-pVTZ, page S-43.

Figure S-12A. NICS (0) values of Li_3^+ at different levels of theory. Numbers 1 to 8 on the horizontal axis denote different basis sets which are employed for optimization and computation of NICS values, (1) Lanl2DZ, (2) DZVP (DFT orbital), (3) Def2-TZVP, (4) Def2-TZVPP, (5) Def2-QZVP, (6) Def2-QZVPP, (7) 6-311G(d) and (8) 6-311+G(d), page S-44.

Figure S-12B. NICS (1) values of Li_3^+ at different levels of theory. Numbers 1 to 8 on the horizontal axis denote different basis sets which are employed for optimization and computation of NICS values, (1) Lanl2DZ, (2) DZVP (DFT orbital), (3) Def2-TZVP, (4) Def2-TZVPP, (5) Def2-QZVP, (6) Def2-QZVPP, (7) 6-311G(d) and (8) 6-311+G(d), page S-44.

Figure S-13. NICS (1) values of Cu_3^+ at different levels of theory. Numbers 1 to 17 on the horizontal axis denote different basis sets which are employed for optimization and computation of NICS values, (1) Aug-cc-pVDZ-PP, (2) Aug-cc-pVTZ-PP, (3) Lanl2DZ, (4) Lanl2TZ, (5) Lanl2TZ(f), (6) DZVP(DFT orbital), (7) cc-pVDZ-PP, (8) cc-pVTZ-PP, (9) Def2-TZVP, (10) Def2-TZVPP, (11) Def2-QZVP, (12) Def2-QZVPP, (13) 6-311G(d), (14) 6-311+G(d), (15) Aug-cc-pVDZ, (16) Aug-cc-pVTZ and (17) Aug-cc-pVQZ, page S-45.

Figure S-14A. NICS (0) values of Ag_3^+ at different levels of theory. Numbers 1 to 14 on the horizontal axis denote different basis sets which are employed for optimization and computation of NICS values, (1) Aug-cc-pVDZ-PP, (2) Aug-cc-pVTZ-PP, (3) Lanl2DZ, (4)

Lanl2TZ, (5) Lanl2TZ(f), (6) DZVP(DFT orbital), (7) cc-pVDZ-PP, (8) cc-pVTZ-PP, (9) Def2-TZVP, (10) Def2-TZVPP, (11) Def2-QZVP and (12) Def2-QZVPP, page S-46.

Figure S-14B. NICS (1) values of Ag_3^+ at different levels of theory. Numbers 1 to 12 on the horizontal axis denote different basis sets which are employed for optimization and computation of NICS values, (1) Aug-cc-pVDZ-PP, (2) Aug-cc-pVTZ-PP, (3) Lanl2DZ, (4) Lanl2TZ, (5) Lanl2TZ(f), (6) DZVP(DFT orbital), (7) cc-pVDZ-PP, (8) cc-pVTZ-PP, (9) Def2-TZVP, (10) Def2-TZVPP, (11) Def2-QZVP and (12) Def2-QZVPP, page S-46.

Figure S-15A. NICS (0) values of Au_3^+ at different levels of theory. Numbers 1 to 14 on the horizontal axis denote different basis sets which are employed for optimization and computation of NICS values, (1) Aug-cc-pVDZ-PP, (2) Aug-cc-pVTZ-PP, (3) Lanl2DZ, (4) Lanl2TZ, (5) Lanl2TZ(f), (6) cc-pVDZ-PP, (7) cc-pVTZ-PP, (8) Def2-TZVP, (9) Def2-TZVPP, (10) Def2-QZVP and (11) Def2-QZVPP. At BP86/Aug-cc-pVTZ-PP levels of theory Self Consistent Field calculations did not converge, page S-47.

Figure S-15B. NICS (1) values of Au_3^+ at different levels of theory. Numbers 1 to 14 on the horizontal axis denote different basis sets which are employed for optimization and computation of NICS values, (1) Aug-cc-pVDZ-PP, (2) Aug-cc-pVTZ-PP, (3) Lanl2DZ, (4) Lanl2TZ, (5) Lanl2TZ(f), (6) cc-pVDZ-PP, (7) cc-pVTZ-PP, (8) Def2-TZVP, (9) Def2-TZVPP, (10) Def2-QZVP and (11) Def2-QZVPP.

At BP86/Aug-cc-pVTZ-PP level of theory Self Consistent Field calculations did not converge, page S-47.

Figure S-16. NICS (1) values of Sc_3^- at different levels of theory. Numbers 1 to 12 on the horizontal axis denote different basis sets which are employed for optimization and computation of NICS values, (1) Lanl2DZ, (2) Lanl2TZ, (3) Lanl2TZ(f), (4) Def2-TZVP, (5) Def2-TZVPP, (6) Def2-QZVP, (7) Def2-QZVPP, (8) 6-311G(d), (9) 6-311+G(d), (10) Aug-cc-pVDZ, (11), Aug-cc-pVTZ and (12) Aug-cc-pVQZ, page S-48.

Figure S-17. NICS (1) values of Y_3^- at different levels of theory. Numbers 1 to 14 on the horizontal axis denote different basis sets which are employed for optimization and computation of NICS values, (1) Lanl2DZ, (2) Lanl2TZ, (3) Lanl2TZ(f), (4) DZVP(DFT orbital), (5) Def2-TZVP, (6) Def2-TZVPP, (7) Def2-QZVP and (8) Def2-QZVPP, page S-49.

Figure S-18. NICS (1) values of La_3^- at different levels of theory. Numbers 1 to 9 on the horizontal axis denote different basis sets which are employed for optimization and computation of NICS values, (1) Lanl2DZ, (2) Lanl2TZ, (3) Lanl2TZ(f), (4) Def2-TZVP, (5) Def2-TZVPP, (6) Def2-QZVP, (7) Def2-QZVPP, page S-50.

Figure S-19A. NICS (0) values of Al_4^{2-} at different levels of theory. Numbers 1 to 8 on the horizontal axis denote different basis sets which are employed for optimization and computation of NICS values, (1) Lanl2DZ, (2) DZVP(DFT orbital), (3) Def2-TZVP, (4)

Def2-TZVPP, (5) Def2-QZVP and (6) Def2-QZVPP, (7) 6-311G(d) and (8) 6-311+G(d) , page S-51.

Figure S-19B. NICS (1) values of Al_4^{2-} at different levels of theory. Numbers 1 to 8 on the horizontal axis denote different basis sets which are employed for optimization and computation of NICS values, (1) Lanl2DZ, (2) DZVP(DFT orbital), (3) Def2-TZVP, (4) Def2-TZVPP, (5) Def2-QZVP and (6) Def2-QZVPP, (7) 6-311G(d) and (8) 6-311+G(d) , page S-51.

Figure S-20A. NICS (0) values of Ga_4^{2-} at different levels of theory. Numbers 1 to 12 on the horizontal axis denote different basis sets which are employed for optimization and computation of NICS values, (1) Aug-cc-pVDZ-PP, (2) Aug-cc-pVTZ-PP, (3) Lanl2DZ, (4) DZVP(DFT orbital), (5) cc-pVDZ-PP, (6) cc-pVTZ-PP, (7) Def2-TZVP, (8) Def2-TZVPP, (9) Def2-QZVP, (10) Def2-QZVPP, (11) 6-311G(d) and (12) 6-311+G(d) , page S-52.

Figure S-20B. NICS (1) values of Ga_4^{2-} at different levels of theory. Numbers 1 to 12 on the horizontal axis denote different basis sets which are employed for optimization and computation of NICS values, (1) Aug-cc-pVDZ-PP, (2) Aug-cc-pVTZ-PP, (3) Lanl2DZ, (4) DZVP(DFT orbital), (5) cc-pVDZ-PP, (6) cc-pVTZ-PP, (7) Def2-TZVP, (8) Def2-TZVPP, (9) Def2-QZVP, (10) Def2-QZVPP, (11) 6-311G(d) and (12) 6-311+G(d), page S-52.

Figure S-21. NICS (1) values of Cu_4^{2-} at different levels of theory. Numbers 1 to 16 on the horizontal axis denote different basis sets which are employed for optimization and computation of NICS values, (1) Aug-cc-pVDZ-PP, (2) Aug-cc-pVTZ-PP, (3) Lanl2DZ, (4) Lanl2TZ, (5) Lanl2TZ(f), (6) DZVP(DFT orbital), (7) cc-pVDZ-PP, (8) cc-pVTZ-PP, (9) Def2-TZVP, (10) Def2-TZVPP, (11) Def2-QZVP, (12) Def2-QZVPP, (13) 6-311G(d), (14) 6-311+G(d), (15) Aug-cc-pVDZ and (16) Aug-cc-pVTZ.

At M06/Aug-cc-pVTZ-PP, BP86/ cc-pVDZ-PP and B3LYP/cc-pVDZ-PP levels of theory Self Consistent Field calculations did not converge, page S-53.

Figure S-22A. NICS (0) values of Ag_4^{2-} at different levels of theory. Numbers 1 to 12 on the horizontal axis denote different basis sets which are employed for optimization and computation of NICS values, (1) Aug-cc-pVDZ-PP, (2) Aug-cc-pVTZ-PP, (3) Lanl2DZ, (4) Lanl2TZ, (5) Lanl2TZ(f), (6) DZVP(DFT orbital), (7) cc-pVDZ-PP, (8) cc-pVTZ-PP, (9) Def2-TZVP, (10) Def2-TZVPP, (11) Def2-QZVP and (12) Def2-QZVPP, page S-54.

Figure S-22B. NICS (1) values of Ag_4^{2-} at different levels of theory. Numbers 1 to 12 on the horizontal axis denote different basis sets which are employed for optimization and computation of NICS values, (1) Aug-cc-pVDZ-PP, (2) Aug-cc-pVTZ-PP, (3) Lanl2DZ, (4) Lanl2TZ, (5) Lanl2TZ(f), (6) DZVP(DFT orbital), (7) cc-pVDZ-PP, (8) cc-pVTZ-PP, (9) Def2-TZVP, (10) Def2-TZVPP, (11) Def2-QZVP and (12) Def2-QZVPP, page S-54.

Figure S-23A. NICS (0) values of Au_4^{2-} at different levels of theory. Numbers 1 to 11 on the horizontal axis denote different basis sets which are employed for optimization and

computation of NICS values, (1) Aug-cc-pVDZ-PP, (2) Aug-cc-pVTZ-PP, (3) Lanl2DZ, (4) Lanl2TZ, (5) Lanl2TZ(f), (6) cc-pVDZ-PP, (7) cc-pVTZ-PP, (8) Def2-TZVP, (9) Def2-TZVPP, (10) Def2-QZVP and (11) Def2-QZVPP, page S-55.

Figure S-23B. NICS (1) values of Au_4^{2-} at different levels of theory. Numbers 1 to 11 on the horizontal axis denote different basis sets which are employed for optimization and computation of NICS values, (1) Aug-cc-pVDZ-PP, (2) Aug-cc-pVTZ-PP, (3) Lanl2DZ, (4) Lanl2TZ, (5) Lanl2TZ(f), (6) cc-pVDZ-PP, (7) cc-pVTZ-PP, (8) Def2-TZVP, (9) Def2-TZVPP, (10) Def2-QZVP and (11) Def2-QZVPP, page S-55.

Figure S-24. NICS(0)_{iso}, dark blue circles, and NICS(0)_{zz}, red circle, in ppm versus bond length in Å in CH_3^+ . This plot includes all data, computed by HF, B3LYP, B3PW91 and BLYP methods and different basis sets. Sky blue circles and orange circles represent NICS values which are different from the other data, page S-56.

Figure S-25. NICS(0)_{iso}, dark blue circles, and NICS(0)_{zz}, red circle, in ppm versus bond length in Å in CH_3^- . This plot includes all data, computed by HF, B3LYP, B3PW91 and BLYP methods and different basis sets, page S-56.

Figure S-26. NICS(0)_{iso}, dark blue circles, and NICS(0)_{zz}, red circle, in ppm versus bond length in Å in $\text{C}_4\text{H}_4^{2+}$. This plot includes all data, computed by HF, B3LYP, B3PW91 and BLYP methods and different basis sets. Orange circles represent NICS values which are different from the other data, page S-57.

Figure S-27. NICS(0)_{iso}, dark blue circles, and NICS(0)_{zz}, red circle, in ppm versus bond length in Å in C_4H_4 . This plot includes all data, computed by HF, B3LYP, B3PW91 and BLYP methods and different basis sets, page S-57.

Figure S-28. NICS(0)_{iso}, dark blue circles, and NICS(0)_{zz}, red circle, in ppm versus bond length in Å in C_5H_5^+ . This plot includes all data, computed by HF, B3LYP, B3PW91 and BLYP methods and different basis sets, page S-58.

Figure S-29. NICS(0)_{iso}, dark blue circles, and NICS(0)_{zz}, red circle, in ppm versus bond length in Å in C_5H_5^- . This plot includes all data, computed by HF, B3LYP, B3PW91 and BLYP methods and different basis sets. Sky blue circles and orange circles represent NICS values which are different from the other data, page S-58.

Figure S-30. NICS(0)_{iso}, dark blue circles, and NICS(0)_{zz}, red circle, in ppm versus bond length in Å in C_6H_6 . This plot includes all data, computed by HF, B3LYP, B3PW91 and BLYP methods and different basis sets. Orange circles represent NICS values which are different from the other data, page S-59.

Figure S-31. NICS(0)_{iso}, dark blue circles, and NICS(0)_{zz}, red circle, in ppm versus bond length in Å in C_7H_7^+ . This plot includes all data, computed by HF, B3LYP, B3PW91 and

BLYP methods and different basis sets. Orange circles represent NICS values which are different from the other data, page S-59.

Figure S-32. NICS(0)_{iso}, dark blue circles, and NICS(0)_{zz}, red circle, in ppm versus bond length in Å in C₈H₈²⁺. This plot includes all data, computed by HF, B3LYP, B3PW91 and BLYP methods and different basis sets. Orange circles represent NICS values which are different from the other data, page S-60.

Figure S-33. NICS(0)_{iso}, dark blue circles, and NICS(0)_{zz}, red circle, in ppm versus bond length in Å in C₈H₈²⁻. This plot includes all data, computed by HF, B3LYP, B3PW91 and BLYP methods and different basis sets. Orange circles represent NICS values which are different from the other data, page S-60.

Figure S-34. NICS(0)_{iso}, dark blue circles, and NICS(0)_{zz}, red circle, in ppm versus bond length in Å in C₉H₉⁻. This plot includes all data, computed by HF, B3LYP, B3PW91 and BLYP methods and different basis sets. Orange circles represent NICS values which are different from the other data, page S-61.

Figure S-35. NICS(0)_{iso}, dark blue circles, and NICS(0)_{zz}, red circle, in ppm versus bond length in Å in Li₃⁺. This plot includes all data, computed by B3LYP and BP86 and M06 methods and different basis sets. Sky blue circles and orange circles represent NICS values which are different from the other data, page S-61.

Figure S-36. NICS(1)_{iso}, dark blue circles, and NICS(0)_{zz}, red circle, in ppm versus bond length in Å in Cu₃⁺. This plot includes all data, computed by B3LYP and BP86 and M06 methods and different basis sets. Sky blue circles and orange circles represent NICS values which are different from the other data, page S-62.

Figure S-37. NICS(0)_{iso}, dark blue circles, and NICS(0)_{zz}, red circle, in ppm versus bond length in Å in Ag₃⁺. This plot includes all data, computed by B3LYP and BP86 and M06 methods and different basis sets. Sky blue circles and orange circles represent NICS values which are different from the other data, page S-62.

Figure S-38. NICS(0)_{iso}, dark blue circles, and NICS(0)_{zz}, red circle, in ppm versus bond length in Å in Au₃⁺. This plot includes all data, computed by B3LYP and BP86 and M06 methods and different basis sets. Sky blue circles and orange circles represent NICS values which are different from the other data, page S-63.

Figure S-39. NICS(0)_{iso}, dark blue circles, and NICS(0)_{zz}, red circle, in ppm versus bond length in Å in Sc₃⁻. This plot includes all data, computed by B3LYP and BP86 and M06 methods and different basis sets. Sky blue circles and orange circles represent NICS values which are different from the other data, page S-63.

Figure S-40. NICS(0)_{iso}, dark blue circles, and NICS(0)_{zz}, red circle, in ppm versus bond length in Å in Y₃⁻. This plot includes all data, computed by B3LYP and BP86 and M06 methods and different basis sets, page S-64.

Figure S-41. NICS(0)_{iso}, dark blue circles, and NICS(0)_{zz}, red circle, in ppm versus bond length in Å in La₃⁻. This plot includes all data, computed by B3LYP and BP86 and M06 methods and different basis sets, page S-64.

Figure S-42. NICS(0)_{iso}, dark blue circles, and NICS(0)_{zz}, red circle, in ppm versus bond length in Å in Al₄²⁻. This plot includes all data, computed by B3LYP and BP86 and M06 methods and different basis sets, page S-65.

Figure S-43. NICS(0)_{iso}, dark blue circles, and NICS(0)_{zz}, red circle, in ppm versus bond length in Å in Ga₄²⁻. This plot includes all data, computed by B3LYP and BP86 and M06 methods and different basis sets, page S-65.

Figure S-44. NICS(0)_{iso}, dark blue circles, and NICS(0)_{zz}, red circle, in ppm versus bond length in Å in Cu₄²⁻. This plot includes all data, computed by B3LYP and BP86 and M06 methods and different basis sets. Sky blue circles and orange circles represent NICS values which are different from the other data, page S-66.

Figure S-45. NICS(0)_{iso}, dark blue circles, and NICS(0)_{zz}, red circle, in ppm versus bond length in Å in Ag₄²⁻. This plot includes all data, computed by B3LYP and BP86 and M06 methods and different basis sets, page S-66.

Figure S-46. NICS(0)_{iso}, dark blue circles, and NICS(0)_{zz}, red circle, in ppm versus bond length in Å in Au₄²⁻. This plot includes all data, computed by B3LYP and BP86 and M06 methods and different basis sets. Orange circles represent NICS values which are different from the other data, page S-67.

Figure S-47A. NICS (0) values of Li₃⁺ at different levels of theory. Numbers 1 to 8 on the horizontal axis denote different basis sets which are employed for computation of NICS values in geometry of molecule optimized by Def2-QZVPP basis set, (1) Lan2DZ, (2) DZVP (DFT orbital), (3) Def2-TZVP, (4) Def2-TZVPP, (5) Def2-QZVP, (6) Def2-QZVPP, (7) 6-311G(d) and (8) 6-311+G(d), page S-68.

Figure S-47B. NICS (1) values of Li₃⁺ at different levels of theory. Numbers 1 to 8 on the horizontal axis denote different basis sets which are employed for computation of NICS values in geometry of molecule optimized by Def2-QZVPP basis set, (1) Lan2DZ, (2) DZVP (DFT orbital), (3) Def2-TZVP, (4) Def2-TZVPP, (5) Def2-QZVP, (6) Def2-QZVPP, (7) 6-311G(d) and (8) 6-311+G(d), page S-68.

Figure S-48A. NICS (0) values of Cu₃⁺ at different levels of theory. Numbers 1 to 17 on the horizontal axis denote different basis sets which are employed for computation of NICS

values in geometry of molecule optimized by Aug-cc-pVQZ basis set, (1) Aug-cc-pVDZ-PP, (2) Aug-cc-pVTZ-PP, (3) Lanl2DZ, (4) Lanl2TZ, (5) Lanl2TZ(f), (6) DZVP(DFT orbital), (7) cc-pVDZ-PP, (8) cc-pVTZ-PP, (9) Def2-TZVP, (10) Def2-TZVPP, (11) Def2-QZVP, (12) Def2-QZVPP, (13) 6-311G(d), (14) 6-311+G(d), (15) Aug-cc-pVDZ, (16) Aug-cc-pVTZ and (17) Aug-cc-pVQZ, page S-69.

Figure S-48B. NICS (1) values of Cu_3^+ at different levels of theory. Numbers 1 to 17 on the horizontal axis denote different basis sets which are employed for computation of NICS values in geometry of molecule optimized by Aug-cc-pVQZ basis set, (1) Aug-cc-pVDZ-PP, (2) Aug-cc-pVTZ-PP, (3) Lanl2DZ, (4) Lanl2TZ, (5) Lanl2TZ(f), (6) DZVP(DFT orbital), (7) cc-pVDZ-PP, (8) cc-pVTZ-PP, (9) Def2-TZVP, (10) Def2-TZVPP, (11) Def2-QZVP, (12) Def2-QZVPP, (13) 6-311G(d), (14) 6-311+G(d), (15) Aug-cc-pVDZ, (16) Aug-cc-pVTZ and (17) Aug-cc-pVQZ, page S-69.

Figure S-49A. NICS (0) values of Ag_3^+ at different levels of theory. Numbers 1 to 14 on the horizontal axis denote different basis sets which are employed for computation of NICS values in geometry of molecule optimized by Def2-QZVPP basis set, (1) Aug-cc-pVDZ-PP, (2) Aug-cc-pVTZ-PP, (3) Lanl2DZ, (4) Lanl2TZ, (5) Lanl2TZ(f), (6) DZVP(DFT orbital), (7) cc-pVDZ-PP, (8) cc-pVTZ-PP, (9) Def2-TZVP, (10) Def2-TZVPP, (11) Def2-QZVP and (12) Def2-QZVPP, page S-70.

Figure S-49B. NICS (1) values of Ag_3^+ at different levels of theory. Numbers 1 to 12 on the horizontal axis denote different basis sets which are employed for computation of NICS values in geometry of molecule optimized by Def2-QZVPP basis set, (1) Aug-cc-pVDZ-PP, (2) Aug-cc-pVTZ-PP, (3) Lanl2DZ, (4) Lanl2TZ, (5) Lanl2TZ(f), (6) DZVP(DFT orbital), (7) cc-pVDZ-PP, (8) cc-pVTZ-PP, (9) Def2-TZVP, (10) Def2-TZVPP, (11) Def2-QZVP and (12) Def2-QZVPP, page S-70.

Figure S-50A. NICS (0) values of Au_3^+ at different levels of theory. Numbers 1 to 14 on the horizontal axis denote different basis sets which are employed for computation of NICS values in geometry of molecule optimized by Def2-QZVPP basis set, (1) Aug-cc-pVDZ-PP, (2) Aug-cc-pVTZ-PP, (3) Lanl2DZ, (4) Lanl2TZ, (5) Lanl2TZ(f), (6) cc-pVDZ-PP, (7) cc-pVTZ-PP, (8) Def2-TZVP, (9) Def2-TZVPP, (10) Def2-QZVP and (11) Def2-QZVPP. At BP86/Aug-cc-pVTZ-PP levels of theory Self Consistent Field calculations did not converge, page S-71.

Figure S-50B. NICS (1) values of Au_3^+ at different levels of theory. Numbers 1 to 14 on the horizontal axis denote different basis sets which are employed for computation of NICS values in geometry of molecule optimized by Def2-QZVPP basis set, (1) Aug-cc-pVDZ-PP, (2) Aug-cc-pVTZ-PP, (3) Lanl2DZ, (4) Lanl2TZ, (5) Lanl2TZ(f), (6) cc-pVDZ-PP, (7) cc-pVTZ-PP, (8) Def2-TZVP, (9) Def2-TZVPP, (10) Def2-QZVP and (11) Def2-QZVPP. At BP86/Aug-cc-pVTZ-PP level of theory Self Consistent Field calculations did not converge, page S-71.

Figure S-51A. NICS (0) values of Sc_3^- at different levels of theory. Numbers 1 to 12 on the horizontal axis denote different basis sets which are employed for computation of NICS values in geometry of molecule optimized by Aug-cc-pVQZ basis set, (1) Lanl2DZ, (2) Lanl2TZ, (3) Lanl2TZ(f), (4) Def2-TZVP, (5) Def2-TZVPP, (6) Def2-QZVP, (7) Def2-QZVPP, (8) 6-311G(d), (9) 6-311+G(d), (10) Aug-cc-pVDZ, (11), Aug-cc-pVTZ and (12) Aug-cc-pVQZ, page S-72.

Figure S-51B. NICS (1) values of Sc_3^- at different levels of theory. Numbers 1 to 12 on the horizontal axis denote different basis sets which are employed for computation of NICS values in geometry of molecule optimized by Aug-cc-pVQZ basis set, (1) Lanl2DZ, (2) Lanl2TZ, (3) Lanl2TZ(f), (4) Def2-TZVP, (5) Def2-TZVPP, (6) Def2-QZVP, (7) Def2-QZVPP, (8) 6-311G(d), (9) 6-311+G(d), (10) Aug-cc-pVDZ, (11), Aug-cc-pVTZ and (12) Aug-cc-pVQZ, page S-72.

Figure S-52A. NICS (0) values of Y_3^- at different levels of theory. Numbers 1 to 14 on the horizontal axis denote different basis sets which are employed for computation of NICS values in geometry of molecule optimized by Def2-QZVPP basis set, (1) Lanl2DZ, (2) Lanl2TZ, (3) Lanl2TZ(f), (4) DZVP(DFT orbital), (5) Def2-TZVP, (6) Def2-TZVPP, (7) Def2-QZVP and (8) Def2-QZVPP, page S-73.

Figure S-52B. NICS (1) values of Y_3^- at different levels of theory. Numbers 1 to 14 on the horizontal axis denote different basis sets which are employed for computation of NICS values in geometry of molecule optimized by Def2-QZVPP basis set, (1) Lanl2DZ, (2) Lanl2TZ, (3) Lanl2TZ(f), (4) DZVP(DFT orbital), (5) Def2-TZVP, (6) Def2-TZVPP, (7) Def2-QZVP and (8) Def2-QZVPP, page S-73.

Figure S-53A. NICS (0) values of La_3^- at different levels of theory. Numbers 1 to 9 on the horizontal axis denote different basis sets which are employed for computation of NICS values in geometry of molecule optimized by Def2-QZVPP basis set, (1) Lanl2DZ, (2) Lanl2TZ, (3) Lanl2TZ(f), (4) Def2-TZVP, (5) Def2-TZVPP, (6) Def2-QZVP, (7) Def2-QZVPP, page S-74.

Figure S-53B. NICS (1) values of La_3^- at different levels of theory. Numbers 1 to 9 on the horizontal axis denote different basis sets which are employed for computation of NICS values in geometry of molecule optimized by Def2-QZVPP basis set, (1) Lanl2DZ, (2) Lanl2TZ, (3) Lanl2TZ(f), (4) Def2-TZVP, (5) Def2-TZVPP, (6) Def2-QZVP, (7) Def2-QZVPP, page S-74.

Figure S-54A. NICS (0) values of Al_4^{2-} at different levels of theory. Numbers 1 to 8 on the horizontal axis denote different basis sets which are employed for computation of NICS values in geometry of molecule optimized by Def2-QZVPP basis set, (1) Lanl2DZ, (2) DZVP(DFT orbital), (3) Def2-TZVP, (4) Def2-TZVPP, (5) Def2-QZVP and (6) Def2-QZVPP, (7) 6-311G(d) and (8) 6-311+G(d), page S-75.

Figure S-54B. NICS (1) values of Al_4^{2-} at different levels of theory. Numbers 1 to 8 on the horizontal axis denote different basis sets which are employed for computation of NICS values in geometry of molecule optimized by Def2-QZVPP basis set, (1) Lanl2DZ, (2) DZVP(DFT orbital), (3) Def2-TZVP, (4) Def2-TZVPP, (5) Def2-QZVP and (6) Def2-QZVPP, (7) 6-311G(d) and (8) 6-311+G(d), page S-75.

Figure S-55A. NICS (0) values of Ga_4^{2-} at different levels of theory. Numbers 1 to 12 on the horizontal axis denote different basis sets which are employed for computation of NICS values in geometry of molecule optimized by Def2-QZVPP basis set, (1) Aug-cc-pVDZ-PP, (2) Aug-cc-pVTZ-PP, (3) Lanl2DZ, (4) DZVP(DFT orbital), (5) cc-pVDZ-PP, (6) cc-pVTZ-PP, (7) Def2-TZVP, (8) Def2-TZVPP, (9) Def2-QZVP, (10) Def2-QZVPP, (11) 6-311G(d) and (12) 6-311+G(d), page S-76.

Figure S-55B. NICS (1) values of Ga_4^{2-} at different levels of theory. Numbers 1 to 12 on the horizontal axis denote different basis sets which are employed for computation of NICS values in geometry of molecule optimized by Def2-QZVPP basis set, (1) Aug-cc-pVDZ-PP, (2) Aug-cc-pVTZ-PP, (3) Lanl2DZ, (4) DZVP(DFT orbital), (5) cc-pVDZ-PP, (6) cc-pVTZ-PP, (7) Def2-TZVP, (8) Def2-TZVPP, (9) Def2-QZVP, (10) Def2-QZVPP, (11) 6-311G(d) and (12) 6-311+G(d), page S-76.

Figure S-56A. NICS (0) values of Cu_4^{2-} at different levels of theory. Numbers 1 to 16 on the horizontal axis denote different basis sets which are employed for computation of NICS values in geometry of molecule optimized by Def2-QZVPP basis set, (1) Aug-cc-pVDZ-PP, (2) Aug-cc-pVTZ-PP, (3) Lanl2DZ, (4) Lanl2TZ, (5) Lanl2TZ(f), (6) DZVP(DFT orbital), (7) cc-pVDZ-PP, (8) cc-pVTZ-PP, (9) Def2-TZVP, (10) Def2-TZVPP, (11) Def2-QZVP, (12) Def2-QZVPP, (13) 6-311G(d), (14) 6-311+G(d), (15) Aug-cc-pVDZ and (16) Aug-cc-pVTZ.

At M06/Aug-cc-pVTZ-PP, BP86/ cc-pVDZ-PP and B3LYP/cc-pVDZ-PP levels of theory Self Consistent Field calculations did not converge, page S-77.

Figure S-56B. NICS (1) values of Cu_4^{2-} at different levels of theory. Numbers 1 to 16 on the horizontal axis denote different basis sets which are employed for computation of NICS values in geometry of molecule optimized by Def2-QZVPP basis set, (1) Aug-cc-pVDZ-PP, (2) Aug-cc-pVTZ-PP, (3) Lanl2DZ, (4) Lanl2TZ, (5) Lanl2TZ(f), (6) DZVP(DFT orbital), (7) cc-pVDZ-PP, (8) cc-pVTZ-PP, (9) Def2-TZVP, (10) Def2-TZVPP, (11) Def2-QZVP, (12) Def2-QZVPP, (13) 6-311G(d), (14) 6-311+G(d), (15) Aug-cc-pVDZ and (16) Aug-cc-pVTZ.

At M06/Aug-cc-pVTZ-PP, BP86/ cc-pVDZ-PP and B3LYP/cc-pVDZ-PP levels of theory Self Consistent Field calculations did not converge, page S-77.

Figure S-57A. NICS (0) values of Ag_4^{2-} at different levels of theory. Numbers 1 to 12 on the horizontal axis denote different basis sets which are employed for computation of NICS values in geometry of molecule optimized by Def2-QZVPP basis set, (1) Aug-cc-pVDZ-PP, (2) Aug-cc-pVTZ-PP, (3) Lanl2DZ, (4) Lanl2TZ, (5) Lanl2TZ(f), (6) DZVP(DFT orbital),

(7) cc-pVDZ-PP, (8) cc-pVTZ-PP, (9) Def2-TZVP, (10) Def2-TZVPP, (11) Def2-QZVP and (12) Def2-QZVPP, page S-78.

Figure S-57B. NICS (1) values of Ag_4^{2-} at different levels of theory. Numbers 1 to 12 on the horizontal axis denote different basis sets which are employed for computation of NICS values in geometry of molecule optimized by Def2-QZVPP basis set, (1) Aug-cc-pVDZ-PP, (2) Aug-cc-pVTZ-PP, (3) Lanl2DZ, (4) Lanl2TZ, (5) Lanl2TZ(f), (6) DZVP(DFT orbital), (7) cc-pVDZ-PP, (8) cc-pVTZ-PP, (9) Def2-TZVP, (10) Def2-TZVPP, (11) Def2-QZVP and (12) Def2-QZVPP, page S-78.

Figure S-58A. NICS (0) values of Au_4^{2-} at different levels of theory. Numbers 1 to 11 on the horizontal axis denote different basis sets which are employed for computation of NICS values in geometry of molecule optimized by Def2-QZVPP basis set, (1) Aug-cc-pVDZ-PP, (2) Aug-cc-pVTZ-PP, (3) Lanl2DZ, (4) Lanl2TZ, (5) Lanl2TZ(f), (6) cc-pVDZ-PP, (7) cc-pVTZ-PP, (8) Def2-TZVP, (9) Def2-TZVPP, (10) Def2-QZVP and (11) Def2-QZVPP, page S-79.

Figure S-58B. NICS (1) values of Au_4^{2-} at different levels of theory. Numbers 1 to 11 on the horizontal axis denote different basis sets which are employed for computation of NICS values in geometry of molecule optimized by Def2-QZVPP basis set, (1) Aug-cc-pVDZ-PP, (2) Aug-cc-pVTZ-PP, (3) Lanl2DZ, (4) Lanl2TZ, (5) Lanl2TZ(f), (6) cc-pVDZ-PP, (7) cc-pVTZ-PP, (8) Def2-TZVP, (9) Def2-TZVPP, (10) Def2-QZVP and (11) Def2-QZVPP, page S-79.

Reference for Basis sets. see page S-80.

Table S-1

Li ₃ ⁺		BP86			B3LYP			M06		
Basis sets	Number of basis functions	NICS(0)	NICS(1)	NICS(2)	NICS(0)	NICS(1)	NICS(2)	NICS(0)	NICS(1)	NICS(2)
Lan2DZ	27	-11.30 -9.19	-7.05 -7.84	-1.65 -4.28	-11.26 -9.05	-7.04 -7.80	-1.63 -4.27	-11.26 -9.70	-7.01 -8.10	-1.72 -4.42
DZVP(DFT orbital)	33	-12.21 -10.91	-7.71 -9.07	-2.03 -4.92	-12.35 -11.05	-7.69 -9.17	-1.96 -4.93	-11.85 -10.52	-7.69 -8.80	-2.15 -4.86
Def2-TZVP	42	-10.82 -8.90	-6.85 -7.69	-1.68 -4.37	-10.66 -8.63	-6.73 -7.54	-1.61 -4.30	-10.94 -9.54	-6.96 -8.12	-1.78 -4.64
Def2-TZVPP	57	-11.14 -9.09	-6.89 -7.62	-1.77 -4.19	-11.05 -8.86	-6.76 -7.48	-1.67 -4.10	-11.38 -9.96	-7.02 -8.22	-1.82 -4.52
Def2-QZVP	105	-11.16 -8.95	-6.84 -7.42	-1.74 -3.94	-11.12 -8.81	-6.75 -7.32	-1.69 -3.88	-11.39 -10.33	-7.01 -8.37	-1.89 -4.49
Def2-QZVPP	105	-11.16 -8.95	-6.84 -7.42	-1.74 -3.94	-11.12 -8.81	-6.75 -7.32	-1.69 -3.88	-11.39 -10.33	-7.01 -8.37	-1.89 -4.49
6-311G(d)	54	-11.21 -9.02	-6.93 -7.49	-1.72 -4.05	-11.07 -8.74	-6.79 -7.32	-1.61 -3.96	-11.41 -9.72	-7.00 -7.97	-1.70 -4.31
6-311+G(d)	66	-11.21 -9.03	-6.94 -7.49	-1.72 -4.04	-11.08 -8.75	-6.79 -7.32	-1.61 -3.96	-11.44 -9.77	-7.01 -6.59	-1.71 -0.46

Table S-2

Cu ₃ ⁺		BP86			B3LYP			M06		
Basis sets	Number of basis functions	NICS(0)	NICS(1)	NICS(2)	NICS(0)	NICS(1)	NICS(2)	NICS(0)	NICS(1)	NICS(2)
Aug-cc-pVDZ-PP	162	-42.60 -28.58	-17.07 -28.16	-2.67 -14.18	-34.86 -16.26	-14.47 -23.34	-2.37 -13.24	-34.55 -14.78	-14.15 -22.94	-2.09 -13.12
Aug-cc-pVTZ-PP	264	-42.27 -28.32	-16.93 -28.29	-2.65 -14.35	-34.17 -15.70	-14.14 -23.19	-2.28 -13.28	-34.55 -15.55	-14.22 -23.34	2.14 -13.32
Lan2DZ	66	-32.507 -13.07	-13.79 -21.78	-1.99 -13.19	-28.27 -7.46	-12.31 -18.98	-1.83 -12.42	-29.07 -7.45	-12.22 -19.31	-1.57 -12.45
Lan2TZ	105	-36.00 -18.53	-14.76 -23.82	-2.15 -13.59	-30.50 -10.33	-12.98 -20.36	-1.96 -12.79	-30.91 -10.09	-12.70 -20.43	-1.69 -12.76
Lan2TZ(f)	126	-35.99 -18.47	-14.75 -23.79	-2.15 -13.58	-30.51 -10.33	-12.98 -20.36	-1.96 -12.78	-30.94 -10.07	-12.70 -20.44	-1.68 -12.75
DZVP(DFT orbital)	72	-33.07 -15.01	-15.40 -24.10	-2.72 -13.68	-28.29 -8.25	-13.56 -20.67	-2.49 -12.88	-29.75 -8.80	-14.14 -21.43	-2.47 -13.06
cc-pVDZ-PP	114	-43.52 -30.52	-17.23 -29.29	-2.91 -14.62	-34.91 -16.72	-14.36 -23.89	-2.52 -13.52	-34.60 -15.39	-14.08 -23.49	-2.29 -13.43
cc-pVTZ-PP	189	-41.66 -27.33	-17.09 -28.03	-2.68 -14.32	-33.66 -14.80	-14.27 -22.92	-2.30 -13.23	-33.96 -14.40	-14.34 -22.94	-2.14 -13.22
Def2-TZVP	135	-33.63 -14.53	-13.94 -22.08	-1.66 -12.77	-28.13 -6.92	-12.09 -18.67	-1.52 -12.05	-28.94 -7.06	-12.17 -19.09	-1.38 -12.15
Def2-TZVPP	192	-34.02 -15.13	-14.17 -22.29	-1.69 -12.84	-28.36 -7.25	-12.25 -18.79	-1.59 -12.09	-29.08 -7.25	-12.34 -19.20	-1.34 -12.20
Def2-QZVP	252	-34.19 -15.20	-13.98 -22.42	-2.09 -12.86	-28.41 -7.17	-12.09 -18.89	-1.92 -12.11	-29.11 -7.12	-12.28 -19.26	-1.80 -12.21
Def2-QZVPP	300	-34.02 -15.13	-14.17 -22.29	-1.69 -12.84	-28.36 -7.25	-12.25 -18.79	-1.59 -12.09	-29.06 -6.91	-12.16 -19.16	-1.71 -12.18
6-311G(d)	138	-30.26 -9.80	-8.59 -14.79	-0.94 -8.47	-23.98 -2.91	-7.98 -14.42	-1.13 -10.36	-23.47 +5.06	-7.69 -14.81	-0.83 -10.75
6-311+G(d)	174	-33.71 -13.86	-14.20 -22.51	-1.93 -13.01	-28.07 -6.22	-12.27 -18.98	-1.77 -12.22	-28.95 -6.57	-12.51 -19.42	-1.73 -12.32
Aug-cc-pVDZ	129	-34.67 -16.81	-14.4 -22.87	-1.96 -12.92	-28.56 -7.96	-12.34 -19.11	-1.80 -12.16	-29.42 -8.08	-12.49 -19.51	-1.68 -12.29
Aug-cc-pVTZ	279	-34.38 -15.19	-14.1 -22.66	-20.01 -12.90	-28.5 -7.12	-12.2 -19.08	-1.87 -12.16	-29.49 -7.56	-12.45 -19.58	-1.75 -12.28
Aug-cc-pVQZ	420	-34.3 -15.11	-14 -22.56	-20.24 -12.88	-28.47 -7.1	-12.12 -19.01	-1.89 -12.15	-29.15 -7.08	-12.25 -19.34	-1.71 -12.23

Table S-3

Ag ₃ ⁺		BP86			B3LYP			M06		
Basis sets	Number of basis functions	NICS(0)	NICS(1)	NICS(2)	NICS(0)	NICS(1)	NICS(2)	NICS(0)	NICS(1)	NICS(2)
Aug-cc-pVDZ-PP	162	-28.43 <i>-1.90</i>	-13.49 <i>-18.18</i>	-2.42 <i>-15.07</i>	-25.91 <i>+0.07</i>	-12.58 <i>-16.36</i>	-2.37 <i>-14.37</i>	-25.88 <i>+0.27</i>	-12.74 <i>-16.23</i>	-2.31 <i>-14.30</i>
Aug-cc-pVTZ-PP	264	-27.61 <i>-0.61</i>	-12.82 <i>-17.45</i>	-2.29 <i>-14.85</i>	-25.15 <i>+1.24</i>	-11.97 <i>-15.69</i>	-2.25 <i>-14.17</i>	-25.88 <i>+0.97</i>	-12.74 <i>-15.88</i>	-2.31 <i>-14.24</i>
Lan12DZ	66	-25.36 <i>+1.12</i>	-12.51 <i>-16.08</i>	-2.04 <i>-14.59</i>	-23.51 <i>+2.38</i>	-11.85 <i>-14.65</i>	-2.06 <i>-13.96</i>	-24.02 <i>+2.04</i>	-12.06 <i>-14.94</i>	-1.99 <i>-14.02</i>
Lan12TZ	105	-26.09 <i>-0.01</i>	-12.73 <i>-16.55</i>	-2.13 <i>-14.63</i>	-24.09 <i>+1.60</i>	-12.01 <i>-15.03</i>	-2.12 <i>-14.01</i>	-24.38 <i>+1.32</i>	-12.14 <i>-15.09</i>	-2.03 <i>-13.99</i>
Lan12TZ(f)	126	-26.19 <i>-0.04</i>	-12.77 <i>-16.61</i>	-2.12 <i>-14.64</i>	-24.14 <i>+1.54</i>	-12.04 <i>-15.06</i>	-2.12 <i>-14.01</i>	-24.40 <i>+1.32</i>	-12.14 <i>-15.10</i>	-2.02 <i>-13.98</i>
DZVP(DFT orbital)	108	-22.61 <i>+4.28</i>	-11.82 <i>-14.08</i>	-2.47 <i>-14.13</i>	-20.98 <i>+5.11</i>	-11.16 <i>-12.75</i>	-2.42 <i>-13.51</i>	-22.45 <i>+4.08</i>	-11.90 <i>-13.69</i>	-2.49 <i>-13.83</i>
cc-pVDZ-PP	114	-27.83 <i>-1.77</i>	-13.29 <i>-17.72</i>	-2.43 <i>-14.93</i>	-25.25 <i>+0.52</i>	-12.31 <i>-15.79</i>	-2.34 <i>-14.18</i>	-25.37 <i>+0.43</i>	-12.46 <i>-15.76</i>	-2.27 <i>-14.15</i>
cc-pVTZ-PP	189	-27.67 <i>-1.29</i>	-13.05 <i>-17.59</i>	-2.40 <i>-14.92</i>	-25.21 <i>+0.68</i>	-12.14 <i>-15.76</i>	-2.32 <i>-14.20</i>	-25.27 <i>+0.47</i>	-12.43 <i>-15.82</i>	-2.21 <i>-14.18</i>
Def2-TZVP	120	-26.98 <i>-0.72</i>	-13.02 <i>-17.17</i>	-2.22 <i>-14.72</i>	-24.63 <i>+1.15</i>	-12.10 <i>-15.44</i>	-2.15 <i>-14.03</i>	-24.95 <i>+0.87</i>	-12.31 <i>-15.52</i>	-2.12 <i>-14.01</i>
Def2-TZVPP	168	-27.14 <i>-0.75</i>	-13.03 <i>-17.28</i>	-2.18 <i>-14.75</i>	-24.80 <i>+1.07</i>	-12.14 <i>-15.58</i>	-2.13 <i>-14.08</i>	-25.01 <i>+0.84</i>	-12.29 <i>-15.56</i>	-2.09 <i>-14.01</i>
Def2-QZVP	216	-27.45 <i>-0.85</i>	-12.70 <i>-17.33</i>	-2.34 <i>-14.79</i>	-25.07 <i>+0.90</i>	-11.90 <i>-15.61</i>	-2.29 <i>-14.12</i>	-25.08 <i>+0.8</i>	-12.13 <i>-15.60</i>	-2.19 <i>-14.10</i>
Def2-QZVPP	264	-27.46 <i>-0.73</i>	-12.70 <i>-17.23</i>	-2.29 <i>-14.74</i>	-25.09 <i>+1.01</i>	-11.91 <i>-15.55</i>	-2.27 <i>-14.10</i>	-24.98 <i>+1.01</i>	-12.09 <i>-15.43</i>	-2.18 <i>-14.03</i>

Table S-4

Au ₃ ⁺		BP86			B3LYP			M06		
Basis sets	Number of basis functions	NICS(0)	NICS(1)	NICS(2)	NICS(0)	NICS(1)	NICS(2)	NICS(0)	NICS(1)	NICS(2)
Aug-cc-pVDZ-PP	162	-32.99 <i>-0.23</i>	-13.45 <i>-18.67</i>	-1.83 <i>-16.40</i>	-30.21 <i>+2.67</i>	-12.63 <i>-17.10</i>	-1.84 <i>-16.01</i>	-28.74 <i>+3.02</i>	-12.55 <i>-16.36</i>	-1.85 <i>-15.72</i>
Aug-cc-pVTZ-PP	264	*	*	*	-33.44 <i>-1.80</i>	-14.34 <i>-19.83</i>	-2.46 <i>-16.94</i>	-31.51 <i>-0.41</i>	-14.03 <i>-18.57</i>	-2.27 <i>-16.50</i>
Lan12DZ	66	-35.89 <i>-6.10</i>	-15.94 <i>-21.86</i>	-2.78 <i>-17.96</i>	-33.07 <i>-3.25</i>	-14.97 <i>-20.08</i>	-2.70 <i>-17.40</i>	-32.05 <i>-3.26</i>	-15.01 <i>-19.69</i>	-2.80 <i>-17.23</i>
Lan12TZ	105	-36.36 <i>-7.12</i>	-16.15 <i>-22.39</i>	-3.02 <i>-17.90</i>	-33.55 <i>-3.82</i>	-15.15 <i>-20.48</i>	-2.89 <i>-17.39</i>	-32.13 <i>-3.54</i>	-15.09 <i>-19.85</i>	-2.90 <i>-17.15</i>
Lan12TZ(f)	126	-36.35 <i>-6.24</i>	-16.08 <i>-22.20</i>	-2.96 <i>-17.85</i>	-33.59 <i>-3.18</i>	-15.11 <i>-20.40</i>	-2.85 <i>-17.38</i>	-32.03 <i>-2.90</i>	-15.00 <i>-19.73</i>	-2.84 <i>-17.12</i>
cc-pVDZ-PP	114	-35.33 <i>-4.76</i>	-15.43 <i>-21.15</i>	-2.66 <i>-17.40</i>	-32.33 <i>-1.32</i>	-14.37 <i>-19.24</i>	-2.57 <i>-16.87</i>	-30.91 <i>-1.06</i>	-14.19 <i>-18.57</i>	-2.54 <i>-16.60</i>
cc-pVTZ-PP	189	-34.88 <i>-2.30</i>	-14.67 <i>-20.61</i>	-2.45 <i>-17.08</i>	-32.06 <i>+0.59</i>	-13.82 <i>-18.93</i>	-2.45 <i>-16.69</i>	-30.33 <i>+1.46</i>	-13.67 <i>-17.97</i>	-2.30 <i>-16.35</i>
Def2-TZVP	120	-32.23 <i>+0.92</i>	-13.31 <i>-18.46</i>	-2.14 <i>-16.44</i>	-29.94 <i>+2.90</i>	-12.71 <i>-17.27</i>	-2.17 <i>-16.18</i>	-28.72 <i>+2.77</i>	-12.66 <i>-16.79</i>	-2.15 <i>-15.94</i>
Def2-TZVPP	168	-32.52 <i>+1.06</i>	-13.15 <i>-18.52</i>	-2.05 <i>-16.42</i>	-30.20 <i>+3.07</i>	-12.60 <i>-17.35</i>	-2.10 <i>-16.20</i>	-28.82 <i>+3.10</i>	-12.51 <i>-16.74</i>	-2.08 <i>-15.91</i>
Def2-QZVP	216	-34.39 <i>-1.56</i>	-14.19 <i>-19.91</i>	-2.29 <i>16.85</i>	-31.80 <i>+0.93</i>	-13.50 <i>-18.50</i>	-2.32 <i>-16.54</i>	-30.21 <i>+1.33</i>	-13.36 <i>-17.72</i>	-2.20 <i>-16.20</i>
Def2-QZVPP	264	-34.50 <i>-1.39</i>	-14.35 <i>-20.16</i>	-2.33 <i>-16.92</i>	-31.85 <i>+1.15</i>	-13.63 <i>-18.68</i>	-2.35 <i>-16.58</i>	-30.14 <i>+1.92</i>	-13.43 <i>-17.79</i>	-2.23 <i>-16.23</i>

*At this level of theory Self Consistent Field (SCF) calculations did not converge.

Table S-5

Sc_3^-		BP86			B3LYP			M06		
Basis sets	Number of basis functions	NICS(0)	NICS(1)	NICS(2)	NICS(0)	NICS(1)	NICS(2)	NICS(0)	NICS(1)	NICS(2)
Lan2DZ	66	-15.88 <i>-50.17</i>	-11.25 <i>+15.73</i>	-2.06 <i>+29.52</i>	-27.82 <i>-49.98</i>	-18.49 <i>+16.26</i>	-4.66 <i>+29.64</i>	-38.59 <i>-62.91</i>	-32.81 <i>+35.26</i>	-10.03 <i>+49.21</i>
Lan2TZ	105	-9.05 <i>-42.07</i>	-8.32 <i>+14.50</i>	-2.17 <i>+26.52</i>	-17.12 <i>-35.84</i>	-14.34 <i>+15.42</i>	-4.83 <i>+25.07</i>	-27.95 <i>-45.88</i>	-26.81 <i>+35.50</i>	-10.01 <i>+45.28</i>
Lan2TZ(f)	126	-11.58 <i>-42.58</i>	-9.09 <i>+14.62</i>	-2.19 <i>+26.65</i>	-19.97 <i>-37.05</i>	-15.36 <i>+15.08</i>	-4.98 <i>+24.97</i>	-34.45 <i>-48.02</i>	-28.48 <i>+34.54</i>	-10.02 <i>+44.78</i>
Def2-TZVP	135	-9.16 <i>-50.32</i>	-14.12 <i>+9.80</i>	-6.62 <i>+25.17</i>	-17.58 <i>-44.94</i>	-21.84 <i>+8.32</i>	-10.21 <i>+21.80</i>	-20.56 <i>-44.69</i>	-33.10 <i>+16.39</i>	-16.66 <i>+28.56</i>
Def2-TZVPP	192	-14.03 <i>-51.15</i>	-15.28 <i>+10.81</i>	-5.60 <i>+25.66</i>	-22.64 <i>-46.68</i>	-22.93 <i>+9.01</i>	-9.23 <i>+22.30</i>	-20.70 <i>-47.19</i>	-32.30 <i>+16.93</i>	-15.01 <i>+28.87</i>
Def2-QZVP	252	-16.55 <i>-52.08</i>	-16.10 <i>+11.00</i>	-5.30 <i>+26.01</i>	-25.54 <i>-48.49</i>	-24.07 <i>+8.76</i>	-9.06 <i>+22.58</i>	-21.80 <i>-48.80</i>	-33.65 <i>+17.05</i>	-14.70 <i>+30.03</i>
Def2-QZVPP	279	-16.09 <i>-51.62</i>	-16.03 <i>+11.05</i>	-5.37 <i>+26.01</i>	-25.06 <i>-48.03</i>	-23.98 <i>+8.86</i>	-9.12 <i>+22.58</i>	-22.23 <i>-48.90</i>	-33.66 <i>+17.47</i>	-15 <i>+29.87</i>
6-311G(d)	138	-35.18 <i>-43.12</i>	-28.98 <i>+6.87</i>	-8.74 <i>+21.12</i>	-47.94 <i>-37.53</i>	-37.82 <i>+7.66</i>	-11.87 <i>+19.87</i>	-147.58 <i>-31.66</i>	-78.87 <i>+15.25</i>	-24.57 <i>+25.46</i>
6-311+G(d)	174	-15.89 <i>-51.92</i>	-15.61 <i>+10.43</i>	-5.18 <i>+25.67</i>	-25.07 <i>-48.13</i>	-23.29 <i>+8.75</i>	-8.67 <i>+22.59</i>	-22.18 <i>-49.22</i>	-33.58 <i>+15.96</i>	-14.67 <i>+29.29</i>
Aug-cc-pVDZ	129	-16.67 <i>-52.48</i>	-15.46 <i>+11.35</i>	-4.88 <i>+26.17</i>	-25.42 <i>-48.71</i>	-22.85 <i>+9.75</i>	-8.43 <i>+23.23</i>	-24.08 <i>-49.63</i>	-32.71 <i>+17.76</i>	-14.35 <i>+30.09</i>
Aug-cc-pVTZ	279	-16.25 <i>-51.7</i>	-15.88 <i>+11.01</i>	-5.45 <i>+25.82</i>	-25.06 <i>-47.97</i>	-23.67 <i>+8.79</i>	-9.15 <i>+22.30</i>	-22.58 <i>-47.65</i>	-33.18 <i>+17.02</i>	-15.04 <i>+29.20</i>
Aug-cc-pVQZ	420	-16.6 <i>-50.81</i>	-16.06 <i>+11.5</i>	-5.36 <i>+26.04</i>	-25.64 <i>-47.53</i>	-23.99 <i>+9.02</i>	-9.12 <i>+22.49</i>	-23.76 <i>-45.93</i>	-34.3 <i>+18</i>	-15.19 <i>+29.73</i>

Table S-6

Y_3^-		BP86			B3LYP			M06		
Basis sets	Number of basis functions	NICS(0)	NICS(1)	NICS(2)	NICS(0)	NICS(1)	NICS(2)	NICS(0)	NICS(1)	NICS(2)
Lan2DZ	66	-11.98 <i>-22.60</i>	-14.43 <i>-0.29</i>	-6.50 <i>+12.39</i>	-13.13 <i>-18.52</i>	-16.72 <i>-0.40</i>	-8.26 <i>+10.11</i>	-11.40 <i>-11.31</i>	-20.29 <i>+5.65</i>	-11.38 <i>+14.62</i>
Lan2TZ	105	-10.52 <i>-18.61</i>	-13.45 <i>+0.95</i>	-6.42 <i>+11.42</i>	-10.80 <i>-14.03</i>	-15.44 <i>+0.97</i>	-8.21 <i>+9.15</i>	-10.28 <i>-6.89</i>	-18.90 <i>+7.22</i>	-11.12 <i>+13.73</i>
Lan2TZ(f)	126	-12.41 <i>-19.35</i>	-14.11 <i>+0.92</i>	-6.43 <i>+11.56</i>	-12.95 <i>-15.43</i>	-16.36 <i>+0.45</i>	-8.36 <i>+9.03</i>	-13.29 <i>-8.45</i>	-20.08 <i>+6.51</i>	-11.25 <i>+13.44</i>
DZVP (DFTorbital)	108	-6.79 <i>-16.46</i>	-11.22 <i>+5.07</i>	-6.48 <i>+15.34</i>	-7.15 <i>-12.63</i>	-13.62 <i>+3.63</i>	-8.61 <i>+11.89</i>	-6.72 <i>-6.89</i>	-18.08 <i>+6.41</i>	-12.56 <i>+12.76</i>
Def2-TZVP	120	-11.60 <i>-19.70</i>	-14.88 <i>-0.64</i>	-7.39 <i>+9.92</i>	-11.78 <i>-16.03</i>	-17.11 <i>-1.14</i>	-9.38 <i>+7.50</i>	-11.32 <i>-11.04</i>	-20.77 <i>+4.19</i>	-12.30 <i>+11.58</i>
Def2-TZVPP	168	-12.05 <i>-19.91</i>	-15.13 <i>-0.71</i>	-7.37 <i>+9.88</i>	-12.22 <i>-16.34</i>	-17.36 <i>-1.32</i>	-9.46 <i>+7.38</i>	-12.07 <i>-11.67</i>	-21.12 <i>+3.71</i>	-12.48 <i>+11.59</i>
Def2-QZVP	216	-12.74 <i>-19.90</i>	-15.35 <i>-0.56</i>	-7.16 <i>+9.99</i>	-13.04 <i>-16.37</i>	-17.66 <i>-1.26</i>	-9.27 <i>+7.39</i>	-12.86 <i>-10.73</i>	-21.49 <i>+3.41</i>	-12.36 <i>+11.17</i>
Def2-QZVPP	243	-12.56 <i>-19.19</i>	-15.23 <i>-0.34</i>	-7.11 <i>+10.02</i>	-12.84 <i>-15.78</i>	-17.54 <i>-1.08</i>	-9.23 <i>+7.42</i>	-12.90 <i>-10.83</i>	-21.31 <i>+3.57</i>	-12.36 <i>+11.23</i>

Table S-7

La ₃ ⁻		BP86			B3LYP			M06		
Basis sets	Number of basis functions	NICS(0)	NICS(1)	NICS(2)	NICS(0)	NICS(1)	NICS(2)	NICS(0)	NICS(1)	NICS(2)
Lan12DZ	66	-7.36 <i>-11.85</i>	-7.71 <i>+15.28</i>	-2.93 <i>+28.64</i>	-11.18 <i>-13.27</i>	-10.95 <i>+12.32</i>	-4.52 <i>+26.51</i>	-25.28 <i>+4.91</i>	-18.85 <i>+18.98</i>	-8.97 <i>+27.09</i>
Lan12TZ	105	-7.70 <i>-11.51</i>	-7.99 <i>+14.15</i>	-2.96 <i>+26.95</i>	-11.04 <i>-11.80</i>	-11.00 <i>+11.48</i>	-4.63 <i>+24.44</i>	-26.38 <i>+8.49</i>	-18.14 <i>+20.08</i>	-7.99 <i>+25.91</i>
Lan12TZ(f)	126	-10.51 <i>-9.75</i>	-8.41 <i>+17.17</i>	-2.30 <i>+29.27</i>	-14.53 <i>-11.69</i>	-12.00 <i>+13.17</i>	-4.28 <i>+26.08</i>	-31.29 <i>+8.33</i>	-19.68 <i>+21.06</i>	-7.68 <i>+26.96</i>
Def2-TZVP	120	-11.08 <i>-10.50</i>	-10.13 <i>+13.67</i>	-3.70 <i>+25.08</i>	-14.78 <i>-11.84</i>	-13.69 <i>+9.67</i>	-5.79 <i>+21.47</i>	-27.72 <i>-0.66</i>	-20.69 <i>+14.25</i>	-9.33 <i>+22.73</i>
Def2-TZVPP	168	-15.90 <i>-11.91</i>	-13.69 <i>+10.30</i>	-5.57 <i>+22.01</i>	-12.07 <i>-9.94</i>	-10.09 <i>+14.72</i>	-3.34 <i>+25.79</i>	-29.06 <i>-1.84</i>	-20.52 <i>+14.09</i>	-9.02 <i>+22.88</i>
Def2-QZVP	216	-9.57 <i>-6.20</i>	-8.02 <i>+18.23</i>	-2.19 <i>+27.70</i>	-13.24 <i>-8.47</i>	-11.78 <i>+13.14</i>	-4.67 <i>+23.41</i>	-29.20 <i>-4.68</i>	-20.04 <i>+13.58</i>	-8.44 <i>+23.01</i>
Def2-QZVPP	243	-11.12 <i>-11.77</i>	-8.47 <i>+16.70</i>	-2.14 <i>+27.85</i>	-14.75 <i>-13.62</i>	-12.19 <i>+11.74</i>	-4.59 <i>+23.54</i>	-29.33 <i>-5.92</i>	-20.06 <i>+13.39</i>	-8.34 <i>+23.22</i>

Table S-8

Al ₄ ²⁻		BP86			B3LYP			M06		
Basis sets	Number of basis functions	NICS(0)	NICS(1)	NICS(2)	NICS(0)	NICS(1)	NICS(2)	NICS(0)	NICS(1)	NICS(2)
Lan12DZ	32	-25.60 <i>-63.39</i>	-22.28 <i>-53.03</i>	-12.56 <i>-33.12</i>	-27.43 <i>-63.50</i>	-23.38 <i>-53.17</i>	-12.94 <i>-33.27</i>	-24.55 <i>-64.57</i>	-21.56 <i>-53.95</i>	-12.45 <i>-33.75</i>
DZVP (DFT orbital)	72	-31.26 <i>-66.69</i>	-25.81 <i>-55.80</i>	-13.68 <i>-34.47</i>	-33.55 <i>-67.09</i>	-27.16 <i>-56.12</i>	-14.19 <i>-34.68</i>	-33.65 <i>-65.86</i>	-26.96 <i>-55.20</i>	-13.93 <i>-34.23</i>
Def2-TZVP	148	-31.90 <i>-66.00</i>	-26.51 <i>-55.10</i>	-14.07 <i>-33.84</i>	-34.61 <i>-66.37</i>	-28.08 <i>-55.38</i>	-14.54 <i>-33.99</i>	-35.31 <i>-65.39</i>	-28.23 <i>-55.07</i>	-14.24 <i>-33.79</i>
Def2-TZVPP	168	-31.96 <i>-66.23</i>	-26.54 <i>-55.24</i>	-14.09 <i>-33.89</i>	-34.64 <i>-66.57</i>	-28.09 <i>-55.50</i>	-14.55 <i>-34.03</i>	-35.36 <i>-65.64</i>	-28.23 <i>-55.20</i>	-14.26 <i>-33.83</i>
Def2-QZVP	280	-33.30 <i>-66.35</i>	-26.94 <i>-55.28</i>	-14.35 <i>-33.99</i>	-36.24 <i>-66.56</i>	-28.57 <i>-55.41</i>	-14.91 <i>-34.09</i>	-35.90 <i>-63.55</i>	-27.95 <i>-53.45</i>	-14.66 <i>-33.22</i>
Def2-QZVPP	280	-33.30 <i>-66.35</i>	-26.94 <i>-55.28</i>	-14.35 <i>-33.99</i>	-36.24 <i>-66.56</i>	-28.57 <i>-55.41</i>	-14.91 <i>-34.09</i>	-35.90 <i>-63.55</i>	-27.95 <i>-53.45</i>	-14.66 <i>-33.22</i>
6-311G(d)	104	-30.65 <i>-65.98</i>	-25.46 <i>-55.15</i>	-13.83 <i>-34.19</i>	-32.77 <i>-66.18</i>	-26.69 <i>-55.27</i>	-14.32 <i>-34.30</i>	-33.09 <i>-65.53</i>	-26.55 <i>-54.50</i>	-14.12 <i>-33.83</i>
6-311+G(d)	120	-32.21 <i>-66.01</i>	-26.07 <i>-54.81</i>	-14.42 <i>-33.71</i>	-34.46 <i>-66.18</i>	-27.39 <i>-54.88</i>	-15.03 <i>-33.74</i>	-34.46 <i>-66.04</i>	-27.17 <i>-54.62</i>	-15.06 <i>-33.33</i>

Table S-9

Ga_4^{2-}		BP86			B3LYP			M06		
Basis sets	Number of basis functions	NICS(0)	NICS(1)	NICS(2)	NICS(0)	NICS(1)	NICS(2)	NICS(0)	NICS(1)	NICS(2)
Aug-cc-pVDZ-PP	128	-37.05 -67.43	-29.29 -59.96	-15.72 -38.19	-38.45 -66.90	-30.22 -59.50	-16.24 -38.07	-33.91 -63.42	-27.98 -56.89	-16.13 -36.84
Aug-cc-pVTZ-PP	220	-38.95 -70.79	-30.15 -61.72	-15.81 -38.79	-40.34 -69.99	-31.05 -61.12	-16.33 -38.62	-30.72 -66.63	-26.44 -58.59	-16.15 -37.61
Lan12DZ	32	-25.19 -64.32	-22.39 -53.62	-12.73 -33.32	-26.65 -64.35	-23.28 -53.75	-13.11 -33.49	-26.27 -64.30	-22.64 -53.73	-12.66 -33.60
DZVP(DFT orbital)	108	-33.70 -62.23	-27.80 -57.57	-14.47 -37.67	-35.40 -62.29	-28.86 -57.57	-14.95 -37.79	-32.19 -60.17	-27.39 -56.16	-14.93 -37.37
cc-pVDZ-PP	92	-34.01 -66.57	-28.27 -60.00	-14.77 -38.32	-35.47 -66.56	-29.23 -59.97	-15.16 -38.39	-34.61 -66.01	-28.84 -59.69	-15.22 -38.46
cc-pVTZ-PP	156	-36.30 -68.87	-29.13 -60.59	-15.38 -38.41	-37.78 -68.81	-30.12 -60.52	-15.82 -38.46	-34.49 -66.16	-28.27 -58.48	-15.64 -37.66
Def2-TZVP	192	-33.61 -63.46	-27.62 -57.73	-14.47 -37.14	-35.38 -63.76	-28.76 -57.89	-14.93 -37.29	-34.86 -63.68	-28.56 -57.82	-15.13 -37.34
Def2-TZVPP	192	-33.61 -63.46	-27.62 -57.73	-14.47 -37.14	-35.38 -63.76	-28.76 -57.89	-14.93 -37.29	-34.86 -63.68	-28.56 -57.82	-15.13 -37.34
Def2-QZVP	300	-34.91 -63.39	-28.12 -57.60	-14.75 -37.27	-36.76 -63.57	-29.27 -57.63	-15.23 -37.36	-34.01 -61.48	-27.76 -55.91	-15.23 -36.68
Def2-QZVPP	356	-34.93 -63.39	-28.13 -57.61	-14.76 -37.28	-36.77 -63.58	-29.28 -57.64	-15.24 -37.37	-34.04 -61.53	-27.78 -55.95	-15.24 -36.70
6-311G(d)	176	-33.69 -62.58	-27.59 -57.45	-14.62 -37.42	-35.26 -62.45	-28.55 -57.27	-15.05 -37.45	-32.12 -60.35	-26.87 -55.60	-14.96 -36.89
6-311+G(d)	192	-42.40 -76.86	-32.17 -67.62	-15.95 -41.90	-39.18 -63.39	-29.86 -57.68	-15.12 -37.29	-31.44 -57.68	-26.39 -53.40	-15.15 -35.51

Table S-10

Cu ₄ ²⁺		BP86			B3LYP			M06		
Basis sets	Number of basis functions	NICS(0)	NICS(1)	NICS(2)	NICS(0)	NICS(1)	NICS(2)	NICS(0)	NICS(1)	NICS(2)
Aug-cc-pVDZ-PP	216	-27.43 -36.09	-15.38 -33.59	-6.28 -22.21	-19.86 -25.75	-11.90 -29.13	-5.53 -21.61	-18.67 -20.88	-11.28 -26.25	-5.42 -20.63
Aug-cc-pVTZ-PP	352	-26.03 -34.68	-14.55 -32.68	-5.80 -21.79	-18.17 -24.10	-10.80 -28.01	-4.98 -21.16	*	*	*
Lan12DZ	88	-19.39 -24.37	-11.25 -28.31	-5.36 -21.65	-14.56 -18.81	-8.84 -25.47	-4.69 -21.00	-14.96 -16.29	-9.14 -24.17	-5.08 -20.58
Lan12TZ	140	-22.01 -27.06	-12.56 -29.77	-5.50 -21.89	-16.17 -20.07	-9.64 -26.41	-4.73 -21.22	-16.72 -17.63	-10.11 -25.05	-5.21 -20.75
Lan12TZ(f)	168	-21.98 -27.00	-12.54 -29.74	-5.49 -21.88	-16.15 -20.05	-9.63 -26.40	-4.73 -21.22	-16.70 -17.70	-10.09 -25.03	-5.20 -20.74
DZVP(DFT orbital)	96	-19.05 -24.10	-13.47 -27.46	-6.48 -20.44	-16.37 -20.82	-12.12 -25.32	-6.32 -19.92	-16.74 -20.81	-12.33 -25.95	-6.40 -20.23
cc-pVDZ-PP	154	*	*	*	*	*	*	-17.68 -24.16	-10.70 -28.60	-5.71 -21.65
cc-pVTZ-PP	352	-24.83 -34.18	-14.52 -33.07	-5.85 -22.07	-17.57 -24.24	-10.88 -28.35	-5.06 -21.26	-16.94 -21.59	-10.64 -26.92	-5.09 -20.82
Def2-TZVP	180	-21.06 -24.82	-13.06 -27.38	-6.02 -20.47	-16.96 -19.50	-11.40 -24.77	-5.89 -20.09	-16.13 -17.66	-10.93 -24.05	-5.85 -20.01
Def2-TZVPP	256	-20.00 -24.92	-12.19 -27.69	-5.68 -20.66	-15.53 -19.41	-10.26 -25.04	-5.50 -20.30	-14.54 -17.39	-9.64 -24.31	-5.44 -20.25
Def2-QZVP	336	-19.24 -25.17	-11.52 -28.37	-5.16 -20.94	-14.04 -19.28	-9.04 -25.43	-4.64 -20.52	-13.71 -16.42	-8.98 -24.20	-4.87 -20.25
Def2-QZVPP	400	-19.11 -25.12	-11.50 -28.31	-5.13 -20.93	-13.92 -19.23	-9.05 -25.42	-4.64 -20.53	-13.58 -16.34	-8.86 -23.98	-4.81 -20.19
6-311G(d)	184	-9.84 -19.15	-5.27 -18.88	-3.67 -12.94	-13.91 -11.56	-8.58 -20.28	-5.09 -16.98	-13.60 -10.21	-8.12 -19.47	-4.86 -16.51
6-311+G(d)	232	-19.65 -24.97	-12.00 -28.53	-4.97 -20.94	-14.25 -19.02	-9.32 -25.52	-4.47 -20.50	-13.38 -14.88	-8.93 -22.80	-4.39 -19.35
Aug-cc-pVDZ	172	-19.81 -26.47	-11.67 -28.6	-5.29 -20.94	-14.37 -20.07	-9.11 -25.61	-4.91 -20.61	-13.68 -17.89	-8.86 -24.59	-4.89 -20.37
Aug-cc-pVTZ-PP	372	-19.82 -25.76	-11.68 -28.68	-5.09 -20.89	-14.28 -19.56	-9.12 -25.77	-4.62 -20.59	-12.8 -14.63	-8.23 -22.74	-4.43 -19.48

*At these levels of theory Self Consistent Field (SCF) calculations did not converge.

Table S-11

Ag ₄ ²⁺		BP86			B3LYP			M06		
Basis sets	Number of basis functions	NICS(0)	NICS(1)	NICS(2)	NICS(0)	NICS(1)	NICS(2)	NICS(0)	NICS(1)	NICS(2)
Aug-cc-pVDZ-PP	216	-14.98 <i>-10.83</i>	-10.22 <i>-21.07</i>	-5.29 <i>-21.37</i>	-13.07 <i>-10.34</i>	-9.22 <i>-20.04</i>	-5.05 <i>-20.78</i>	-12.74 <i>-8.57</i>	-9.08 <i>-18.99</i>	-5.01 <i>-20.38</i>
Aug-cc-pVTZ-PP	352	-14.34 <i>-9.61</i>	-9.72 <i>-20.31</i>	-5.03 <i>-21.04</i>	-12.46 <i>-9.29</i>	-8.74 <i>-19.40</i>	-4.82 <i>-20.53</i>	-11.95 <i>-9.00</i>	-8.70 <i>-19.65</i>	-5.01 <i>-20.94</i>
Lan12DZ	88	-13.38 <i>-8.50</i>	-9.28 <i>-19.06</i>	-5.00 <i>-20.70</i>	-11.88 <i>-8.60</i>	-8.45 <i>-18.39</i>	-4.73 <i>-20.13</i>	-12.60 <i>-7.11</i>	-9.04 <i>-17.86</i>	-5.10 <i>-20.11</i>
Lan12TZ	140	-14.13 <i>-9.84</i>	-9.72 <i>-20.08</i>	-5.00 <i>-21.05</i>	-12.35 <i>-9.35</i>	-8.73 <i>-19.06</i>	-4.73 <i>-20.41</i>	-12.91 <i>-7.90</i>	-9.28 <i>-18.36</i>	-5.23 <i>-20.33</i>
Lan12TZ(f)	168	-14.09 <i>-9.74</i>	-9.70 <i>-20.06</i>	-4.99 <i>-21.05</i>	-12.30 <i>-9.26</i>	-8.69 <i>-19.04</i>	-4.71 <i>-20.41</i>	-12.85 <i>-7.78</i>	-9.24 <i>-18.31</i>	-5.21 <i>-20.32</i>
DZVP(DFT orbital)	144	-12.37 <i>-9.11</i>	-9.74 <i>-18.86</i>	-6.01 <i>-20.42</i>	-11.39 <i>-9.04</i>	-9.24 <i>-17.83</i>	-5.94 <i>-19.61</i>	-11.30 <i>-7.80</i>	-9.20 <i>-18.06</i>	-6.06 <i>-20.26</i>
cc-pVDZ-PP	152	-14.42 <i>-10.90</i>	-9.99 <i>-20.76</i>	-5.19 <i>-21.15</i>	-12.46 <i>-10.27</i>	-8.90 <i>-19.66</i>	-4.93 <i>-20.47</i>	-12.96 <i>-9.66</i>	-9.40 <i>-19.53</i>	-5.18 <i>-20.61</i>
cc-pVTZ-PP	252	-14.45 <i>-10.70</i>	-10.12 <i>-20.89</i>	-5.18 <i>-21.22</i>	-12.58 <i>-10.24</i>	-9.08 <i>-19.87</i>	-4.91 <i>-20.61</i>	-12.71 <i>-9.63</i>	-9.32 <i>-19.76</i>	-5.18 <i>-20.85</i>
Def2-TZVP	160	-14.04 <i>-10.95</i>	-9.75 <i>-20.62</i>	-5.11 <i>-21.05</i>	-12.28 <i>-10.45</i>	-8.81 <i>-19.61</i>	-4.95 <i>-20.43</i>	-12.65 <i>-9.67</i>	-9.22 <i>-19.48</i>	-5.21 <i>-20.70</i>
Def2-TZVPP	224	-14.00 <i>-10.83</i>	-9.69 <i>-20.66</i>	-5.07 <i>-21.09</i>	-12.27 <i>-10.43</i>	-8.77 <i>-19.70</i>	-4.92 <i>-20.50</i>	-12.57 <i>-9.51</i>	-9.14 <i>-19.49</i>	-5.16 <i>-20.74</i>
Def2-QZVP	288	-14.16 <i>-10.13</i>	-9.82 <i>-20.52</i>	-5.09 <i>-21.10</i>	-12.40 <i>-9.82</i>	-8.90 <i>-19.60</i>	-4.87 <i>-20.55</i>	-12.33 <i>-8.55</i>	-9.01 <i>-19.11</i>	-5.07 <i>-20.66</i>
Def2-QZVPP	352	-14.08 <i>-10.05</i>	-9.80 <i>-20.56</i>	-5.11 <i>-21.14</i>	-12.38 <i>-9.78</i>	-8.90 <i>-19.66</i>	-4.90 <i>-20.61</i>	-12.15 <i>-8.47</i>	-8.95 <i>-19.01</i>	-5.06 <i>-20.56</i>

Table S-12

Au ₄ ²⁺		BP86			B3LYP			M06		
Basis sets	Number of basis functions	NICS(0)	NICS(1)	NICS(2)	NICS(0)	NICS(1)	NICS(2)	NICS(0)	NICS(1)	NICS(2)
Aug-cc-pVDZ-PP	216	-16.54 <i>-4.69</i>	-10.57 <i>-18.00</i>	-4.65 <i>-20.53</i>	-15.23 <i>-4.95</i>	-10.01 <i>-17.75</i>	-4.67 <i>-20.46</i>	-14.05 <i>-4.28</i>	-9.47 <i>-16.74</i>	-4.56 <i>-20.02</i>
Aug-cc-pVTZ-PP	352	-19.45 <i>-9.84</i>	-12.58 <i>-21.55</i>	-5.60 <i>-22.32</i>	-18.06 <i>-9.93</i>	-11.96 <i>-21.23</i>	-5.61 <i>-22.26</i>	-15.87 <i>-6</i>	-10.79 <i>-17.97</i>	-5.20 <i>-20.70</i>
Lan12DZ	88	-17.46 <i>-5.27</i>	-11.69 <i>-17.58</i>	-5.25 <i>-20.55</i>	-16.19 <i>-5.63</i>	-11.10 <i>-17.38</i>	-5.25 <i>-20.41</i>	-16.42 <i>-6.74</i>	-11.46 <i>-18.18</i>	-5.55 <i>-20.89</i>
Lan12TZ	140	-18.75 <i>-6.85</i>	-12.44 <i>-18.91</i>	-5.45 <i>-21.08</i>	-17.30 <i>-6.78</i>	-11.74 <i>-18.55</i>	-5.44 <i>-21.00</i>	-16.94 <i>-7.76</i>	-11.76 <i>-18.89</i>	-5.68 <i>-21.26</i>
Lan12TZ(f)	168	-18.65 <i>-6.32</i>	-12.36 <i>-18.80</i>	-5.39 <i>-21.09</i>	-17.21 <i>-6.31</i>	-11.66 <i>-18.48</i>	-5.38 <i>-21.04</i>	-16.76 <i>-7.25</i>	-11.62 <i>-18.72</i>	-5.61 <i>-21.25</i>
cc-pVDZ-PP	152	-18.01 <i>-6.85</i>	-11.82 <i>-18.93</i>	-5.28 <i>-20.98</i>	-16.48 <i>-6.68</i>	-11.09 <i>-18.50</i>	-5.23 <i>-20.83</i>	-15.87 <i>-6.65</i>	-10.99 <i>-18.17</i>	-5.36 <i>-20.74</i>
cc-pVTZ-PP	252	-18.12 <i>-6.41</i>	-11.85 <i>-19.36</i>	-5.37 <i>-21.22</i>	-16.75 <i>-6.77</i>	-11.26 <i>-19.19</i>	-5.38 <i>-21.21</i>	-15.65 <i>-5.81</i>	-10.75 <i>-17.85</i>	-5.27 <i>-20.60</i>
Def2-TZVP	160	-17.11 <i>-5.37</i>	-11.27 <i>-18.32</i>	-5.11 <i>-20.79</i>	-15.77 <i>-5.76</i>	-10.69 <i>-18.14</i>	-5.14 <i>-20.75</i>	-15.33 <i>-5.60</i>	-10.55 <i>-17.48</i>	-5.20 <i>-20.44</i>
Def2-TZVPP	224	-17.05 <i>-5.13</i>	-11.19 <i>-18.31</i>	-5.05 <i>-20.82</i>	-15.74 <i>-5.60</i>	-10.65 <i>-18.18</i>	-5.11 <i>-20.81</i>	-15.23 <i>-5.28</i>	-10.47 <i>-17.43</i>	-5.15 <i>-20.47</i>
Def2-QZVP	288	-17.59 <i>-5.67</i>	-11.56 <i>-18.95</i>	-5.19 <i>-21.18</i>	-16.28 <i>-6.04</i>	-11.00 <i>-18.79</i>	-5.22 <i>-21.19</i>	-15.25 <i>-5.38</i>	-10.52 <i>-17.55</i>	-5.08 <i>-20.44</i>
Def2-QZVPP	352	-17.73 <i>-6.19</i>	-11.61 <i>-19.27</i>	-5.19 <i>-21.22</i>	-16.44 <i>-6.56</i>	-11.05 <i>-19.10</i>	-5.22 <i>-21.25</i>	-15.17 <i>-5.69</i>	-10.53 <i>-17.85</i>	-5.12 <i>-20.58</i>

Table S-13

Li_3^+	BP86				B3LYP				M06			
	Δ NICS (0)		Δ NICS (1)		Δ NICS (0)		Δ NICS (1)		Δ NICS (0)		Δ NICS (1)	
<i>Basis sets</i>	NICS_{iso}	NICS_z	NICS_{iso}	NICS_z	NICS_{iso}	NICS_z	NICS_{iso}	NICS_z	NICS_{iso}	NICS_z	NICS_{iso}	NICS_z
Lan12DZ	0.02	-0.08	0.02	-0.03	0.02	-0.08	0.01	-0.03	0	0.01	0	0.01
DZVP(DFT orbital)	0.13	-0.03	0.05	0.01	0.12	-0.03	0.04	0	0.03	0	0	0
Def2-TZVP	0.01	-0.12	-0.01	-0.05	0.01	-0.14	-0.01	-0.06	0.01	-0.02	0	-0.01
Def2-TZVPP	0.02	-0.05	-0.01	-0.02	0.01	-0.05	-0.01	-0.03	-0.05	0.06	0.01	0.03
Def2-QZVP	0	0	0	0	0	0	0	0	0	0	0	0
Def2-QZVPP	0	0	0	0	0	0	0	0	0	0	0	0
6-311G(d)	0	-0.02	0	-0.01	0.01	-0.02	-0.01	-0.01	-0.04	0.13	0	0.08
6-311+G(d)	0.01	-0.02	0	0.29	0.01	-0.02	-0.01	0	-0.04	0.15	0.01	1.5

Table S-14

Cu_3^+	BP86				B3LYP				M06			
	Δ NICS (0)		Δ NICS (1)		Δ NICS (0)		Δ NICS (1)		Δ NICS (0)		Δ NICS (1)	
<i>Basis sets</i>	NICS_{iso}	NICS_z	NICS_{iso}	NICS_z	NICS_{iso}	NICS_z	NICS_{iso}	NICS_z	NICS_{iso}	NICS_z	NICS_{iso}	NICS_z
Aug-cc-pVDZ-PP	-0.7	-0.28	-0.13	-0.36	-0.79	-0.16	-0.15	-0.46	-0.56	0.02	-0.08	-0.32
Aug-cc-pVTZ-PP	-1.35	-0.91	-0.34	-0.75	-1.34	-0.74	-0.36	-0.83	0.87	0.42	0.22	0.54
Lan12DZ	0.513	0.12	0.12	0.32	0.06	0.01	0.02	0.04	-0.14	-0.02	-0.03	-0.1
Lan12TZ	0.24	0.1	0.06	0.14	-0.31	-0.1	-0.09	-0.2	-0.19	-0.05	-0.06	-0.12
Lan12TZ(f)	0.23	0.1	0.06	0.14	-0.3	-0.09	-0.08	-0.19	-0.21	-0.04	-0.06	-0.13
DZVP(DFT orbital)	1.06	0.13	0.31	0.72	0.69	-0.01	0.23	0.53	0.35	-0.04	0.11	0.25
cc-pVDZ-PP	-1.55	-0.92	-0.4	-0.88	-1.61	-0.79	-0.44	-1.02	-1.18	-0.44	-0.31	-0.75
cc-pVTZ-PP	-0.78	-0.5	-0.21	-0.44	-0.92	-0.48	-0.26	-0.58	-0.57	-0.24	-0.15	-0.36
Def2-TZVP	0.6	0.25	0.26	0.38	0.37	0.07	0.11	0.25	0.28	0.03	0.08	0.19
Def2-TZVPP	0.49	0.19	0.13	0.31	0.32	0.06	0.09	0.22	0.24	0.02	0.07	0.18
Def2-QZVP	0.19	0.07	0.05	0.11	0.09	0.02	0.03	0.06	0.07	-0.01	0.02	0.05
Def2-QZVPP	0.3	-0.05	-0.26	0.13	0.1	-0.21	-0.2	0.1	0.05	0	0.01	0.03
6-311G(d)	-1.21	0.94	-0.04	-0.48	-1.81	-4.66	-0.15	-0.93	-1.83	1.02	-0.2	-1.02
6-311+G(d)	0.23	0.09	0.06	0.13	0.13	0.02	0.03	0.08	0.12	0.01	0.03	0.08
Aug-cc-pVDZ	0.74	0.33	0.2	0.45	0.48	0.13	0.14	0.33	0.35	0.06	0.1	0.23
Aug-cc-pVTZ	-0.74	-0.27	-0.17	-0.43	0.69	0.11	0.17	0.45	0	0	0.01	0.01
Aug-cc-pVQZ	0	0	0	0	0	0	0	0	0	0	0	0

Table S-15

Ag_3^+	BP86				B3LYP				M06			
	Δ NICS (0)		Δ NICS (1)		Δ NICS (0)		Δ NICS (1)		Δ NICS (0)		Δ NICS (1)	
<i>Basis sets</i>	NICS_{iso}	NICS_z	NICS_{iso}	NICS_z	NICS_{iso}	NICS_z	NICS_{iso}	NICS_z	NICS_{iso}	NICS_z	NICS_{iso}	NICS_z
Aug-cc-pVDZ-PP	0.08	-0.01	0.03	0.06	0.06	-0.02	0.02	0.05	-0.04	0.02	-0.02	-0.03
Aug-cc-pVTZ-PP	-0.12	0.01	-0.04	-0.07	-0.09	0.02	-0.03	-0.06	-0.79	0.03	-0.51	-0.05
Lan12DZ	1.18	-0.09	0.37	0.87	0.89	-0.2	0.29	0.68	0.5	-0.17	0.16	0.38
Lan12TZ	1.25	-0.07	0.43	0.9	0.87	-0.18	0.3	0.64	0.62	-0.21	0.21	0.45
Lan12TZ(f)	1.18	-0.09	0.41	0.85	0.86	-0.2	0.29	0.63	0.6	-0.22	0.21	0.43
DZVP(DFT orbital)	2.94	-1.18	1.04	2.24	2.49	-1.43	0.89	1.94	1.81	-1.21	0.67	1.39
cc-pVDZ-PP	0.51	0.02	0.17	0.35	0.34	-0.05	0.1	0.24	0.14	-0.04	0.05	0.1
cc-pVTZ-PP	0.22	-0.01	0.06	0.15	0.15	-0.03	0.05	0.11	0.12	-0.04	0.03	0.09
Def2-TZVP	0.73	-0.03	0.25	0.51	0.52	-0.1	0.19	0.36	0.27	-0.1	0.09	0.19
Def2-TZVPP	0.47	-0.04	0.15	0.33	0.33	-0.08	0.11	0.23	0.17	-0.07	0.06	0.13
Def2-QZVP	0.04	0	0.01	0.03	0.03	-0.01	0.01	0.03	0	0	0	0
Def2-QZVPP	0	0	0	0	0	0	0	0	0	0	0	0

Table S-16

Au_3^+	BP86				B3LYP				M06			
	Δ NICS (0)		Δ NICS (1)		Δ NICS (0)		Δ NICS (1)		Δ NICS (0)		Δ NICS (1)	
<i>Basis sets</i>	$NICS_{iso}$	$NICS_z$	$NICS_{iso}$	$NICS_z$	$NICS_{iso}$	$NICS_z$	$NICS_{iso}$	$NICS_z$	$NICS_{iso}$	$NICS_z$	$NICS_{iso}$	$NICS_z$
Aug-cc-pVDZ-PP	0.17	0.02	0.04	0.1	0.15	0	0.04	0.09	0.15	-0.01	0.03	0.09
Aug-cc-pVTZ-PP	-	-	-	-	-0.02	0	0	-0.01	-0.05	0	-0.01	-0.02
Lan12DZ	2.06	1.14	0.6	1.32	1.76	0.86	0.52	1.14	1.23	0.56	0.38	0.8
Lan12TZ	1.24	0.35	0.33	0.74	1.01	0.29	0.28	0.62	0.83	0.21	0.24	0.54
Lan12TZ(f)	0.67	0.12	0.17	0.4	0.5	0.09	0.13	0.31	0.46	0.07	0.13	0.28
cc-pVDZ-PP	0.74	0.18	0.22	0.47	0.61	0.1	0.17	0.4	0.47	0.04	0.14	0.32
cc-pVTZ-PP	0.09	-0.01	0.02	0.05	0.11	-0.01	0.02	0.06	0.09	-0.03	0.02	0.06
Def2-TZVP	0.5	0.01	0.12	0.33	0.43	-0.04	0.1	0.28	0.3	-0.06	0.08	0.2
Def2-TZVPP	0.15	0	0.04	0.1	0.12	-0.02	0.03	0.08	0.09	-0.02	0.02	0.06
Def2-QZVP	0.11	0	0.03	0.06	0.07	-0.01	0.02	0.05	0.09	-0.02	0.02	0.05
Def2-QZVPP	0	0	0	0	0	0	0	0	0	0	0	0

Table S-17

Sc_3^-	BP86				B3LYP				M06			
	Δ NICS (0)		Δ NICS (1)		Δ NICS (0)		Δ NICS (1)		Δ NICS (0)		Δ NICS (1)	
<i>Basis sets</i>	$NICS_{iso}$	$NICS_z$	$NICS_{iso}$	$NICS_z$	$NICS_{iso}$	$NICS_z$	$NICS_{iso}$	$NICS_z$	$NICS_{iso}$	$NICS_z$	$NICS_{iso}$	$NICS_z$
Lan12DZ	0.01	-0.46	-0.11	-0.45	-0.17	-0.34	-0.21	-0.3	1.51	1.64	2.19	1.11
Lan12TZ	0	-2.22	-0.46	-2.12	-0.71	-1.84	-0.92	-1.68	-1.07	-1.05	-1.41	-0.74
Lan12TZ(f)	0.01	-2.04	-0.44	-2.02	-0.63	-1.6	-0.85	-1.53	-0.98	-0.8	-1.14	-0.58
Def2-TZVP	0.09	-0.16	-0.02	-0.18	0	0.05	0.04	0.06	-0.01	0.16	0.3	0.12
Def2-TZVPP	0.06	-0.15	-0.02	-0.18	-0.01	-0.02	-0.02	-0.02	-0.02	0.08	0.13	0.07
Def2-QZVP	0.03	-0.08	-0.02	-0.1	-0.01	-22.96	-0.02	-0.02	-0.02	0.25	0.31	0.18
Def2-QZVPP	0.04	-0.11	-0.02	-0.13	-0.01	-22.97	-0.02	-0.02	-0.01	0.2	0.27	0.16
6-311G(d)	4.96	2.21	2.73	2.34	12.21	22.62	6.77	2.11	-569.51	1.78	-137.27	1.17
6-311+G(d)	0.12	-0.37	-0.09	-0.44	-0.07	-0.2	-0.19	-0.24	0.01	-0.24	-10.47	-0.18
Aug-cc-pVDZ	0.07	-0.25	-0.07	-0.29	-0.06	-0.17	-0.15	-0.2	-0.01	-0.06	-10.02	-0.05
Aug-cc-pVTZ	0.01	-0.05	-0.01	-0.06	0	0	0	0	0	0	-9.51	0
Aug-cc-pVQZ	0	0	0	0	0	0	0	0	0	0	0	0

Table S-18

Y_3^-	BP86				B3LYP				M06			
	Δ NICS (0)		Δ NICS (1)		Δ NICS (0)		Δ NICS (1)		Δ NICS (0)		Δ NICS (1)	
<i>Basis sets</i>	$NICS_{iso}$	$NICS_z$	$NICS_{iso}$	$NICS_z$	$NICS_{iso}$	$NICS_z$	$NICS_{iso}$	$NICS_z$	$NICS_{iso}$	$NICS_z$	-0.13	$NICS_z$
Lan12DZ	-0.03	-0.14	-0.06	-0.13	-0.03	-0.09	-0.05	-0.07	-0.04	-0.12	-0.42	-0.07
Lan12TZ	-0.08	-0.49	-0.19	-0.43	-0.12	-0.41	-0.22	-0.32	-0.1	-0.44	-0.28	-0.26
Lan12TZ(f)	-0.05	-0.31	-0.12	-0.29	-0.06	-0.26	-0.16	-0.22	-0.07	-0.27	-0.65	-0.15
DZVP(DFT orbital)	-0.01	-0.11	-0.04	-0.09	-0.03	-0.25	-0.13	-0.21	0.11	-0.89	0	-0.51
Def2-TZVP	0.02	-0.08	-0.02	-0.08	0.01	-0.05	-0.02	-0.04	0	-0.01	-0.01	0
Def2-TZVPP	0.01	-0.08	-0.02	-0.07	0.01	-0.04	-0.03	-0.04	0	-0.01	0	0
Def2-QZVP	0	-0.02	-0.01	-0.02	0	-0.01	-0.01	-0.01	0	0	0	0
Def2-QZVPP	0	0	0	0	0	0	0	0	0	0	-0.13	0

Table S-19

La_3^-	BP86				B3LYP				M06			
	Δ NICS (0)		Δ NICS (1)		Δ NICS (0)		Δ NICS (1)		Δ NICS (0)		Δ NICS (1)	
<i>Basis sets</i>	$NICS_{iso}$	$NICS_z$	$NICS_{iso}$	$NICS_z$	$NICS_{iso}$	$NICS_z$	$NICS_{iso}$	$NICS_z$	$NICS_{iso}$	$NICS_z$	$NICS_{iso}$	$NICS_z$
Lan12DZ	-0.9	-3.1	-1.36	-3.26	-1.76	-3.07	-0.89	-3.13	-2.3	13.3	4.13	-3.32
Lan12TZ	-0.89	-2.76	-1.36	-3.28	-1.16	-2.77	-1.6	-3.18	-2.28	20.08	5.96	-3.03
Lan12TZ(f)	-0.32	-1.09	-0.5	-1.27	-0.53	-1.42	2	-1.62	-0.91	18.08	10.7	-1.39
Def2-TZVP	-0.12	-0.57	-0.25	-0.7	-0.1	-0.38	0.99	-0.45	-0.14	-0.27	6.89	-0.29
Def2-TZVPP	-3.89	-2.26	-3.72	-4.77	3.81	1.86	3.55	4.29	-0.05	-0.1	8.48	-0.1
Def2-QZVP	-0.01	-0.02	-0.019	-0.02	-0.01	-0.03	1.45	-0.03	0.01	0	9.17	0.01
Def2-QZVPP	0	0	0	0	0	0	0	0	0	0	0	0

Table S-20

Al_4^{2-}	BP86				B3LYP				M06			
	Δ NICS (0)		Δ NICS (1)		Δ NICS (0)		Δ NICS (1)		Δ NICS (0)		Δ NICS (1)	
<i>Basis sets</i>	$NICS_{iso}$	$NICS_z$	$NICS_{iso}$	$NICS_z$	$NICS_{iso}$	$NICS_z$	$NICS_{iso}$	$NICS_z$	$NICS_{iso}$	$NICS_z$	$NICS_{iso}$	$NICS_z$
Lan12DZ	0.13	1.73	0.04	1.06	0.14	1.66	0.01	1.01	-0.91	2.7	-0.44	1.67
DZVP(DFT orbital)	0.11	0.38	0.06	0.26	0.11	0.38	0.05	0.26	0.05	0.32	0.04	0.22
Def2-TZVP	-0.01	-0.04	-0.01	-0.03	-0.04	-0.11	-0.02	-0.07	-0.05	-0.23	-0.03	-0.16
Def2-TZVPP	-0.02	-0.05	-0.01	-0.03	-0.04	-0.11	-0.02	-0.07	-0.06	-0.25	-0.04	-0.17
Def2-QZVP	-0.01	0	0	0	0	0	0	0	0	0	0	0
Def2-QZVPP	0	0	0	0	0	0	0	0	0	0	0	0
6-311G(d)	0.07	0.26	0.04	0.17	0.07	0.26	0.04	0.17	0.03	0.19	0.01	0.12
6-311+G(d)	0.08	0.26	0.04	0.17	0.07	0.25	0.03	0.17	0.08	0.32	0.04	0.22

Table S-21

Ga_4^{2-}	BP86				B3LYP				M06			
	Δ NICS (0)		Δ NICS (1)		Δ NICS (0)		Δ NICS (1)		Δ NICS (0)		Δ NICS (1)	
<i>Basis sets</i>	$NICS_{iso}$	$NICS_z$	$NICS_{iso}$	$NICS_z$	$NICS_{iso}$	$NICS_z$	$NICS_{iso}$	$NICS_z$	$NICS_{iso}$	$NICS_z$	$NICS_{iso}$	$NICS_z$
Aug-cc-pVDZ-PP	0.46	0.92	0.3	0.94	0.41	0.85	0.26	0.89	0.43	0.42	0.24	0.49
Aug-cc-pVTZ-PP	0.28	0.63	0.15	0.52	0.26	0.61	0.14	0.51	0.63	0.65	0.33	0.54
Lan12DZ	0.22	2.27	0.16	1.52	0.22	1.89	0.13	1.27	-0.37	1.88	-0.14	1.26
DZVP(DFT orbital)	0.31	0.43	0.19	0.55	0.26	0.36	0.15	0.46	0.21	0.28	0.13	0.34
cc-pVDZ-PP	0.31	0.52	0.2	0.55	0.23	0.35	0.13	0.37	-0.01	-0.02	0	-0.01
cc-pVTZ-PP	0.13	0.23	0.08	0.21	0.08	0.13	0.05	0.13	0.07	0.1	0.04	0.09
Def2-TZVP	-0.08	-0.11	-0.05	-0.12	-0.12	-0.16	-0.07	-0.18	-0.4	-0.4	-0.21	-0.49
Def2-TZVPP	-0.08	-0.12	-0.05	-0.12	-0.12	-0.16	-0.07	-0.18	-0.4	-0.4	-0.21	-0.49
Def2-QZVP	0.01	0	0	0	0	0	0	0	0	0.01	0	0
Def2-QZVPP	0	0	0	0	0	0	0	0	0	0	0	0
6-311G(d)	0.15	0.24	0.09	0.28	0.13	0.22	0.08	0.26	0.19	0.27	0.11	0.32
6-311+G(d)	1.2	4.09	0.94	3.17	0.02	0.61	0.07	0.64	0.37	0.34	0.2	0.43

Table S-22

Cu_4^{2-}	BP86				B3LYP				M06			
	Δ NICS (0)		Δ NICS (1)		Δ NICS (0)		Δ NICS (1)		Δ NICS (0)		Δ NICS (1)	
<i>Basis sets</i>	$NICS_{iso}$	$NICS_z$	$NICS_{iso}$	$NICS_z$	$NICS_{iso}$	$NICS_z$	$NICS_{iso}$	$NICS_z$	$NICS_{iso}$	$NICS_z$	$NICS_{iso}$	$NICS_z$
Aug-cc-pVDZ-PP	-0.81	-0.76	-0.21	-0.56	-0.71	-0.51	-0.14	-0.65	-0.31	-0.09	-0.03	-0.23
Aug-cc-pVTZ-PP	-1.25	-1.28	-0.45	-1.02	-1.02	-1	-0.34	-1.1	-	-	-	-
Lan12DZ	0.1	0.08	0.02	0.08	-0.15	-0.1	-0.01	-0.19	-0.22	-0.11	-0.03	-0.24
Lan12TZ	-0.58	-0.49	-0.18	-0.5	-0.67	-0.5	-0.16	-0.77	-0.56	-0.35	-0.13	-0.58
Lan12TZ(f)	-0.59	-0.48	-0.18	-0.5	-0.67	-0.5	-0.16	-0.77	-0.57	6.75	-0.13	-0.58
DZVP(DFT orbital)	1.62	1.4	0.85	2.05	1.12	0.84	0.62	1.65	0.73	0.52	0.41	1.15
cc-pVDZ-PP	-	-	-	-	-	-	-	-	-0.61	-0.67	-0.16	-0.75
cc-pVTZ-PP	-0.74	-0.81	-0.29	-0.68	-0.58	-0.55	-0.21	-0.68	-0.26	-0.24	-0.08	-0.33
Def2-TZVP	0.59	0.49	0.23	0.53	0.36	0.21	0.14	0.39	0.43	0.23	0.17	0.51
Def2-TZVPP	0.23	0.21	0.08	0.22	0.08	0.05	0.03	0.09	0.16	0.07	0.04	0.2
Def2-QZVP	0.03	0.02	0.01	0.03	0.01	0.01	0.01	0.03	0.01	0	-0.01	0.02
Def2-QZVPP	0	0	0	0	0	0	0	0	0	0	0	0
6-311G(d)	-7.33	0.53	-3.12	-2.2	-3.59	1.33	-1.41	-2.02	-3.98	1.26	-1.53	-2.09
6-311+G(d)	-0.12	-0.11	-0.05	-0.14	-0.09	-0.05	-0.03	-0.15	0.01	7.94	0	0.02
Aug-cc-pVDZ	0.42	0.43	0.14	0.43	0.25	0.21	0.07	0.36	0.27	0.24	0.05	0.49
Aug-cc-pVTZ	-0.23	-0.18	-0.07	-0.24	-0.16	-0.1	-0.04	-0.25	-0.02	0	0	-0.03

Table S-23

Ag_2^{2-}	BP86				B3LYP				M06			
	$\Delta \text{NICS} (0)$		$\Delta \text{NICS} (1)$		$\Delta \text{NICS} (0)$		$\Delta \text{NICS} (1)$		$\Delta \text{NICS} (0)$		$\Delta \text{NICS} (1)$	
<i>Basis sets</i>	NICS_{iso}	NICS_z	NICS_{iso}	NICS_z	NICS_{iso}	NICS_z	NICS_{iso}	NICS_z	NICS_{iso}	NICS_z	NICS_{iso}	NICS_z
Aug-cc-pVDZ-PP	-0.06	0.02	-0.02	-0.07	-0.05	0.02	-0.01	-0.06	-0.03	0.02	-0.01	-0.06
Aug-cc-pVTZ-PP	-0.15	0.05	-0.05	-0.18	-0.11	0.07	-0.04	-0.15	-0.02	0.03	0.01	-0.05
Lan12DZ	0	0	0	0	0.3	-0.24	0.08	0.47	0.11	-0.13	0.03	0.16
Lan12TZ	0.3	-0.02	0.13	0.39	0.19	-0.08	0.07	0.3	0.13	-0.08	0.04	0.16
Lan12TZ(f)	0.26	-0.03	0.1	0.33	0.16	-0.07	0.06	0.26	-1.14	-0.07	0.03	0.14
DZVP(DFT orbital)	1.1	-0.82	0.51	1.83	0.93	-0.98	0.44	1.77	0.41	-0.71	0.19	1.05
cc-pVDZ-PP	0.16	0.01	0.07	0.22	0.11	-0.02	0.05	0.18	0.06	-0.01	0.03	0.12
cc-pVTZ-PP	0.06	-0.01	0.03	0.08	0.05	-0.02	0.02	0.06	0.03	-0.02	0.01	0.05
Def2-TZVP	0.31	0.02	0.13	0.44	0.24	-0.06	0.08	0.38	0.14	-0.03	0.06	0.25
Def2-TZVPP	0.2	-0.01	0.08	0.27	0.16	-0.05	0.06	0.26	0.06	-0.03	0.02	0.12
Def2-QZVP	0.01	0	0.01	0.01	0.01	-0.01	0	0.01	-0.01	0.01	0	0
Def2-QZVPP	0	0	0	0	0	0	0	0	0	0	0	0

Table S-24

Au_2^{2-}	BP86				B3LYP				M06			
	$\Delta \text{NICS} (0)$		$\Delta \text{NICS} (1)$		$\Delta \text{NICS} (0)$		$\Delta \text{NICS} (1)$		$\Delta \text{NICS} (0)$		$\Delta \text{NICS} (1)$	
<i>Basis sets</i>	NICS_{iso}	NICS_z	NICS_{iso}	NICS_z	NICS_{iso}	NICS_z	NICS_{iso}	NICS_z	NICS_{iso}	NICS_z	NICS_{iso}	NICS_z
Aug-cc-pVDZ-PP	-0.01	0	0	-0.01	0	0	0	0.01	-0.03	0.02	-0.01	-0.04
Aug-cc-pVTZ-PP	-0.13	-0.04	-0.06	-0.15	-0.1	-0.03	-0.04	-0.11	-0.05	0.04	-0.02	-0.07
Lan12DZ	1.37	0.46	0.65	1.32	1.21	0.3	0.59	1.23	0.46	0	0.23	0.45
Lan12TZ	-6.06	0.17	0.25	0.5	0.47	0.11	0.23	0.47	0.21	0	0.1	0.2
Lan12TZ(f)	0.17	0.04	0.08	0.17	0.16	0.02	0.08	0.16	0.02	0	0.01	0.02
cc-pVDZ-PP	0.33	0.09	0.16	0.32	0.28	0.04	0.13	0.29	0.11	-0.04	0.05	0.11
cc-pVTZ-PP	0	0	0	0.01	0.03	-0.01	0.01	0.03	0.01	0	0	0.01
Def2-TZVP	0.29	-0.03	0.12	0.29	0.26	-0.06	0.11	0.28	0.17	-0.09	0.07	0.17
Def2-TZVPP	0.12	-0.02	0.05	0.13	0.13	-0.05	0.05	0.14	0.07	-0.04	0.03	0.06
Def2-QZVP	0.01	0	0.01	0.01	0.02	-0.01	0.01	0.03	0.03	-0.02	0.01	0.02
Def2-QZVPP	0	0	0	0	0	0	0	0	0	0	0	0

Table S-25

Li₃⁺	BP86	B3LYP	M06
Lan2DZ	0.03	0.027	-0.007
DZVP(DFT orbital)	0.063	0.057	0.003
Def2-TZVP	0.044	0.044	0.007
Def2-TZVPP	0.022	0.018	-0.043
Def2-QZVP	0	-0.001	0
Def2-QZVPP	0	0	0
6-311G(d)	0.008	0.005	-0.055
6-311+G(d)	0.008	0.005	-0.059

Table S-26

Cu₃⁺	BP86	B3LYP	M06
Aug-cc-pVDZ-PP	-0.02	-0.029	-0.024
Aug-cc-pVTZ-PP	-0.03	-0.036	-0.029
Lan2DZ	0.017	0.002	-0.006
Lan2TZ	0.007	-0.01	-0.006
Lan2TZ(f)	0.007	-0.01	-0.007
DZVP(DFT orbital)	0.037	0.029	0.014
cc-pVDZ-PP	-0.035	-0.044	-0.035
cc-pVTZ-PP	-0.017	-0.025	-0.017
Def2-TZVP	0.018	0.014	0.01
Def2-TZVPP	0.015	0.012	0.009
Def2-QZVP	0.006	0.004	0.002
Def2-QZVPP	0.003	0.002	0.001
6-311G(d)	-0.048	-0.081	-0.08
6-311+G(d)	0.007	0.005	0.004
Aug-cc-pVDZ	0.021	0.017	0.012
Aug-cc-pVTZ	0	0	0
Aug-cc-pVQZ	0	0	0

Table S-27

Ag₃⁺	BP86	B3LYP	M06
Aug-cc-pVDZ-PP	0.003	0.004	0
Aug-cc-pVTZ-PP	-0.005	-0.003	-0.004
Lan2DZ	0.049	0.043	0.026
Lan2TZ	0.049	0.04	0.03
Lan2TZ(f)	0.047	0.04	0.03
DZVP(DFT orbital)	0.14	0.138	0.106
cc-pVDZ-PP	0.018	0.015	0.008
cc-pVTZ-PP	0.008	0.008	0.008
Def2-TZVP	0.028	0.024	0.014
Def2-TZVPP	0.018	0.015	0.01
Def2-QZVP	0.048	-0.045	0.002
Def2-QZVPP	0	0	0

Table S-28

Au₃⁺	BP86	B3LYP	M06
Aug-cc-pVDZ-PP	0.005	0.005	0.005
Aug-cc-pVTZ-PP	-0.01	-0.001	-0.002
Lan2DZ	0.046	0.042	0.032
Lan2TZ	0.032	0.027	0.025
Lan2TZ(f)	0.019	0.014	0.014
cc-pVDZ-PP	0.02	0.018	0.015
cc-pVTZ-PP	0.003	0.004	0.003
Def2-TZVP	0.016	0.014	0.011
Def2-TZVPP	0.005	0.004	0.003
Def2-QZVP	0.003	0.002	0.003
Def2-QZVPP	0	0	0

Table S-29

Sc_3^-	BP86	B3LYP	M06
Lan12DZ	0.007	0.006	-0.016
Lan12TZ	0.036	0.036	0.013
Lan12TZ(f)	0.035	0.033	0.01
Def2-TZVP	0.004	-0.001	-0.004
Def2-TZVPP	0.004	0.001	-0.002
Def2-QZVP	0.002	0.001	-0.004
Def2-QZVPP	0.003	0.001	-0.004
6-311G(d)	-0.078	-0.088	-0.075
6-311+G(d)	0.009	0.007	0.006
Aug-cc-pVDZ	0.006	0.006	0.002
Aug-cc-pVTZ	0.001	0	0
Aug-cc-pVQZ	0	0	0

Table S-30

Y_3^-	BP86	B3LYP	M06
Lan12DZ	0.005	0.003	0.004
Lan12TZ	0.017	0.019	0.017
Lan12TZ(f)	0.012	0.014	0.012
DZVP(DFT orbital)	0.003	0.007	0.024
Def2-TZVP	0.005	0.004	0
Def2-TZVPP	0.004	0.003	0
Def2-QZVP	0.002	0.001	0
Def2-QZVPP	0	0	0

Table S-31

La_3^-	BP86	B3LYP	M06
Lan12DZ	0.03	0.031	0.03
Lan12TZ	0.037	0.039	0.035
Lan12TZ(f)	0.014	0.019	0.014
Def2-TZVP	0.009	0.007	0.004
Def2-TZVPP	0.005	0.002	0
Def2-QZVP	0.001	0.001	0
Def2-QZVPP	0	0	0

Table S-32

Al_4^{2-}	BP86	B3LYP	M06
Lan12DZ	0.082	0.081	0.109
DZVP(DFT orbital)	0.019	0.019	0.015
Def2-TZVP	-0.003	-0.005	-0.01
Def2-TZVPP	-0.003	-0.006	-0.011
Def2-QZVP	0	0	0
Def2-QZVPP	0	0	0
6-311G(d)	0.012	0.012	0.008
6-311+G(d)	0.012	0.014	0.015

Table S-33

Ga²⁺	BP86	B3LYP	M06
Aug-cc-pVDZ-PP	0.038	0.036	0.024
Aug-cc-pVTZ-PP	0.019	0.02	0.02
Lan2DZ	0.105	0.09	0.07
DZVP(DFT orbital)	0.025	0.021	0.015
cc-pVDZ-PP	0.023	0.016	0
cc-pVTZ-PP	0.01	0.005	0.004
Def2-TZVP	-0.006	-0.009	-0.024
Def2-TZVPP	-0.006	-0.009	-0.024
Def2-QZVP	0	0	0.001
Def2-QZVPP	0	0	0
6-311G(d)	0.013	0.012	0.016
6-311+G(d)	0.019	0.022	0.022

Table S-34

Cu²⁺	BP86	B3LYP	M06
Aug-cc-pVDZ-PP	-0.03	-0.044	-0.023
Aug-cc-pVTZ-PP	-0.041	-0.053	-
Lan2DZ	0.005	-0.013	-0.017
Lan2TZ	-0.024	-0.045	-0.035
Lan2TZ(f)	-0.024	-0.045	-0.035
DZVP(DFT orbital)	0.095	0.09	0.062
cc-pVDZ-PP	-	-	-0.036
cc-pVTZ-PP	-0.024	-0.031	-0.016
Def2-TZVP	0.025	0.023	0.031
Def2-TZVPP	0.011	0.006	0.013
Def2-QZVP	0.002	0.001	0.001
Def2-QZVPP	0	0	0
6-311G(d)	-0.119	-0.147	-0.145
6-311+G(d)	-0.007	-0.01	0.002
Aug-cc-pVDZ	0.02	0.02	0.028
Aug-cc-pVTZ-PP	-0.013	-0.016	-0.004

Table S-35

Ag²⁺	BP86	B3LYP	M06
Aug-cc-pVDZ-PP	-0.006	-0.006	-0.006
Aug-cc-pVTZ-PP	-0.015	-0.016	-0.005
Lan2DZ	0.05	0.047	0.019
Lan2TZ	0.028	0.025	0.016
Lan2TZ(f)	0.025	0.023	0.014
DZVP(DFT orbital)	0.157	0.175	0.104
cc-pVDZ-PP	0.014	0.015	0.009
cc-pVTZ-PP	0.006	0.005	0.004
Def2-TZVP	0.03	0.032	0.02
Def2-TZVPP	0.02	0.022	0.01
Def2-QZVP	0.001	0	-0.001
Def2-QZVPP	0	0	0

Table S-36

Au₄²⁺	BP86	B3LYP	M06
Aug-cc-pVDZ-PP	0	0.001	-0.002
Aug-cc-pVTZ-PP	-0.007	-0.006	-0.005
Lan12DZ	0.067	0.069	0.032
Lan12TZ	0.026	0.026	0.015
Lan12TZ(f)	0.01	0.01	0.002
cc-pVDZ-PP	0.017	0.017	0.009
cc-pVTZ-PP	0.001	0.003	0.001
Def2-TZVP	0.018	0.019	0.015
Def2-TZVPP	0.008	0.01	0.006
Def2-QZVP	0.001	0.002	0.003
Def2-QZVPP	0	0	0

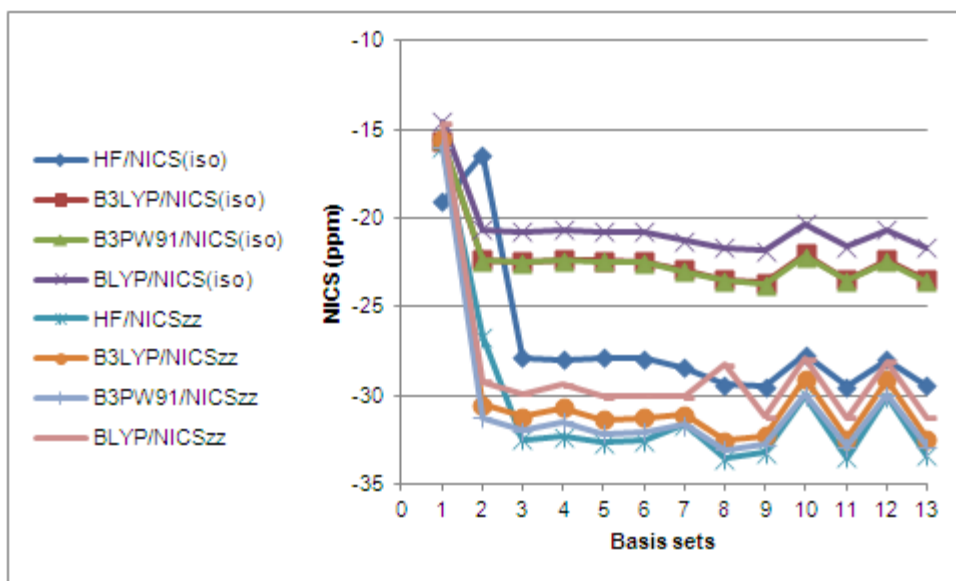


Figure S-1A

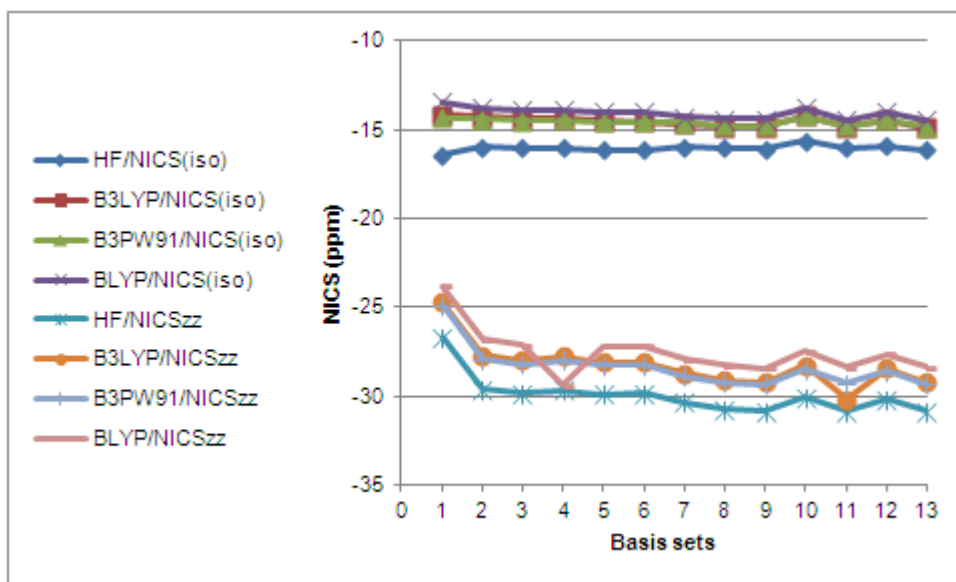


Figure S-1B

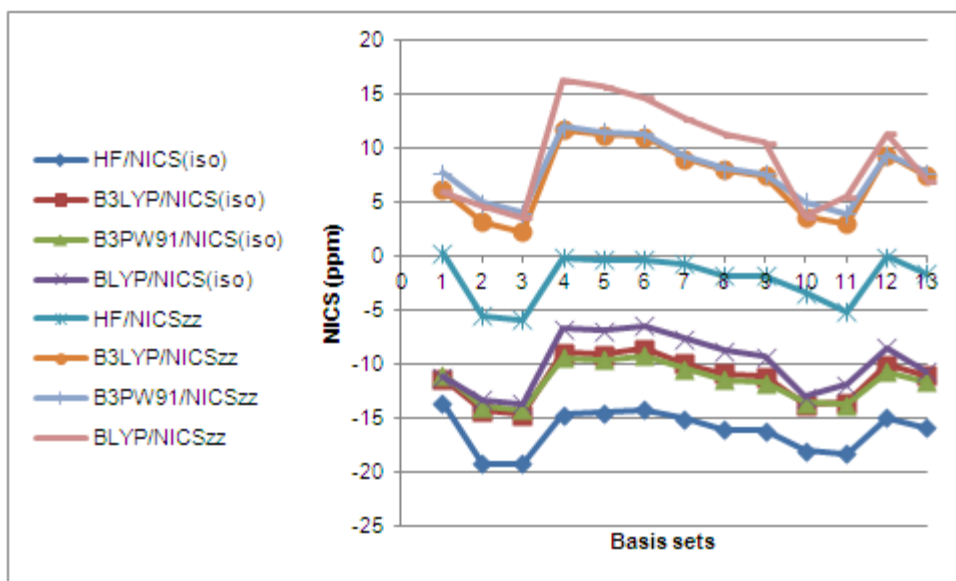


Figure S-2A

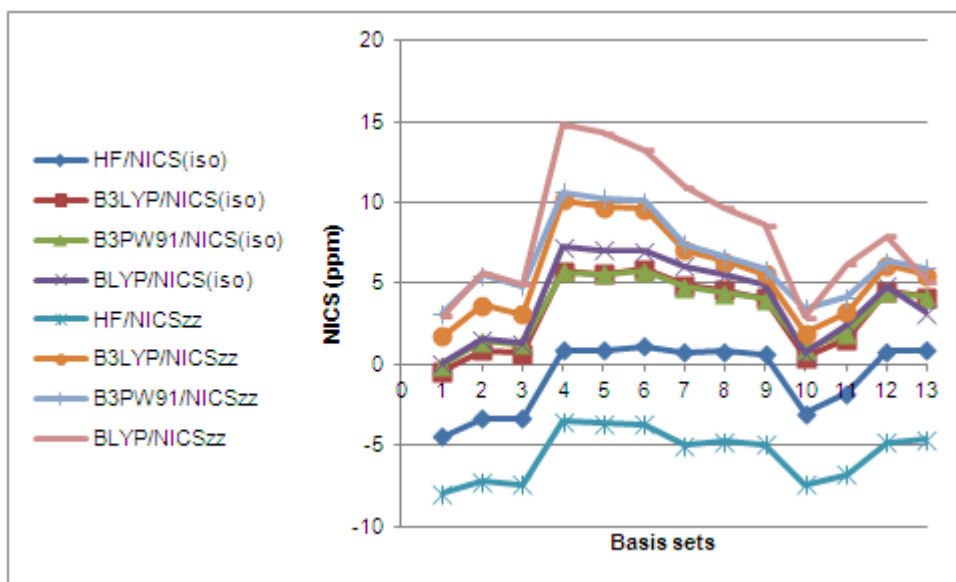


Figure S-2B

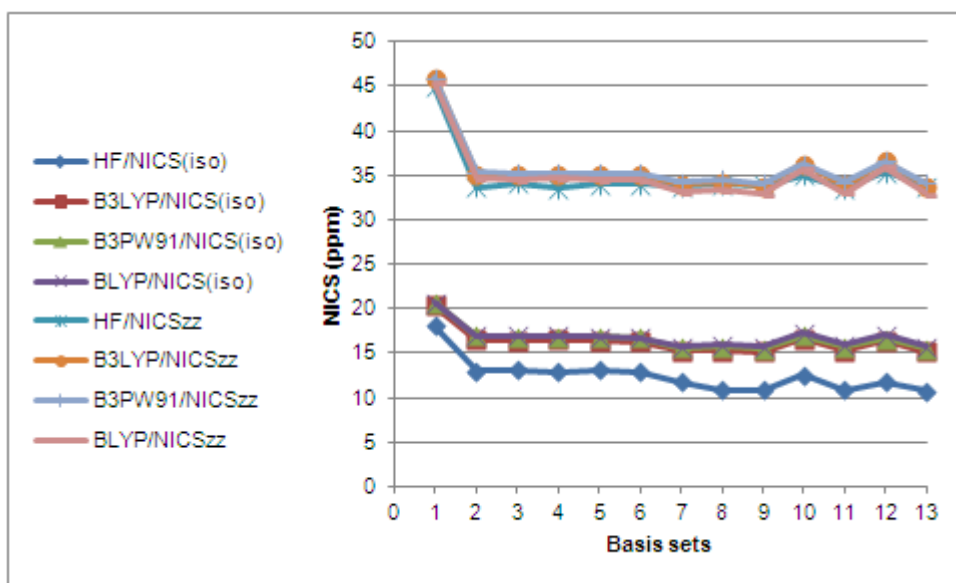


Figure S-3A

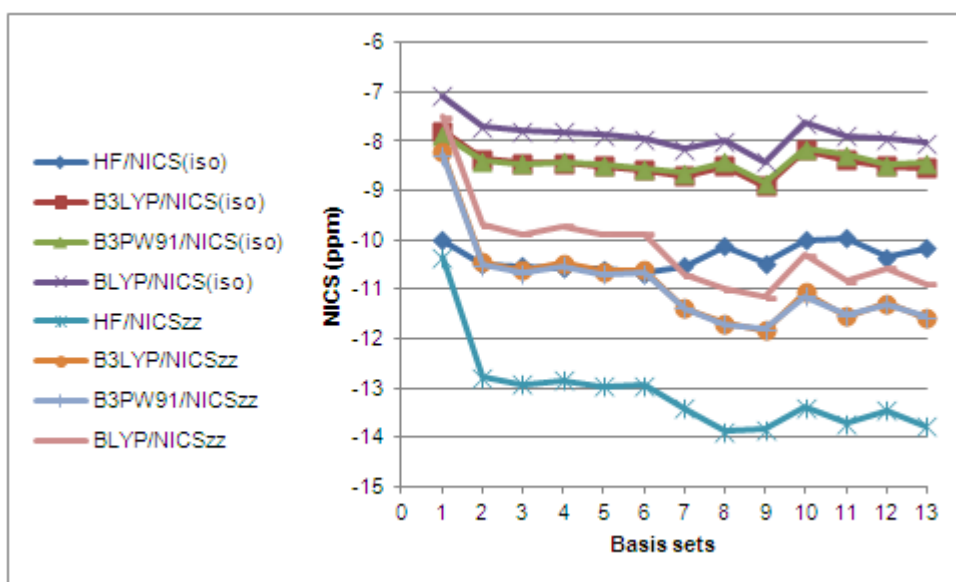


Figure S-3B

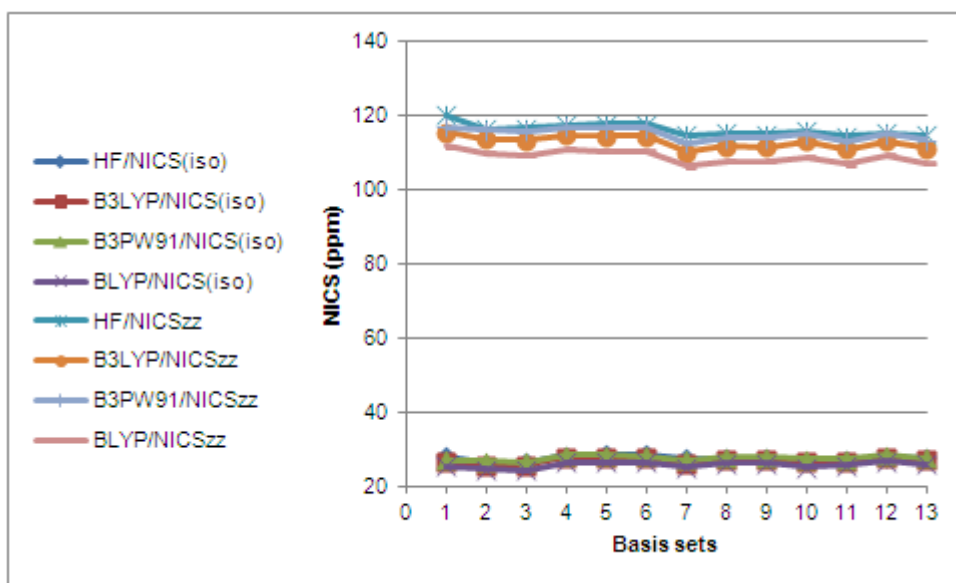


Figure S-4A

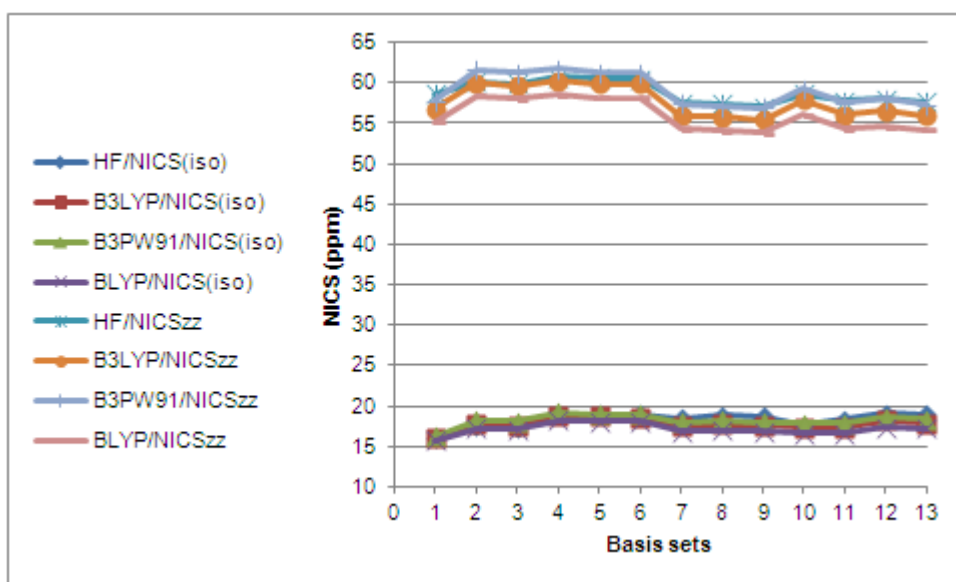


Figure S-4B

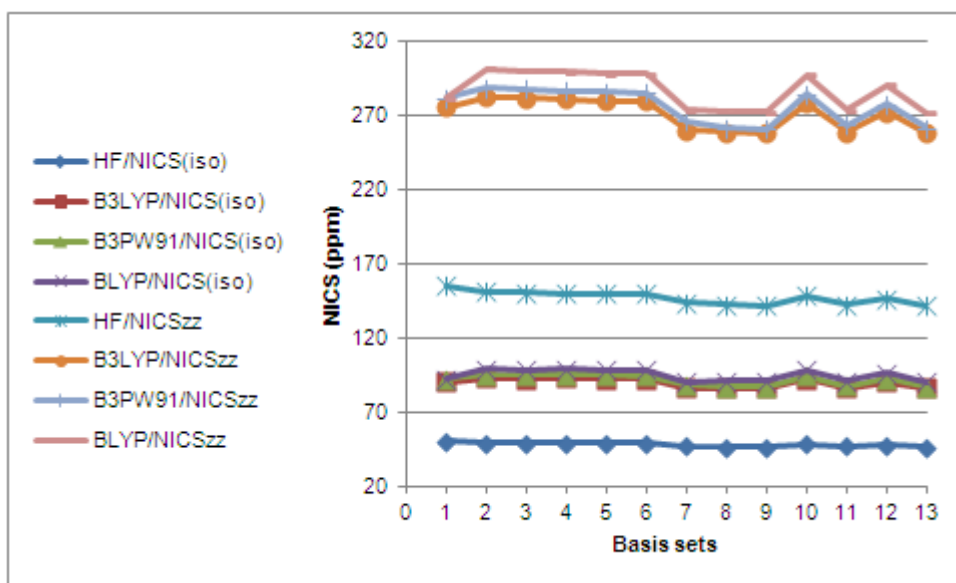


Figure S-5A

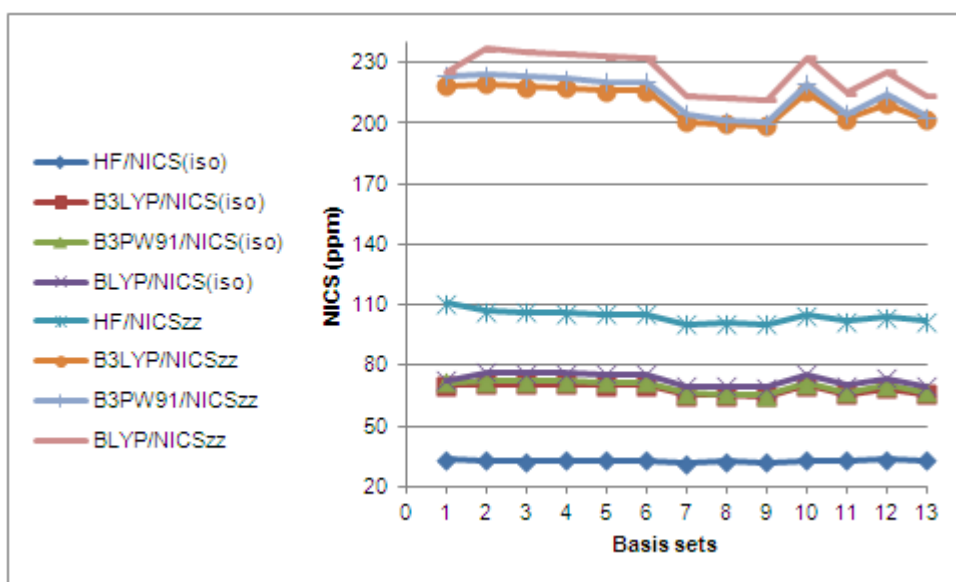


Figure S-5B

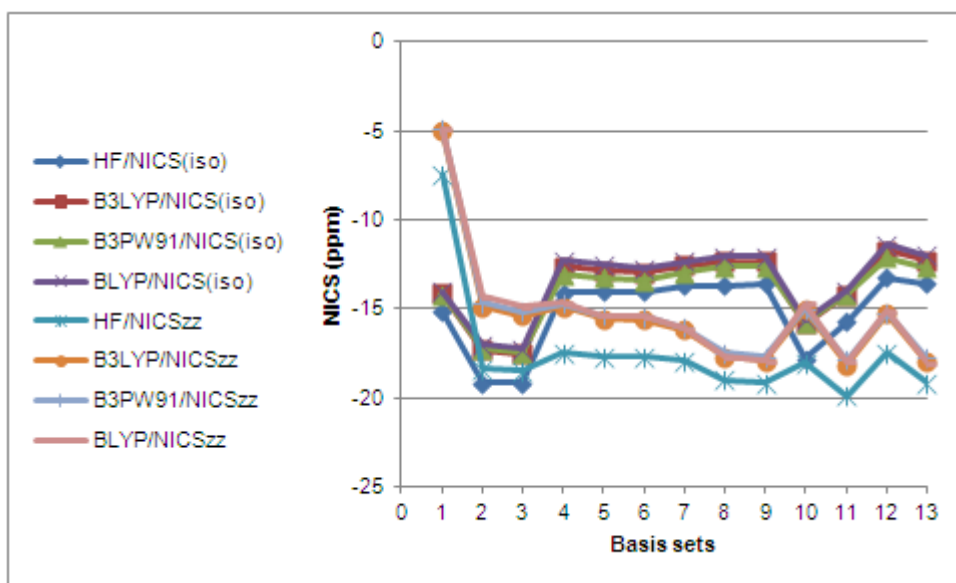


Figure S-6A

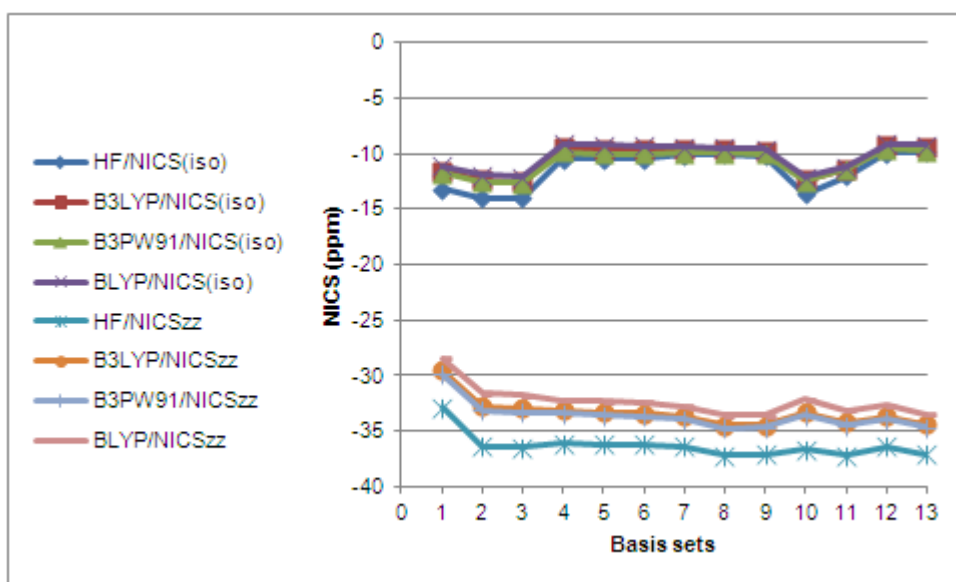


Figure S-6B

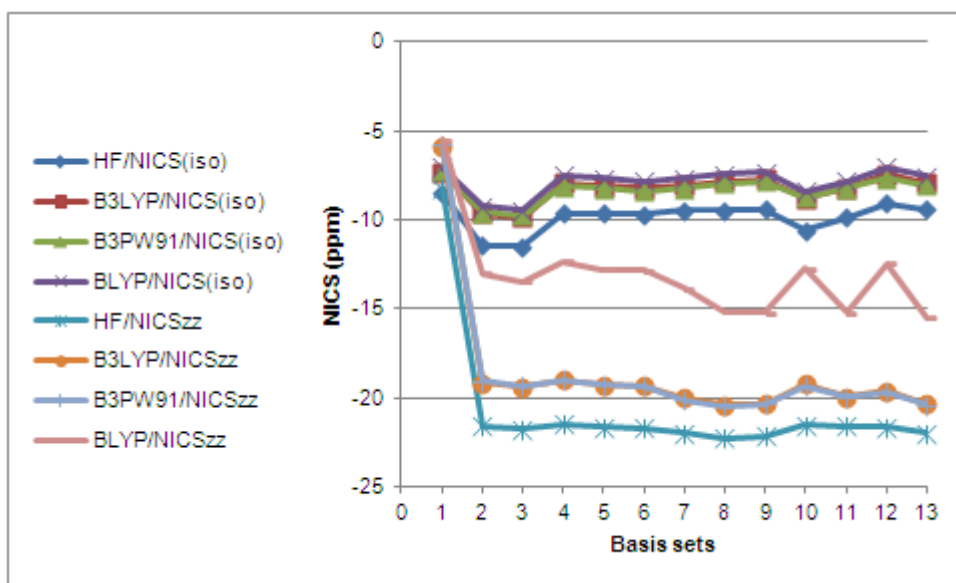


Figure S-7A

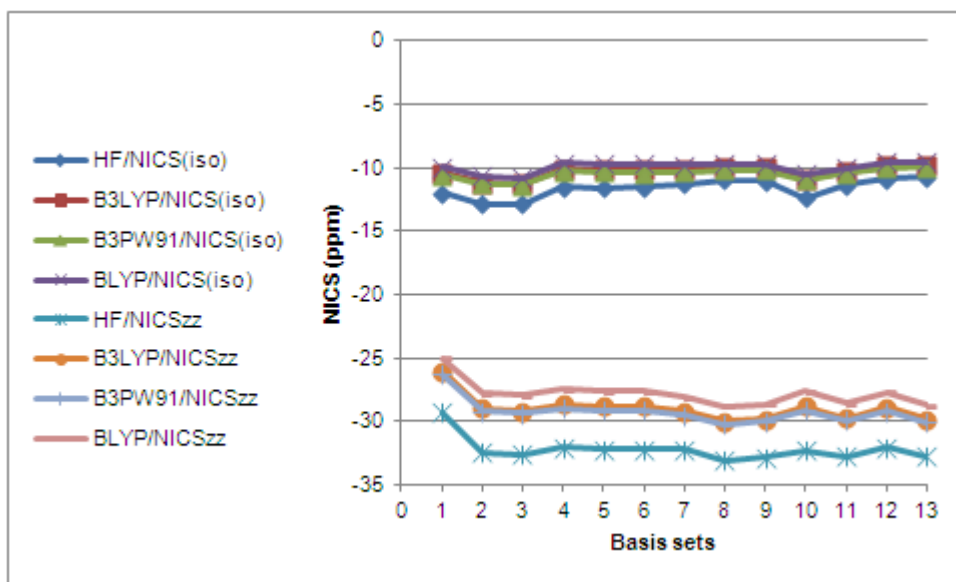


Figure S-7B

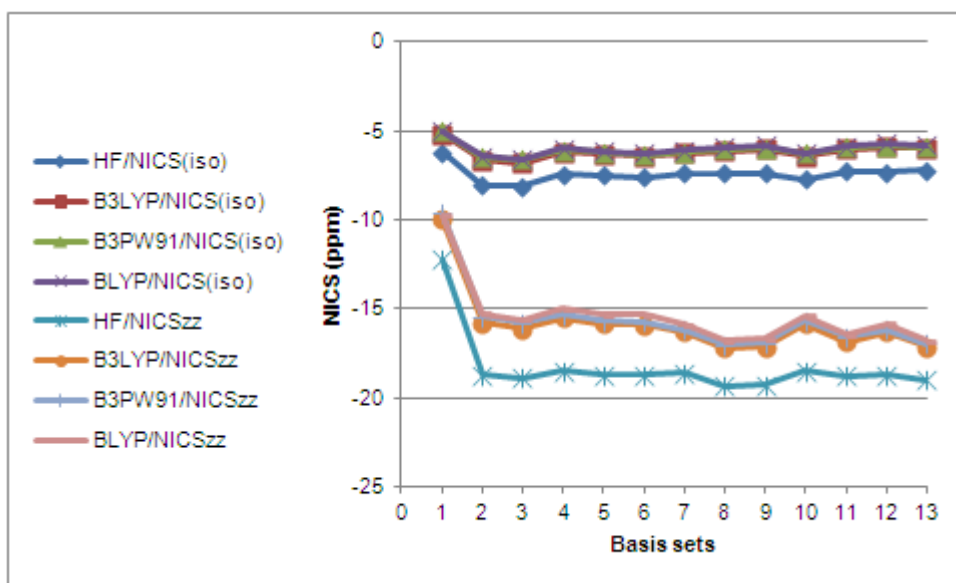


Figure S-8A

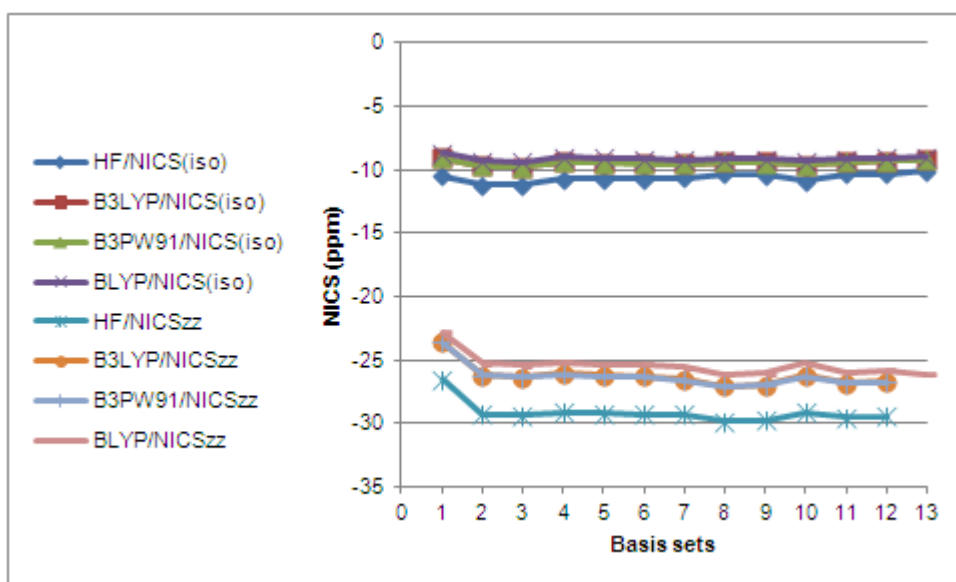


Figure S-8B

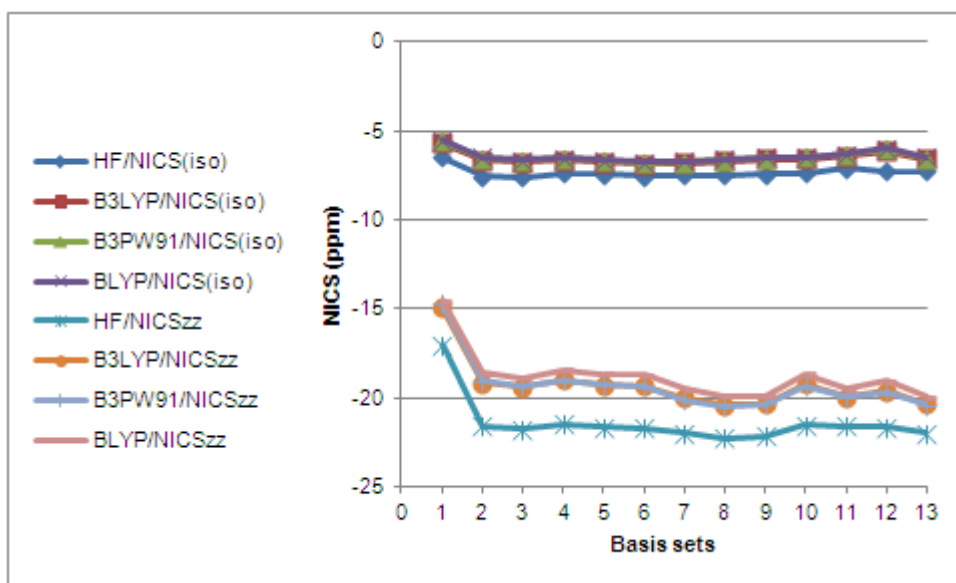


Figure S-9A

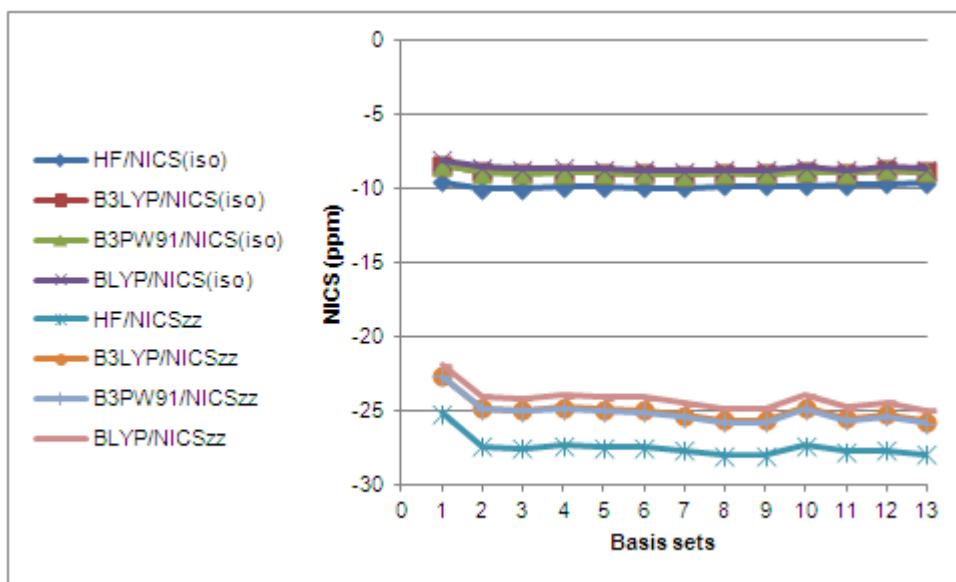


Figure S-9B

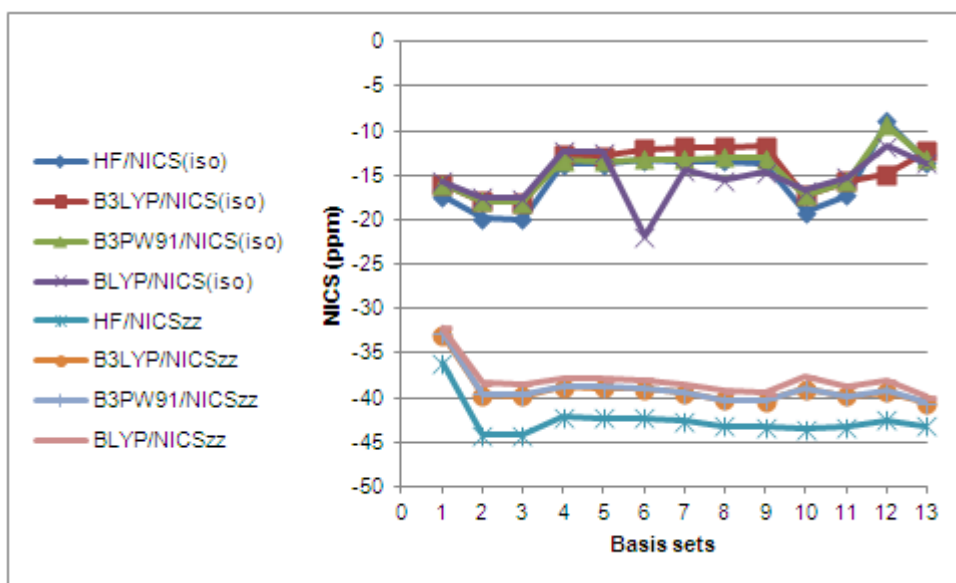


Figure S-10A

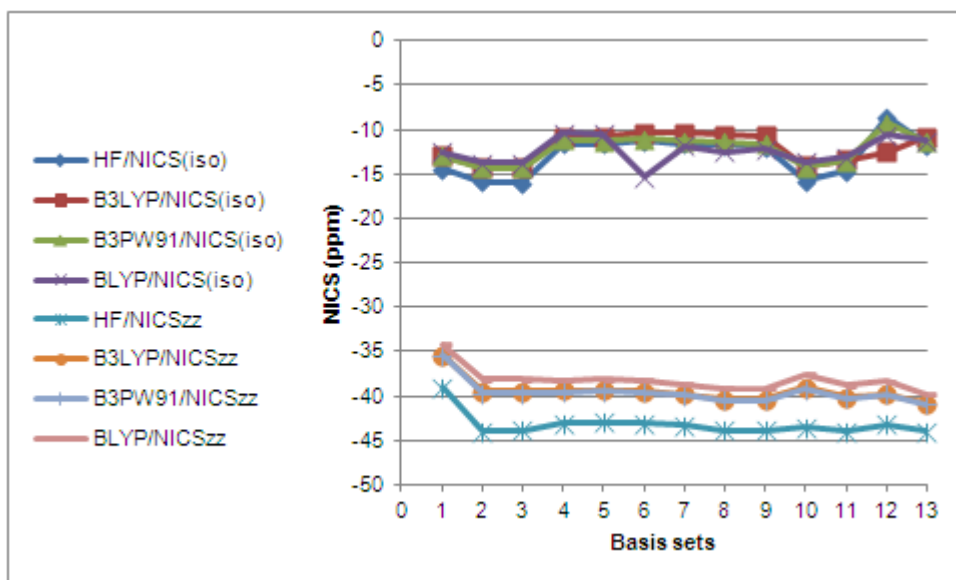


Figure S-10B

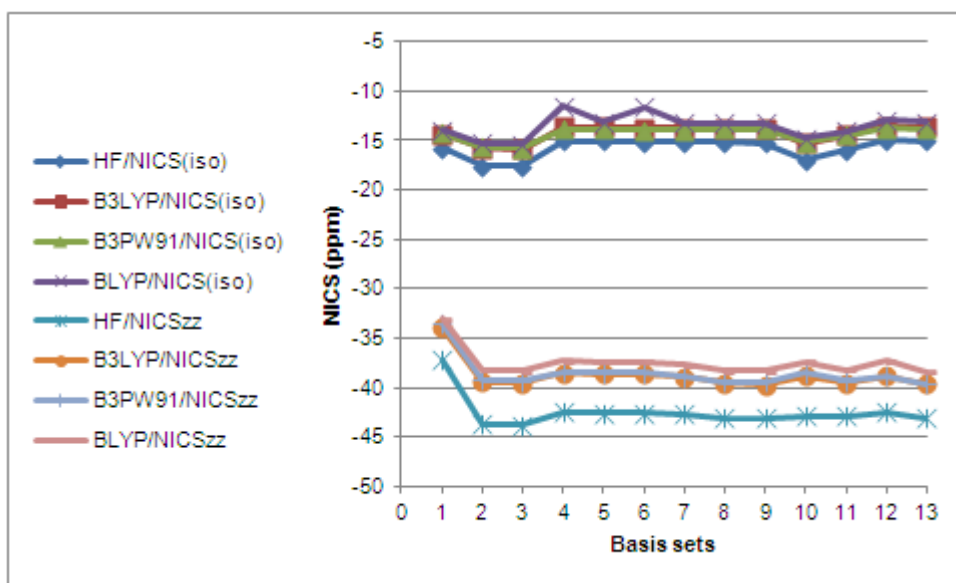


Figure S-11A

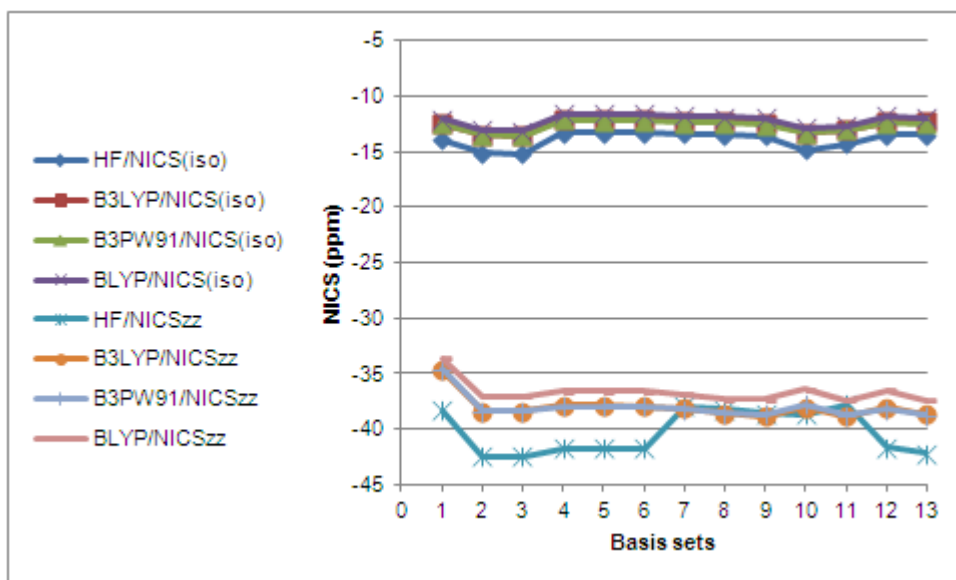


Figure S-11B

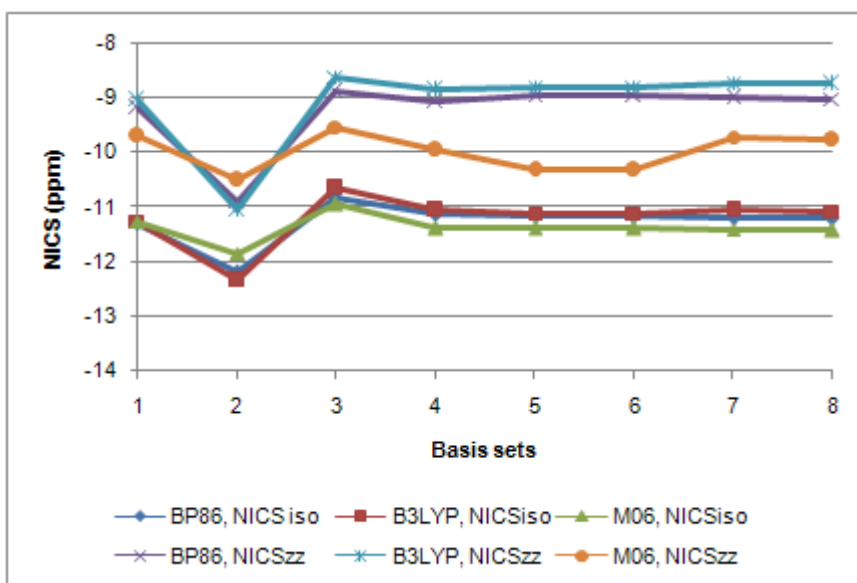


Figure S-12A

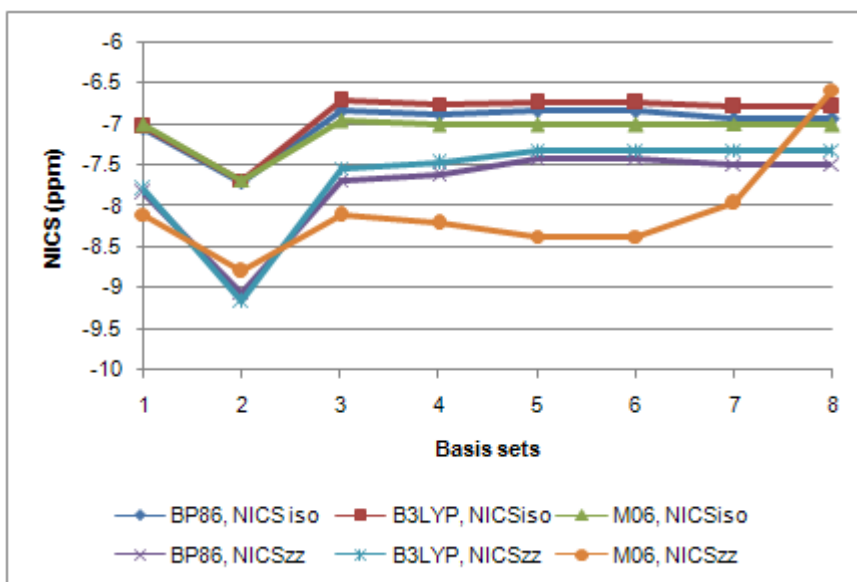


Figure S-12B

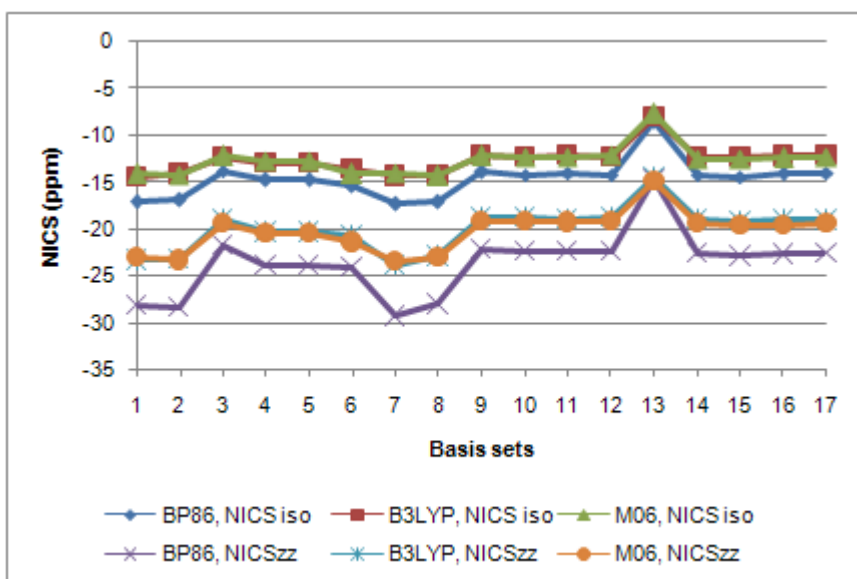


Figure S-13

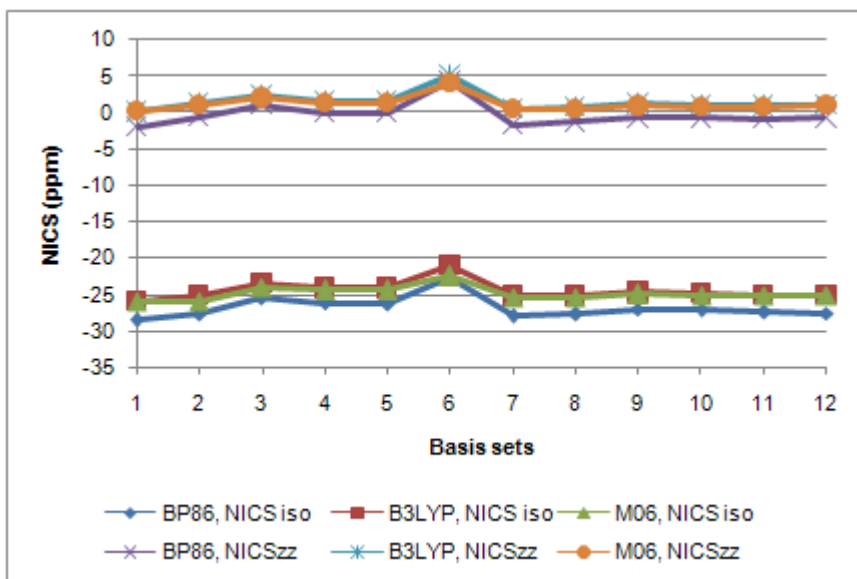


Figure S-14A

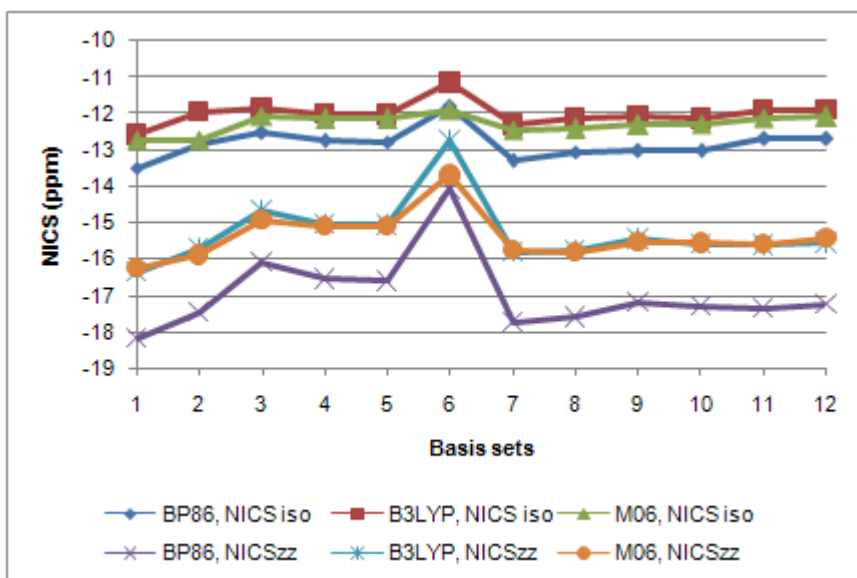


Figure S-14B

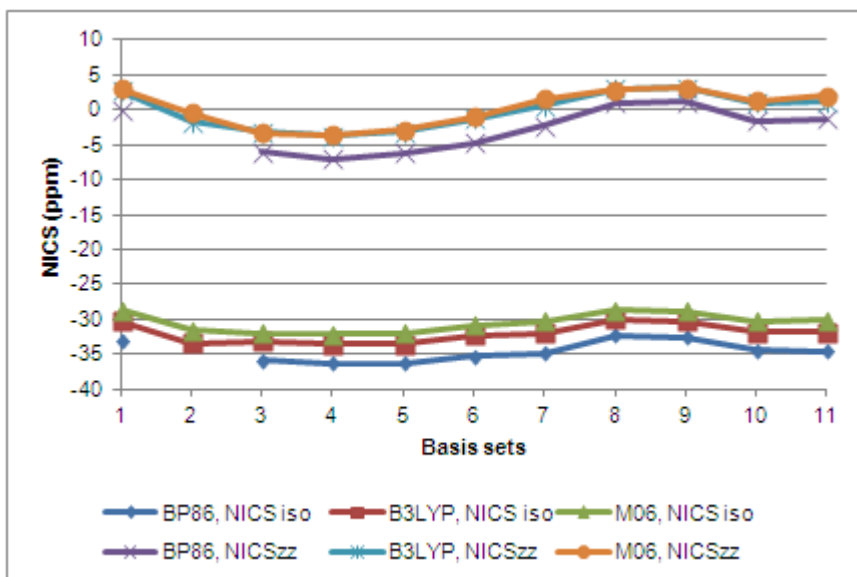


Figure S-15A

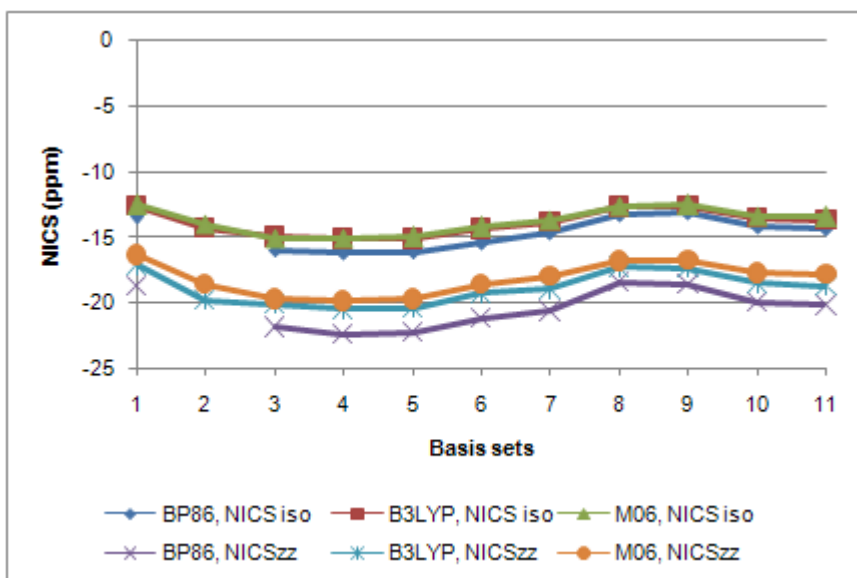


Figure S-15B

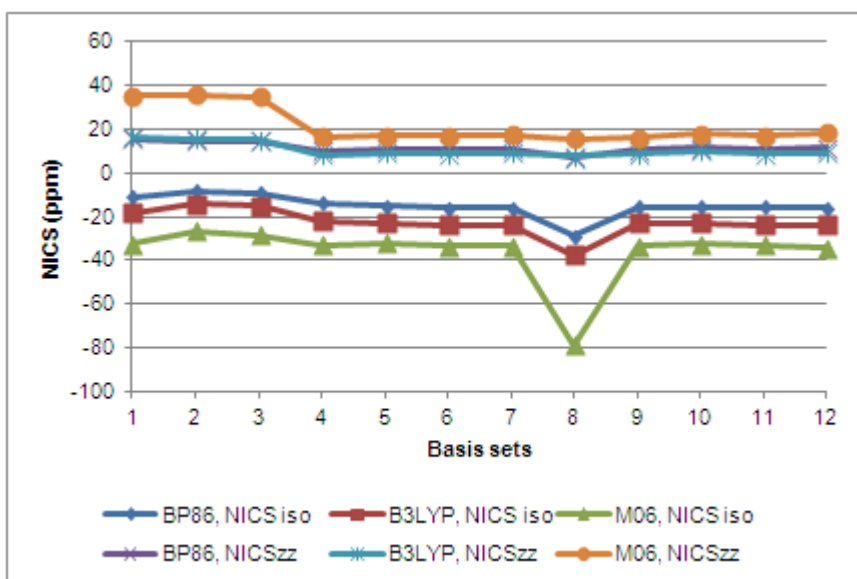


Figure S-16

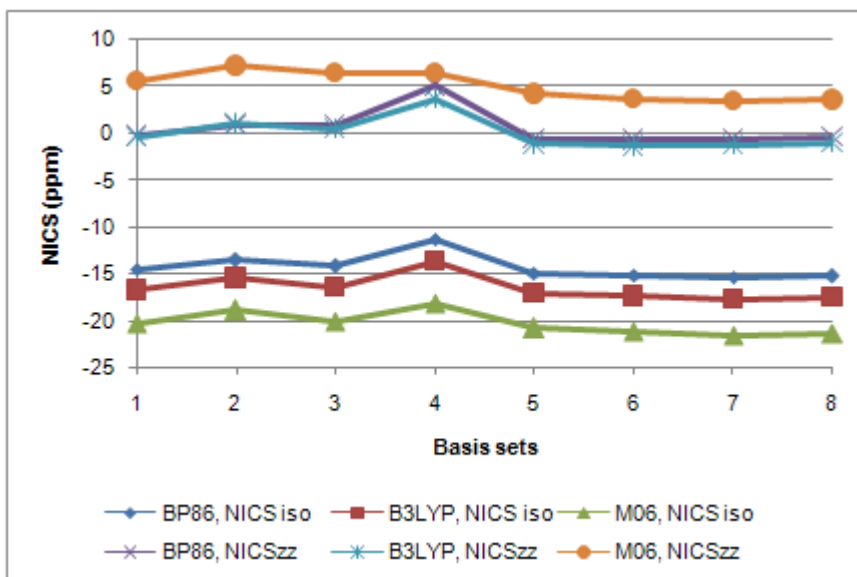


Figure S-17

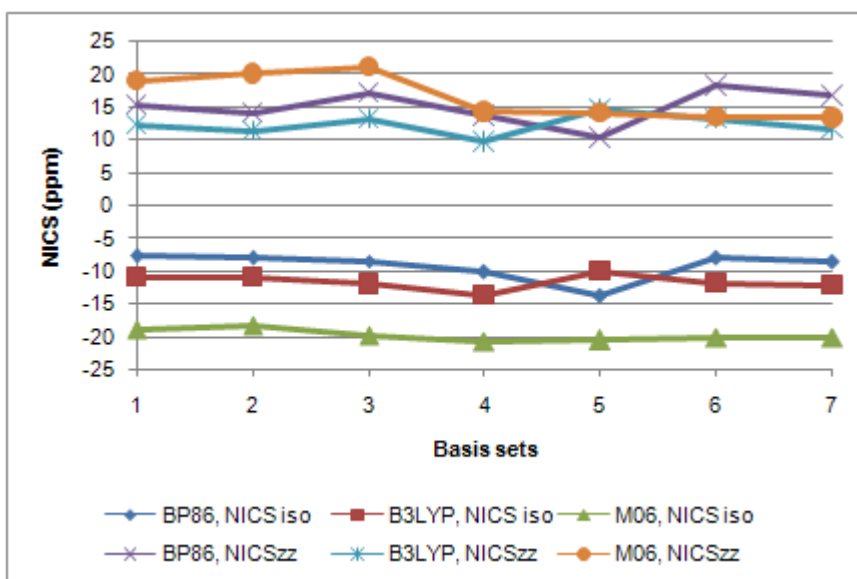


Figure S-18

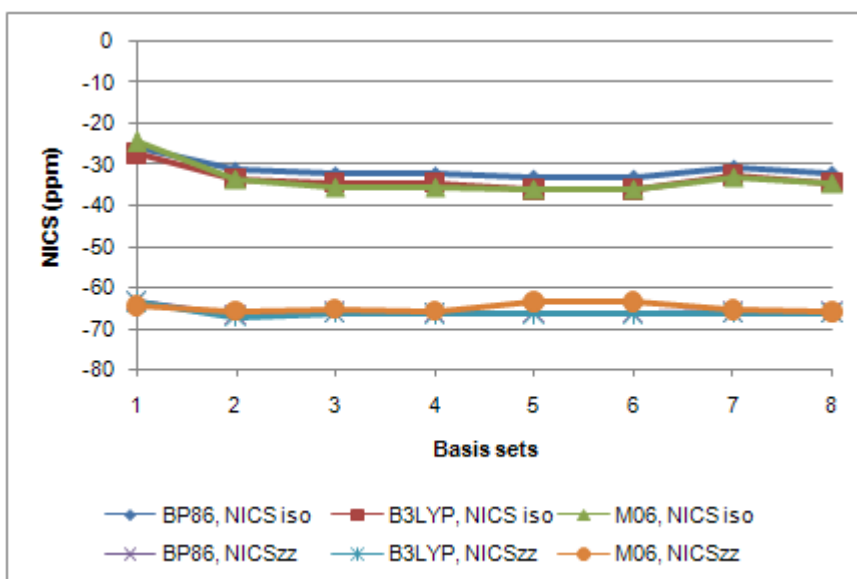


Figure S-19A

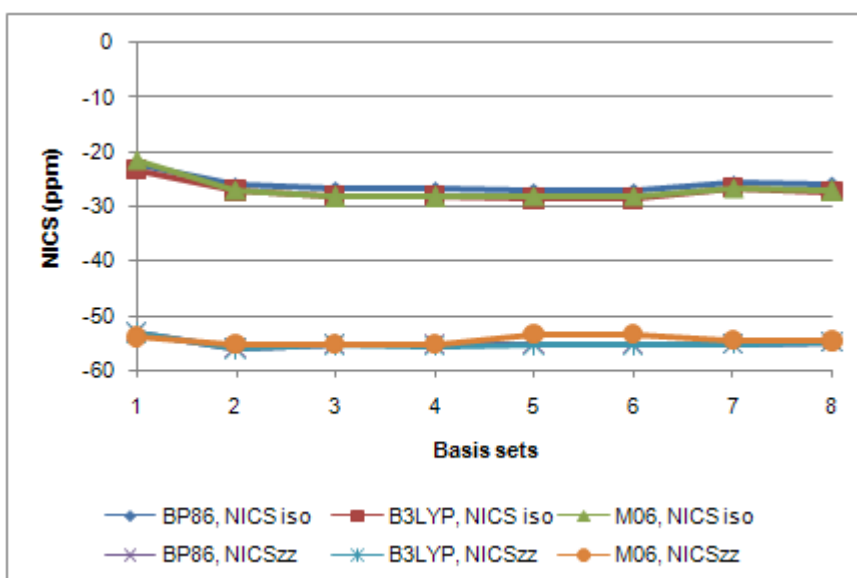


Figure S-19B

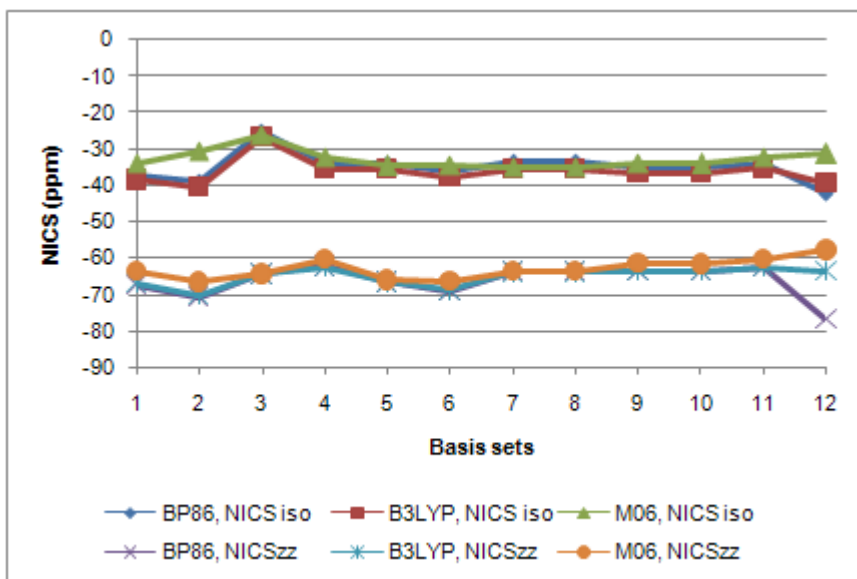


Figure S-20A

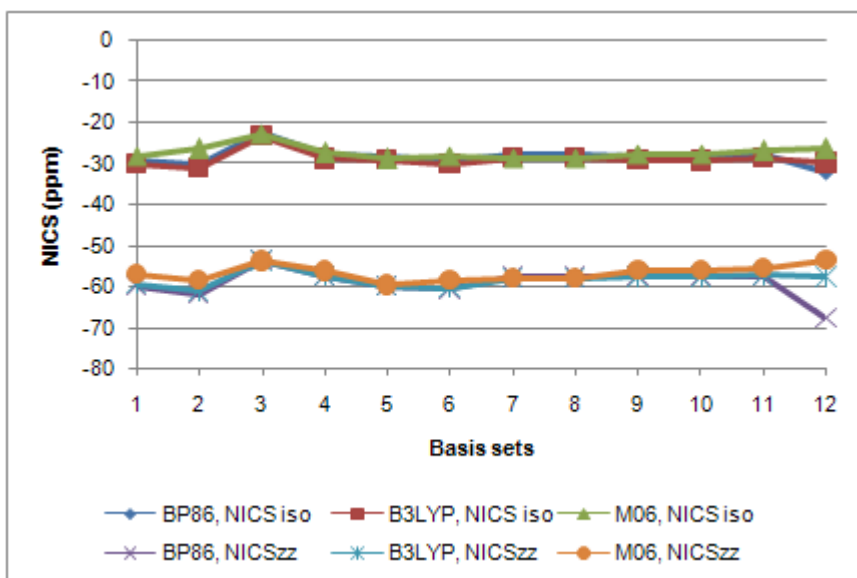


Figure S-20B

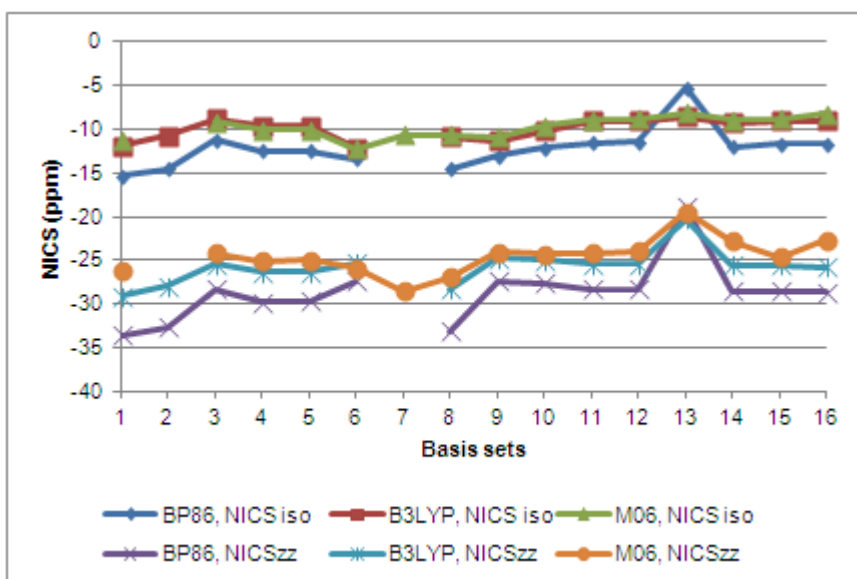


Figure S-21

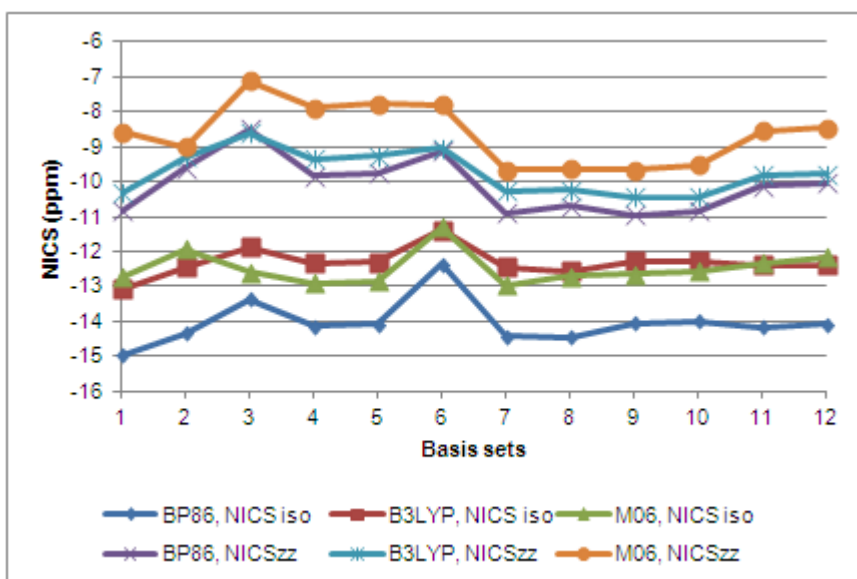


Figure S-22A

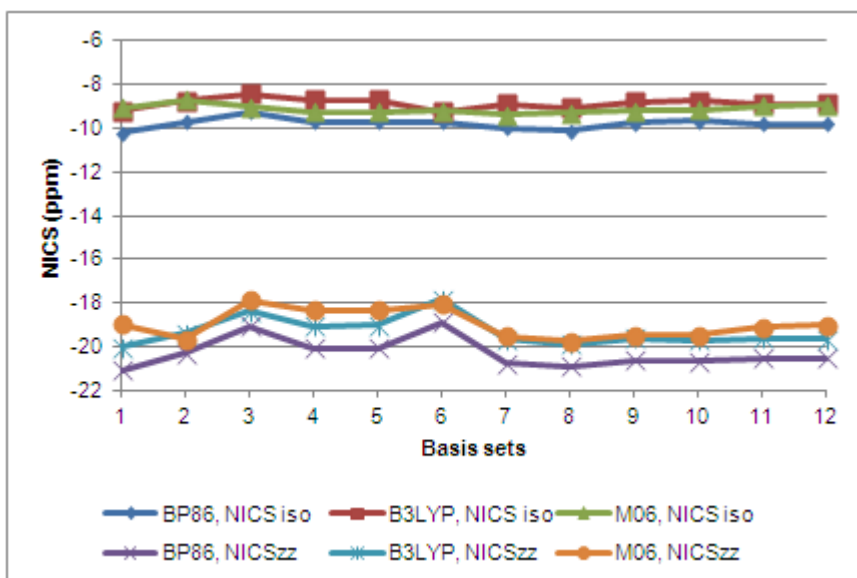


Figure S-22B

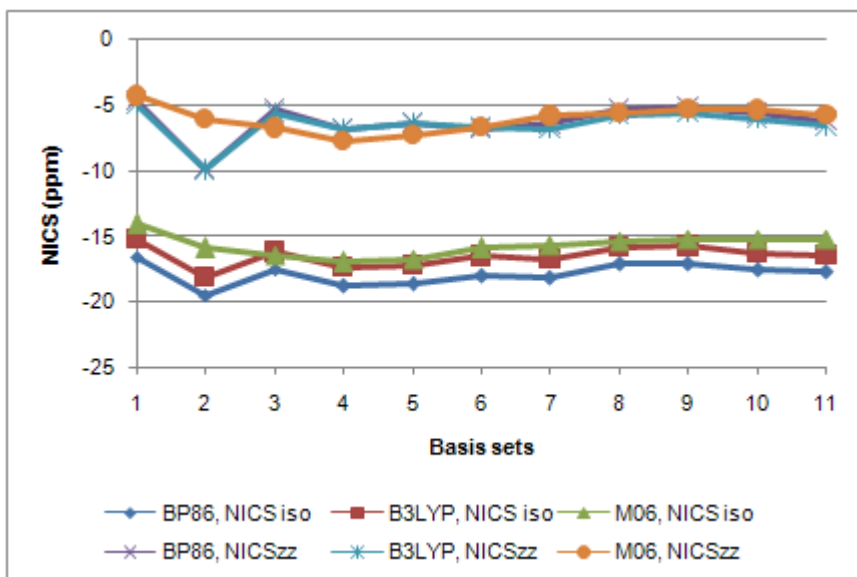


Figure S-23A

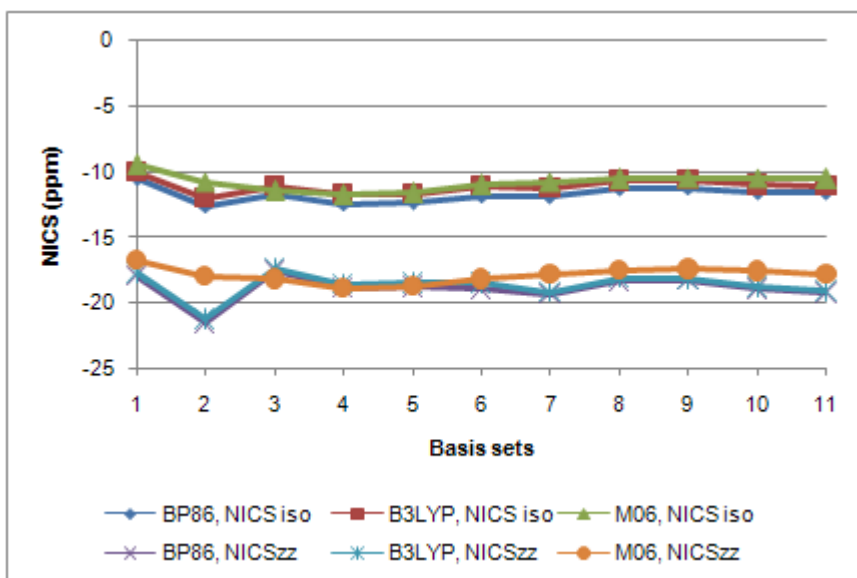


Figure S-23B

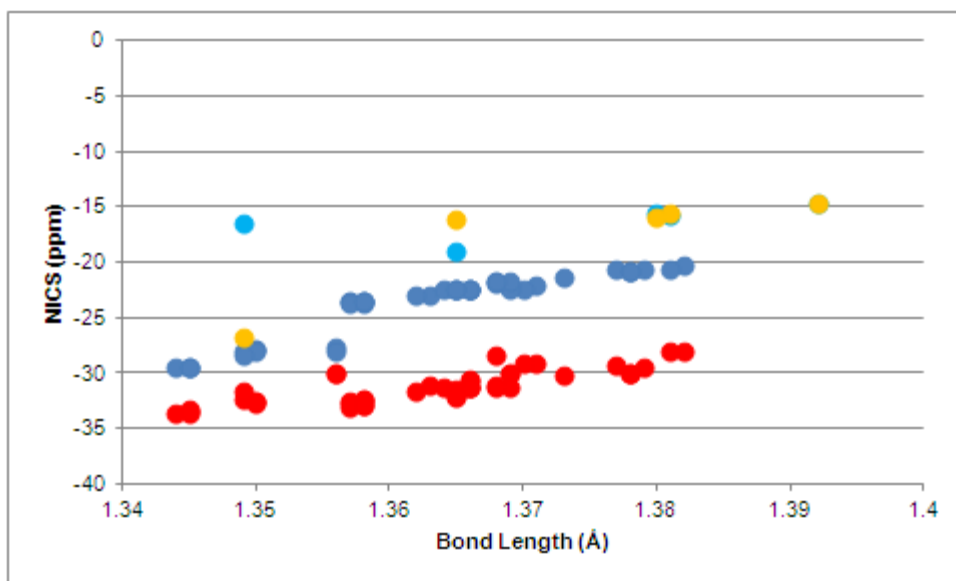


Figure S-24

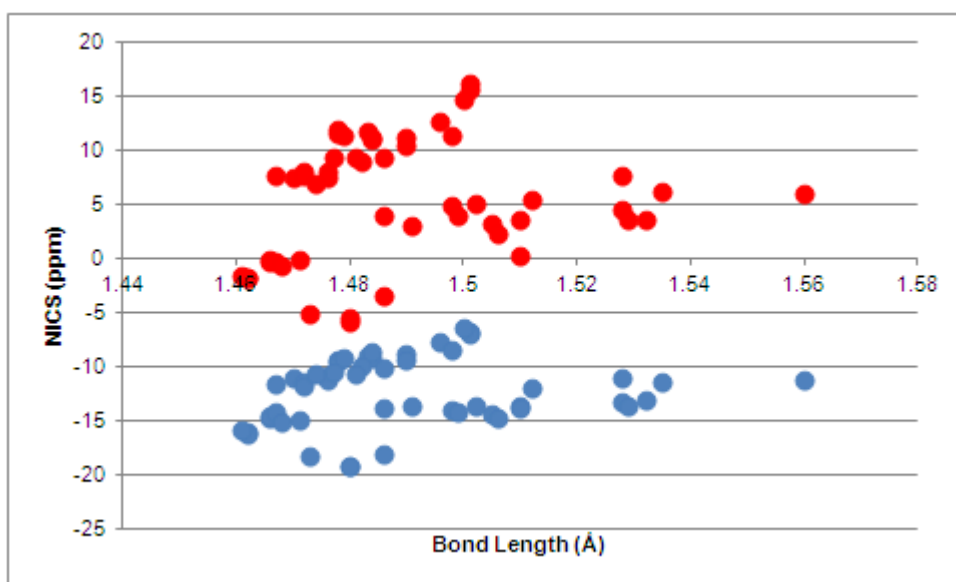


Figure S-25

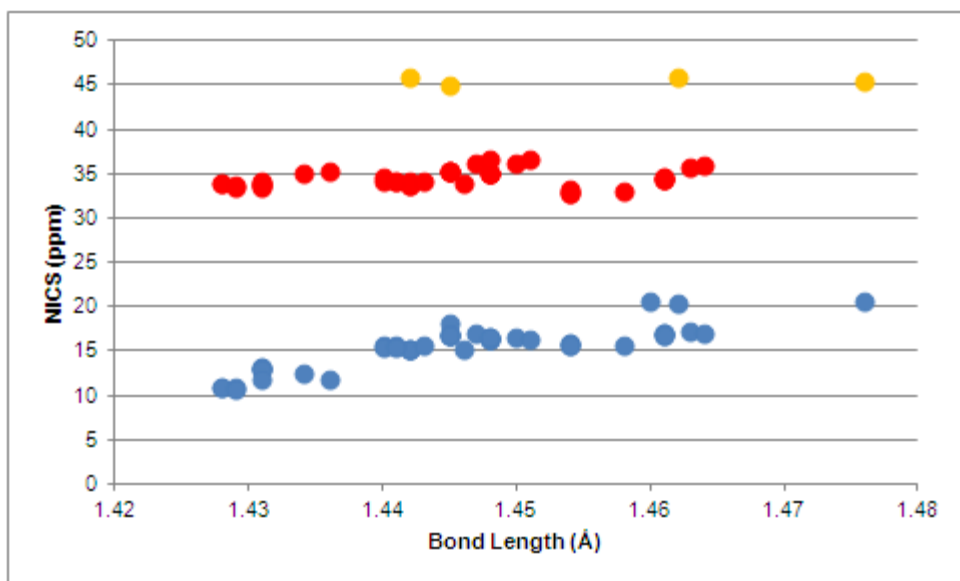


Figure S-26

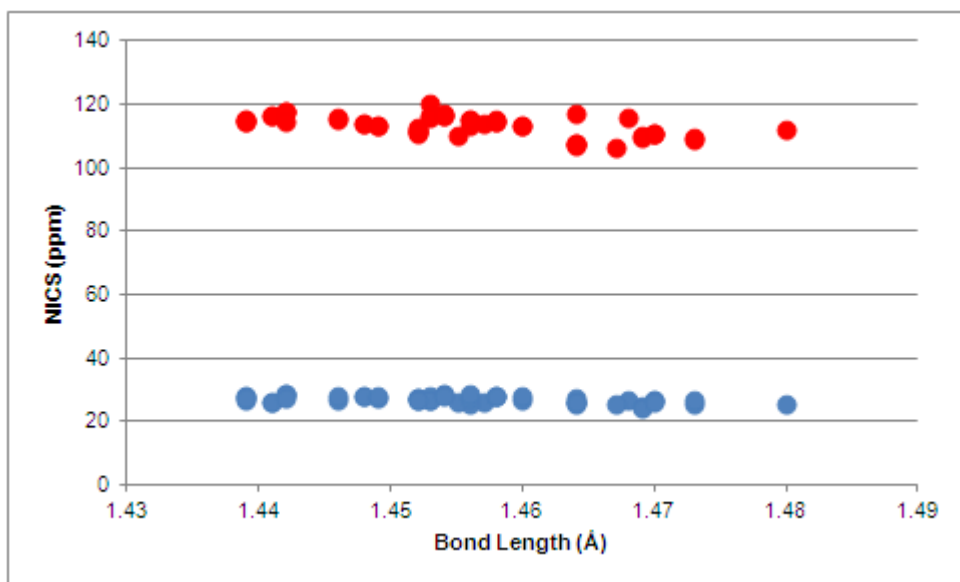


Figure S-27

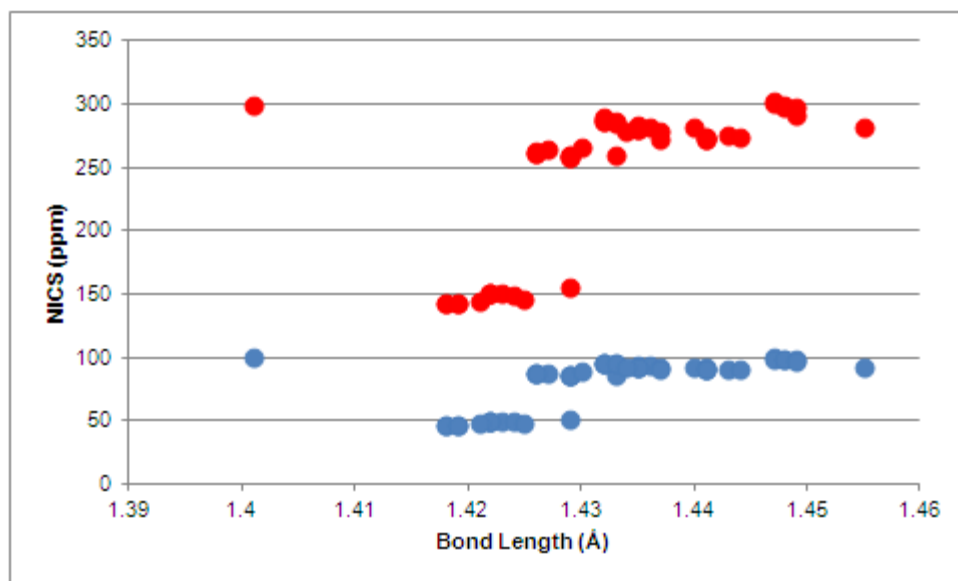


Figure S-28

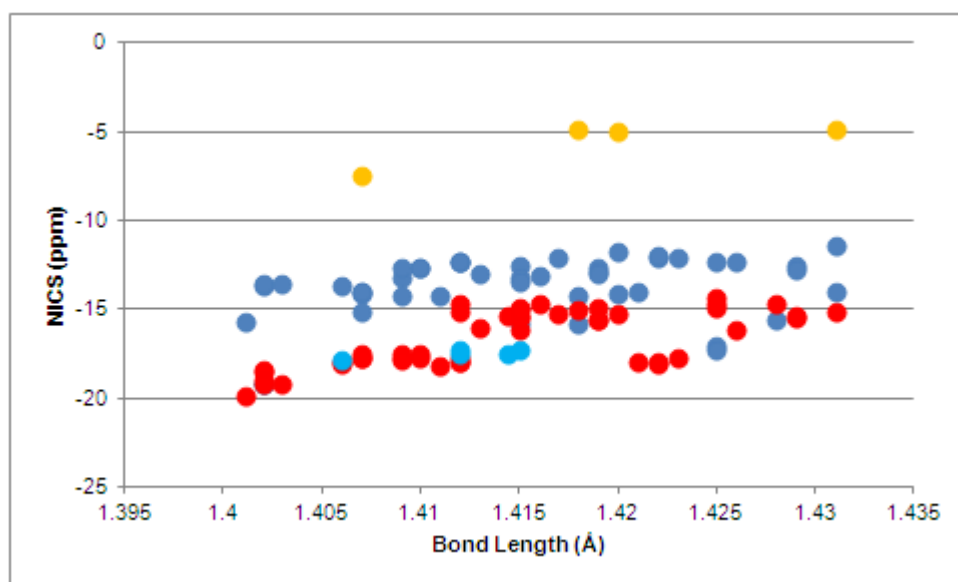


Figure S-29

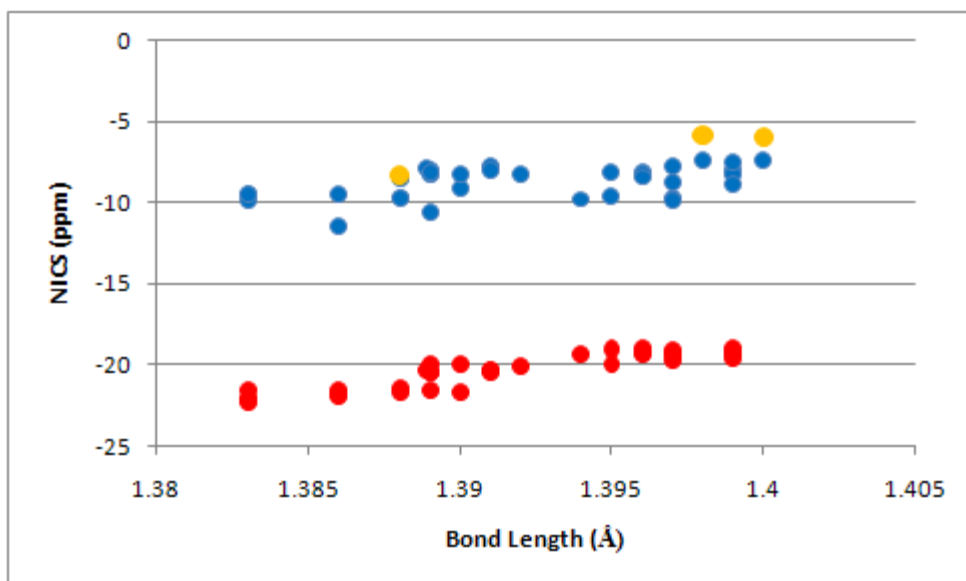


Figure S-30

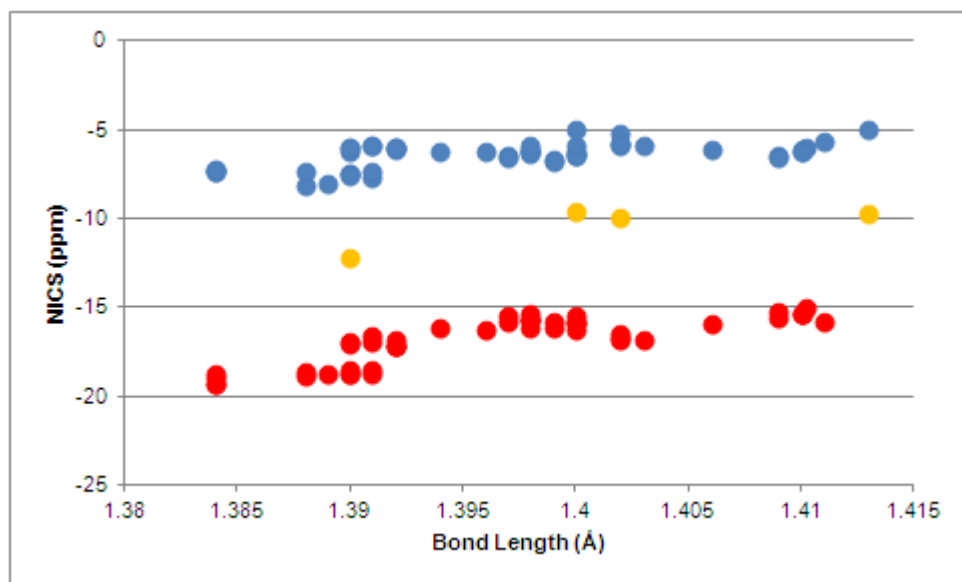


Figure S-31

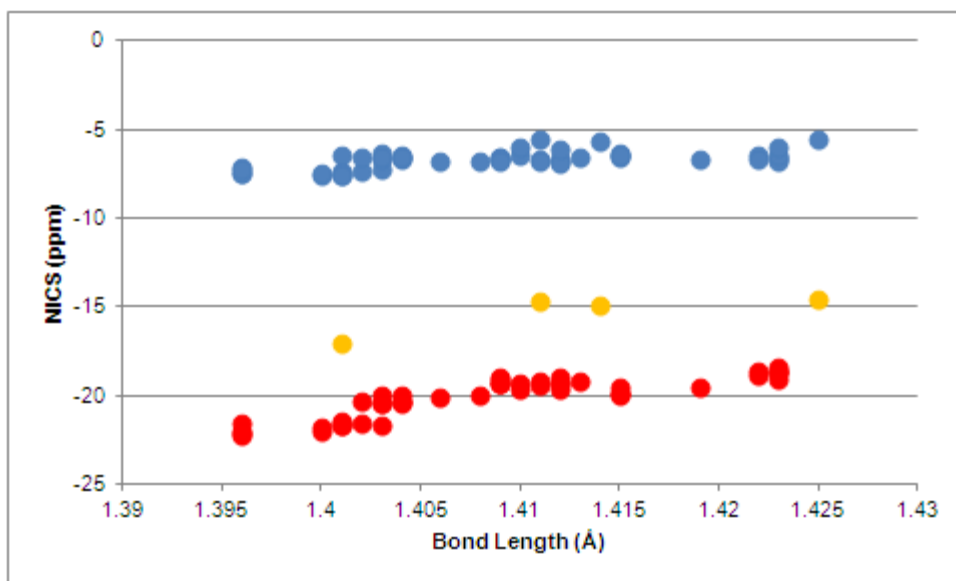


Figure S-32

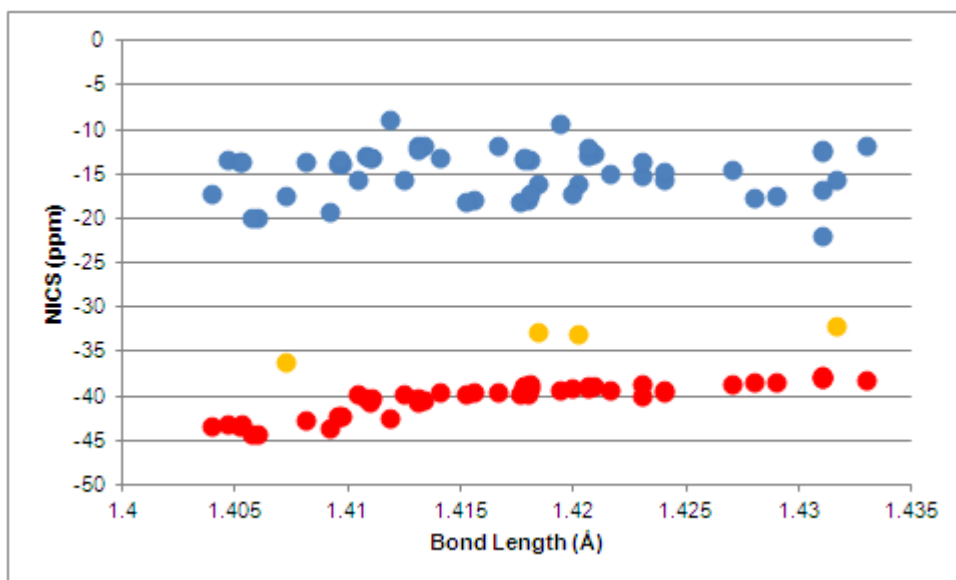


Figure S-33

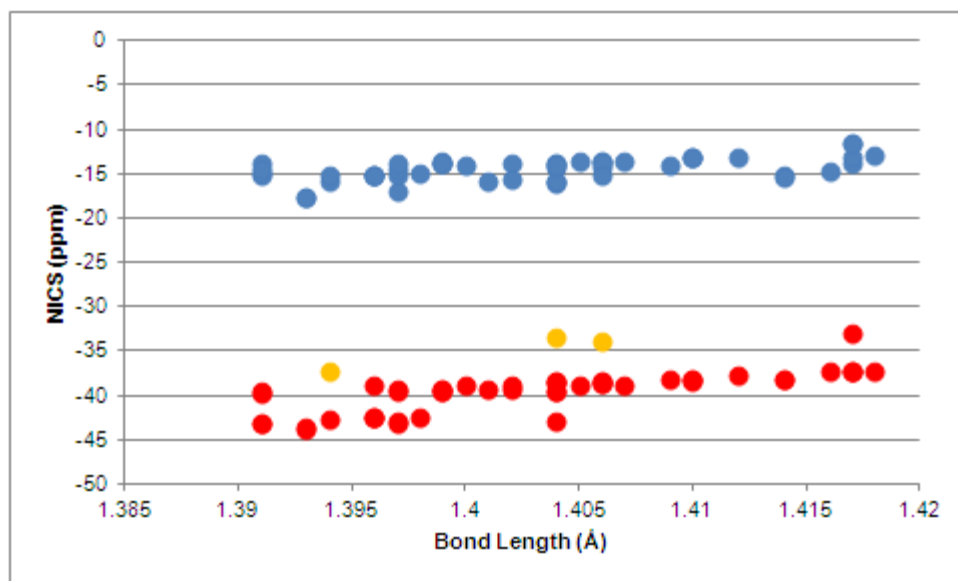


Figure S-34

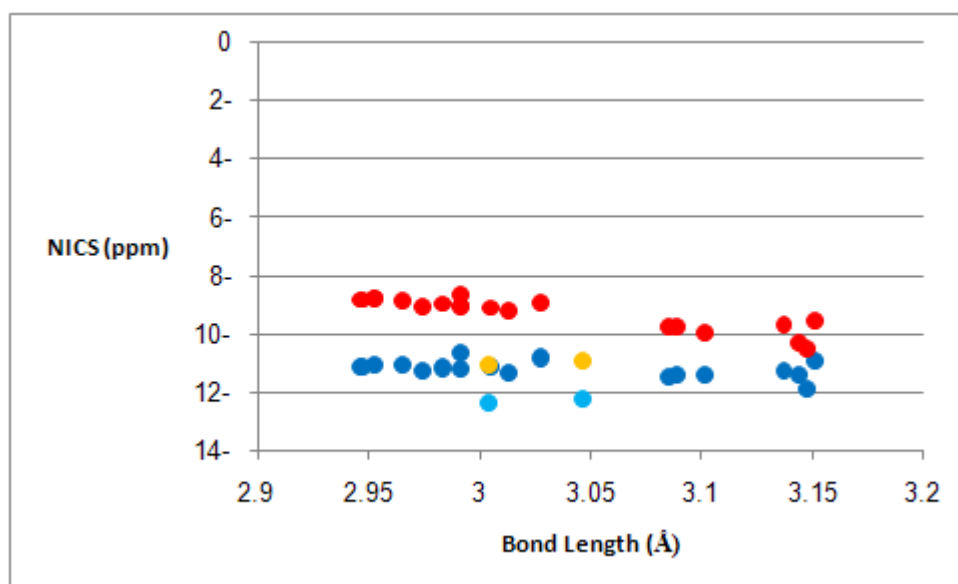


Figure S-35

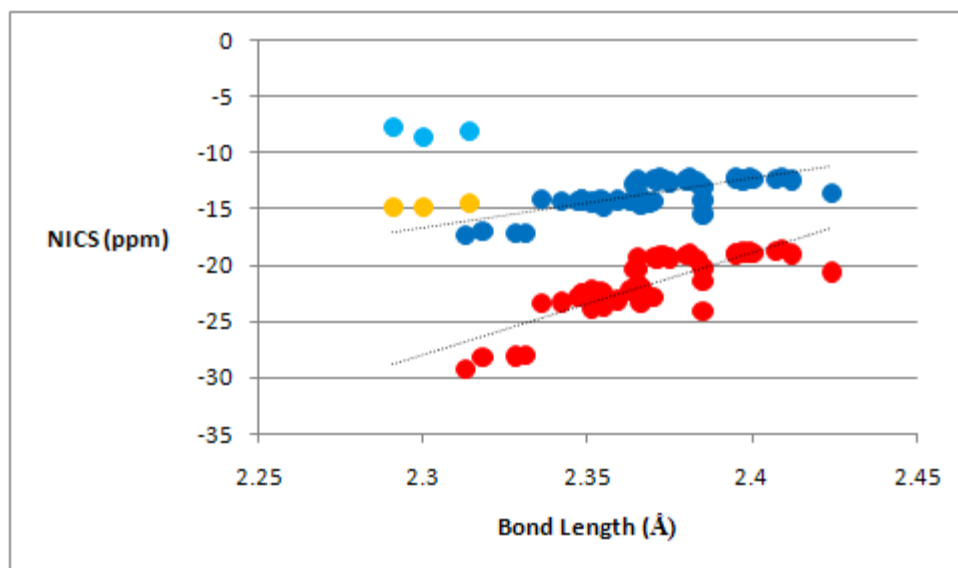


Figure S-36

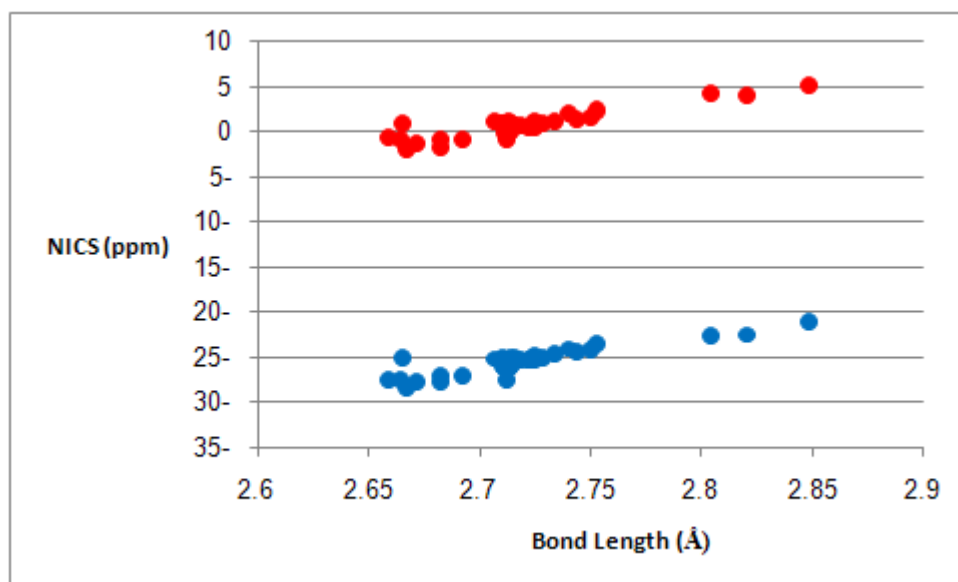


Figure S-37

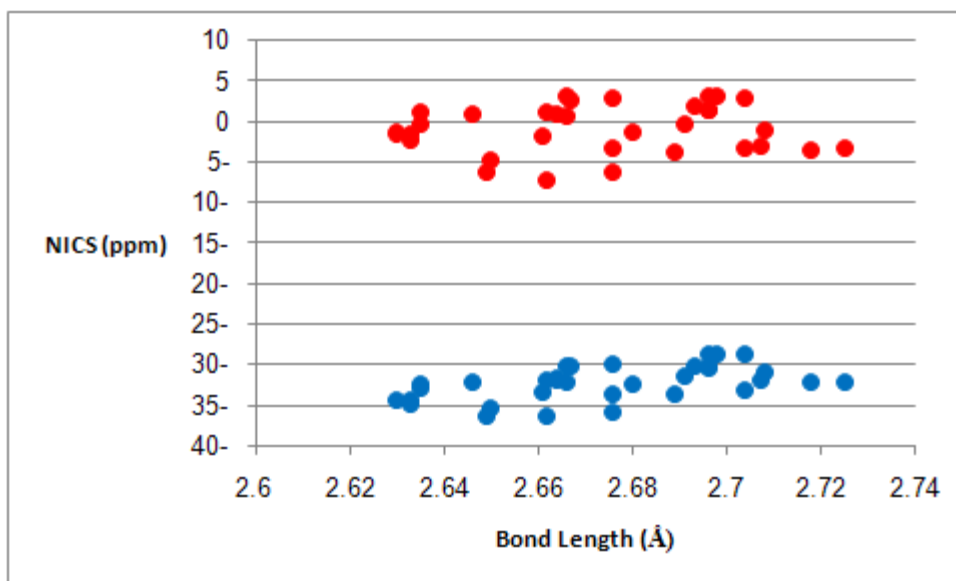


Figure S-38

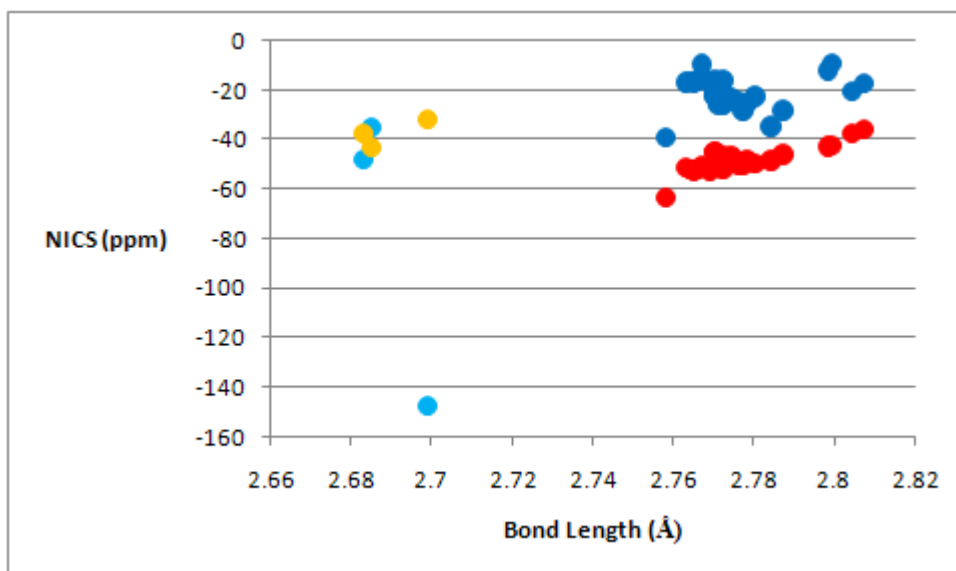


Figure S-39

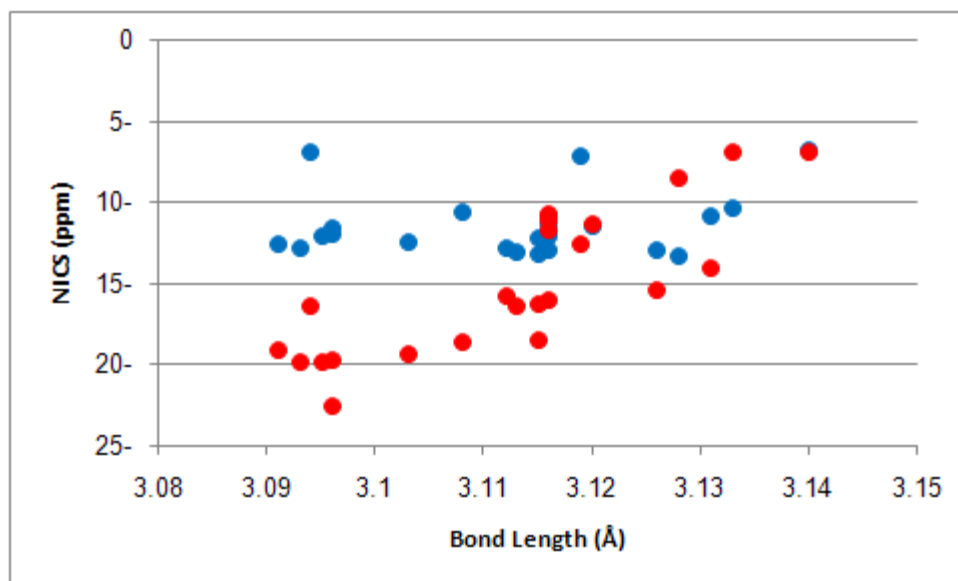


Figure S-40

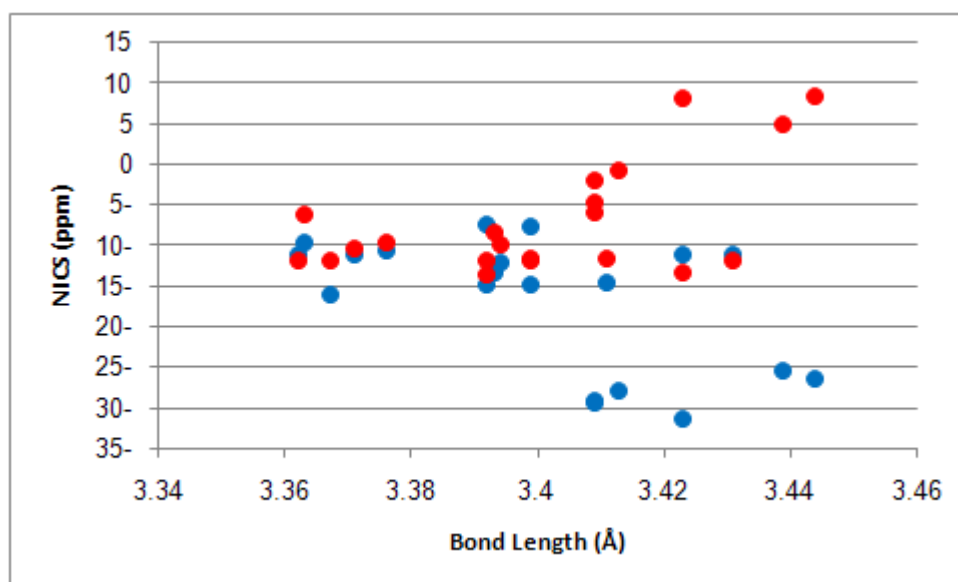


Figure S-41

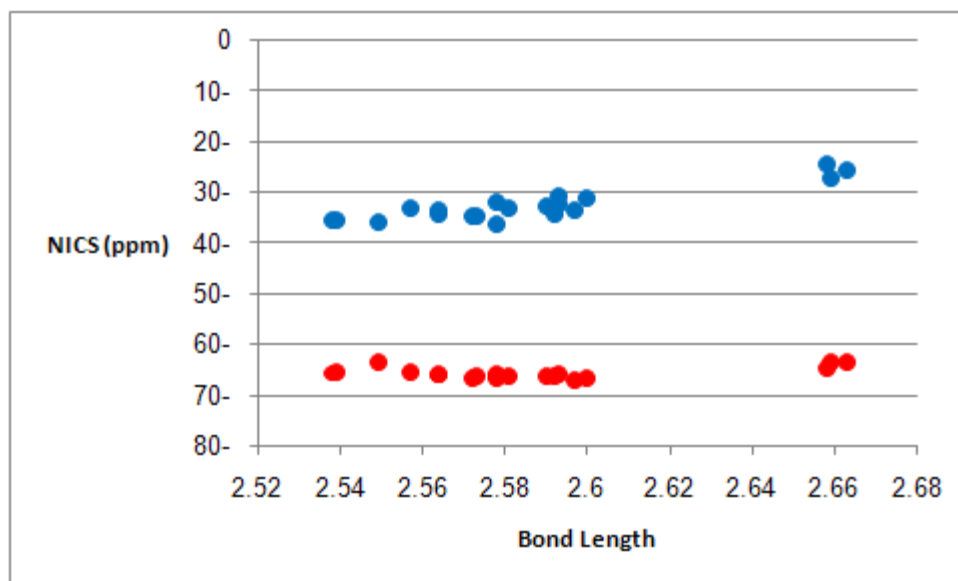


Figure S-42

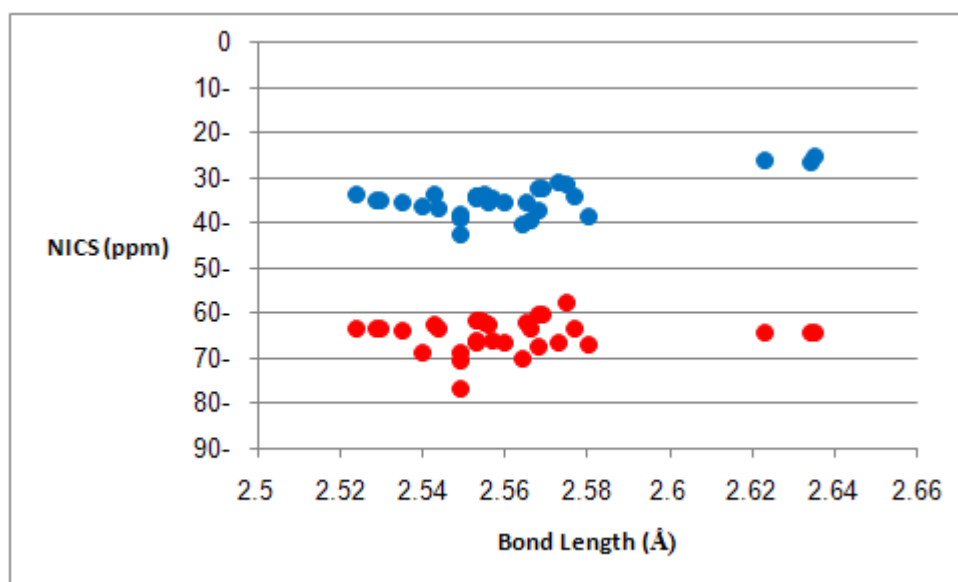


Figure S-43

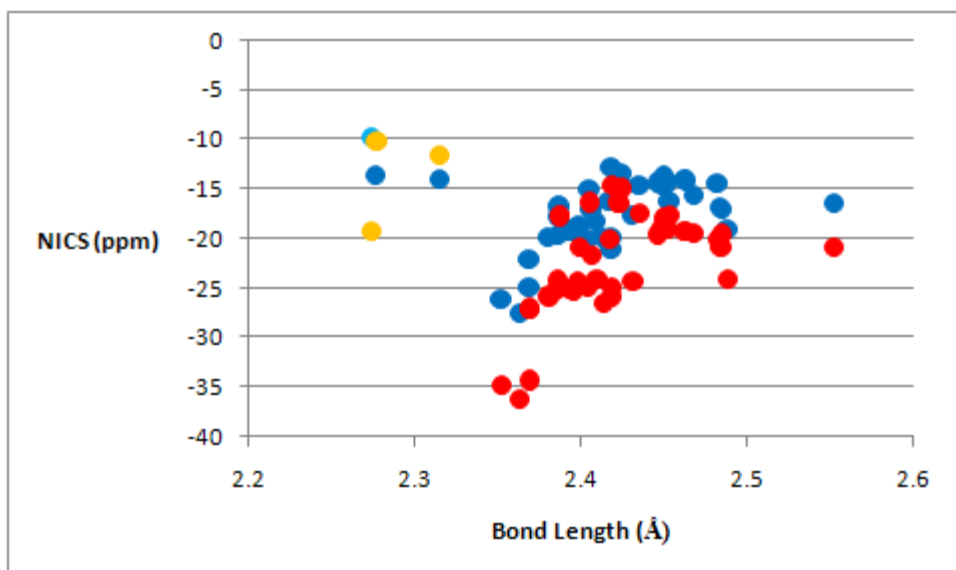


Figure S-44

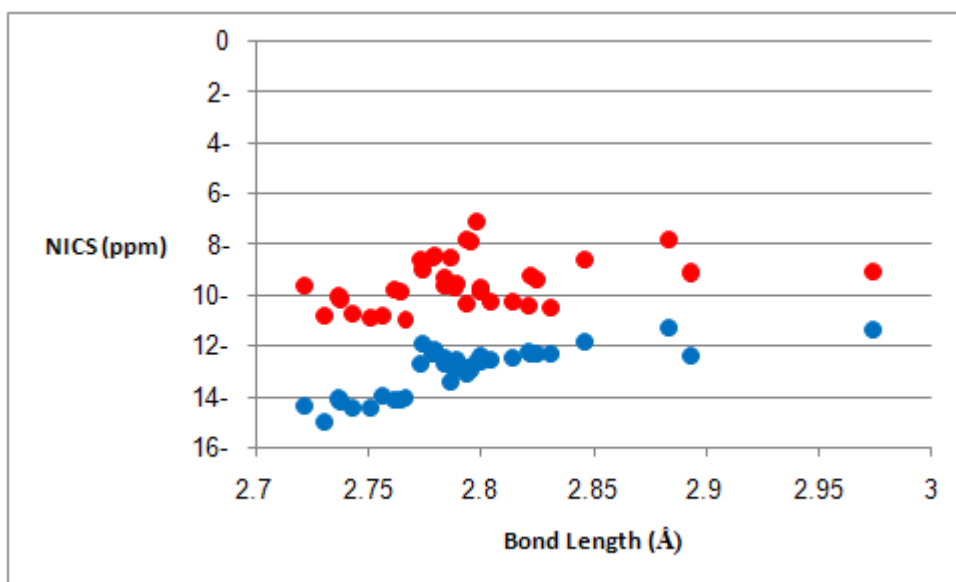


Figure S-45

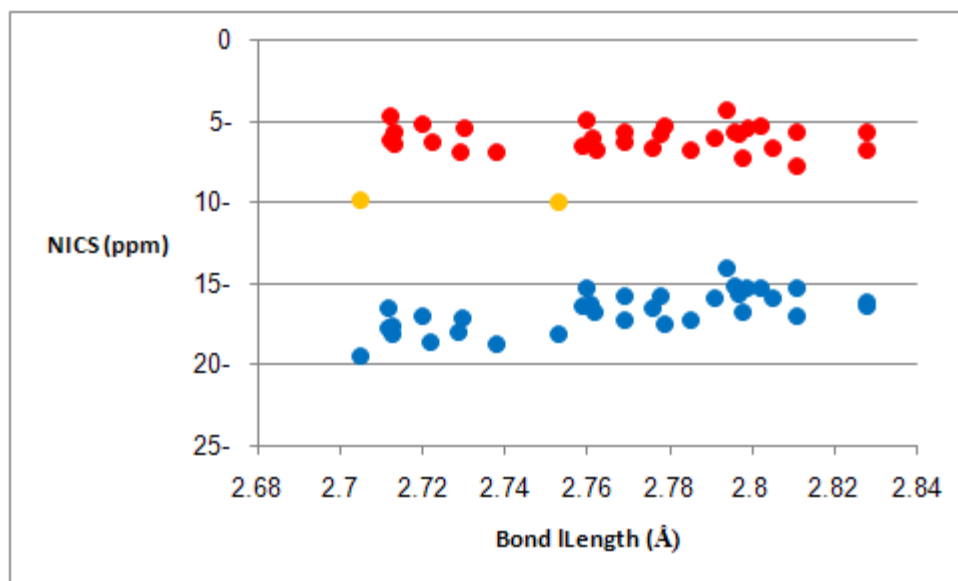


Figure S-46

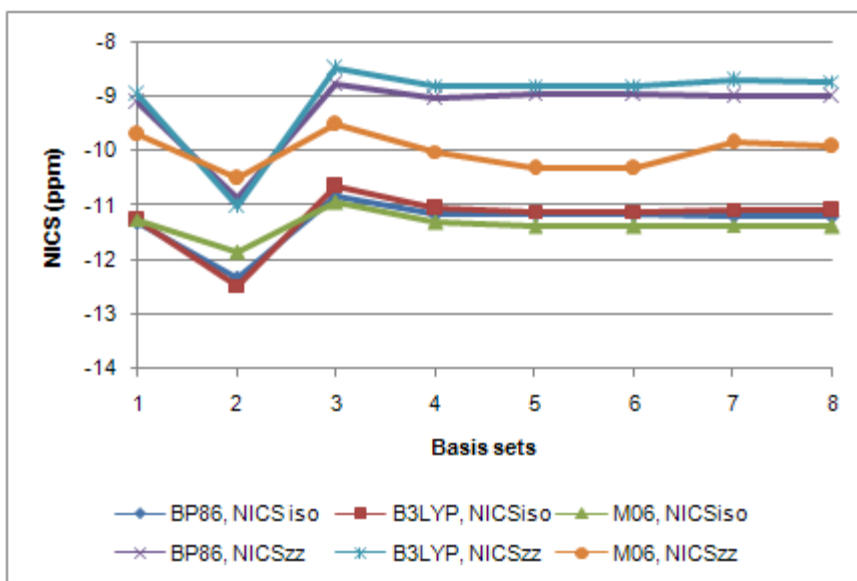


Figure S-47A

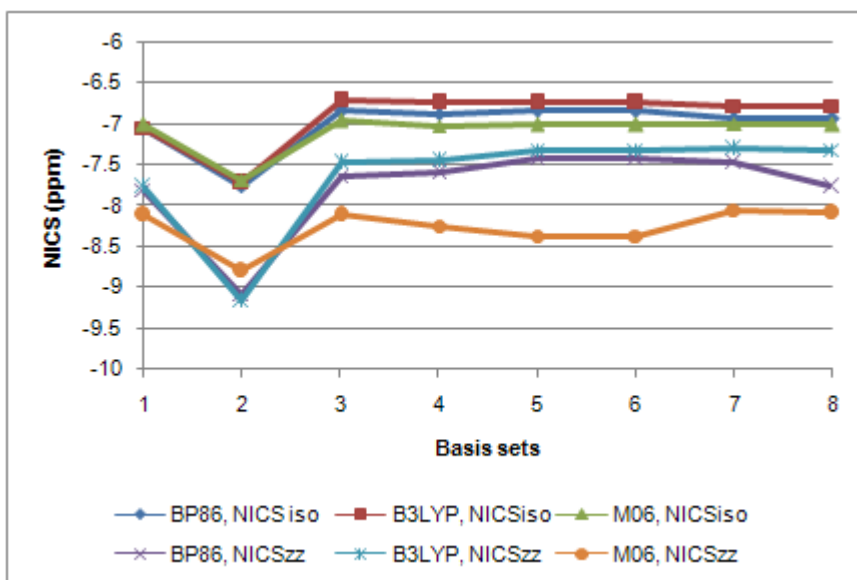


Figure S-47B

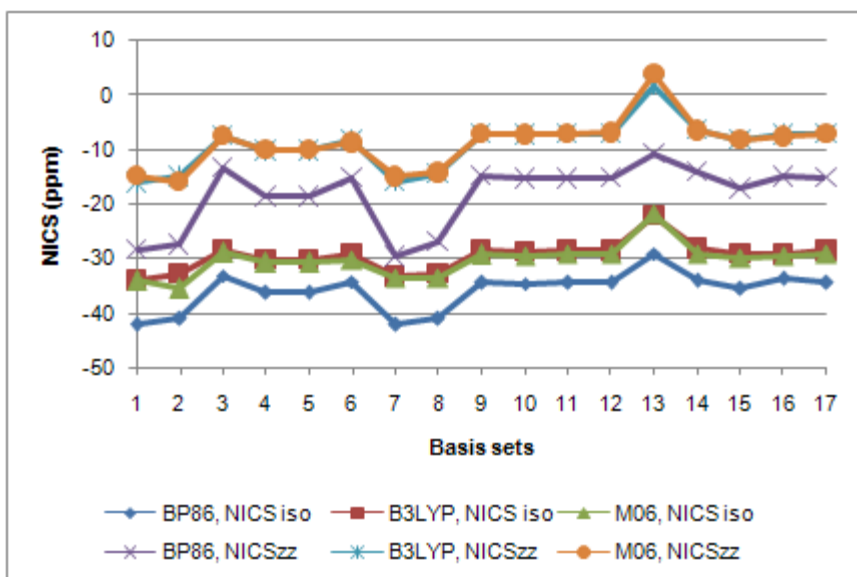


Figure S-48A

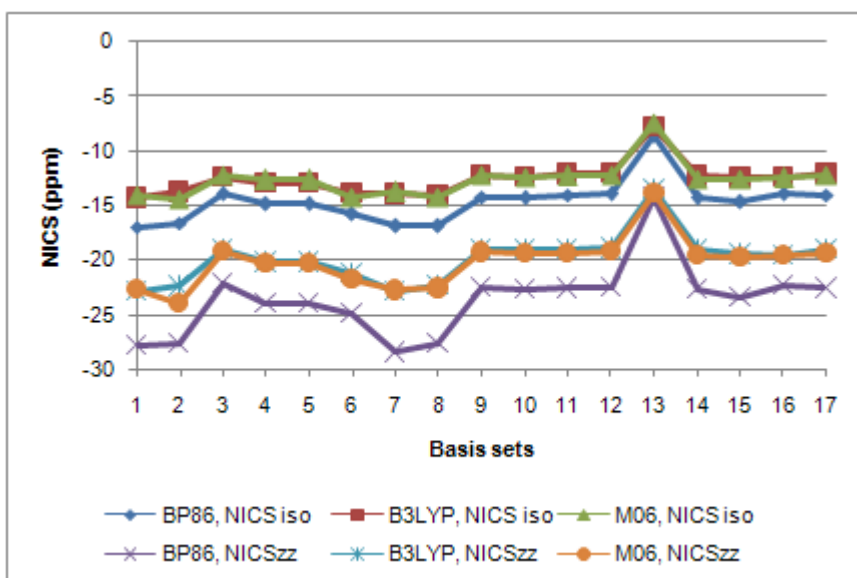


Figure S-48B

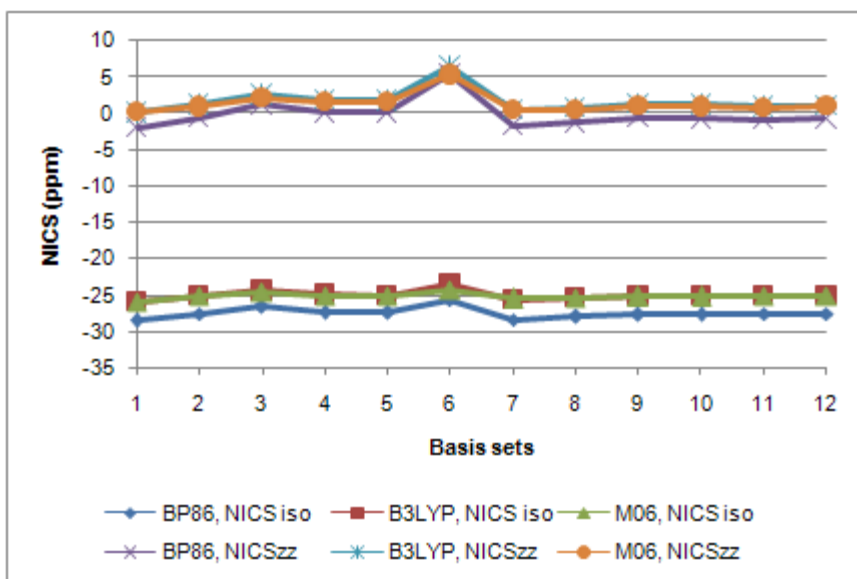


Figure S-49A

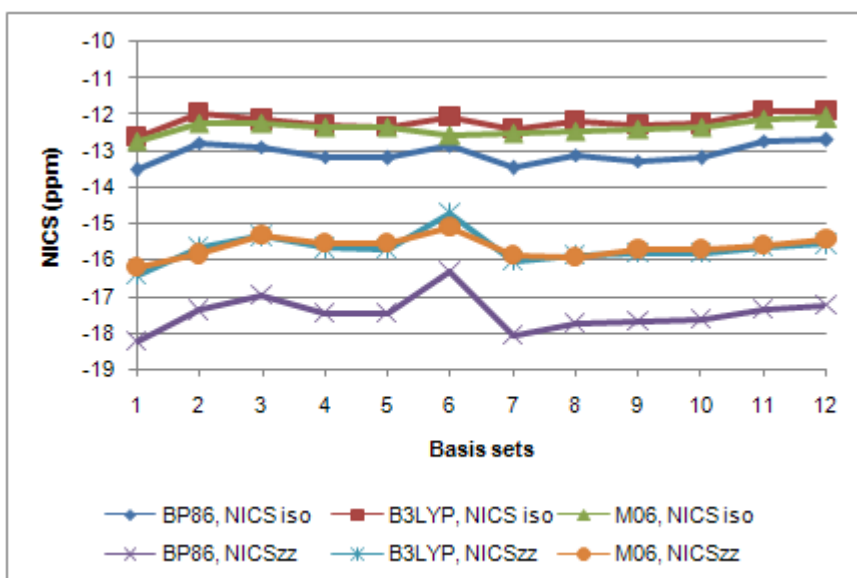


Figure S-49B

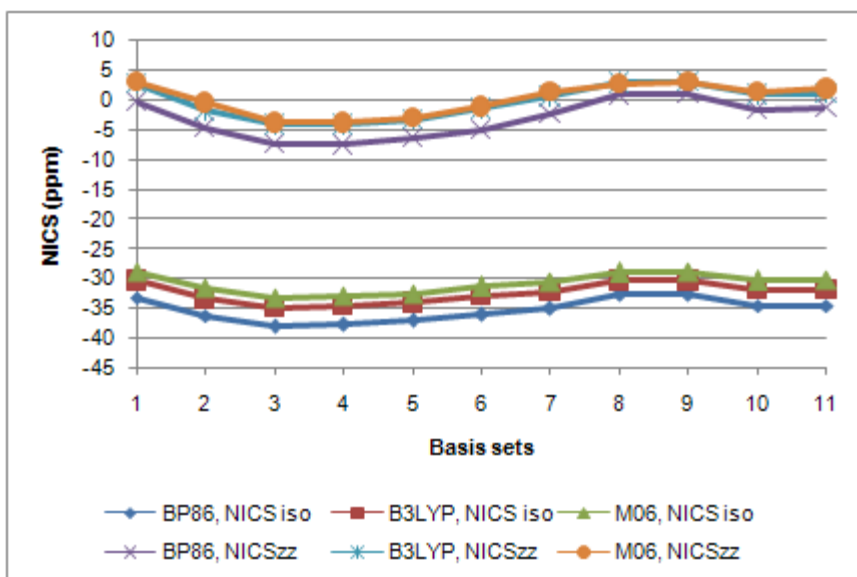


Figure S-50A

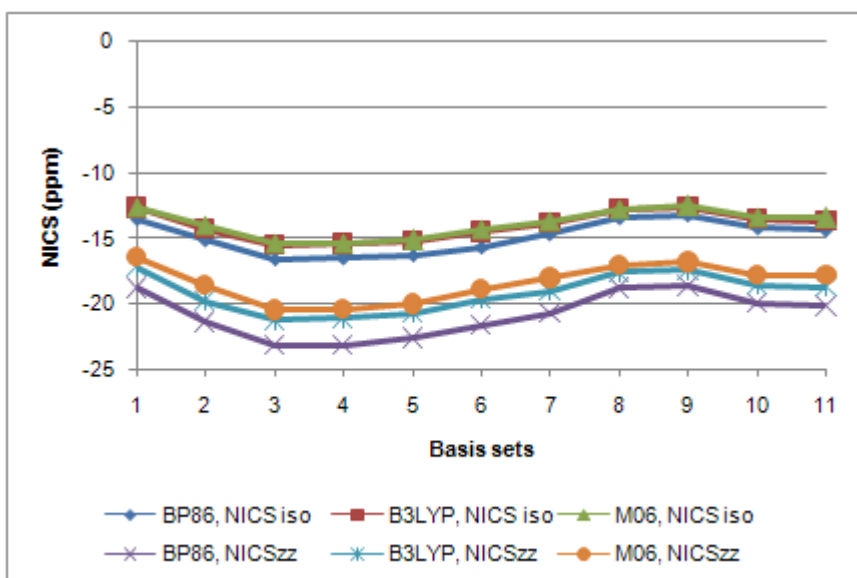


Figure S-50B

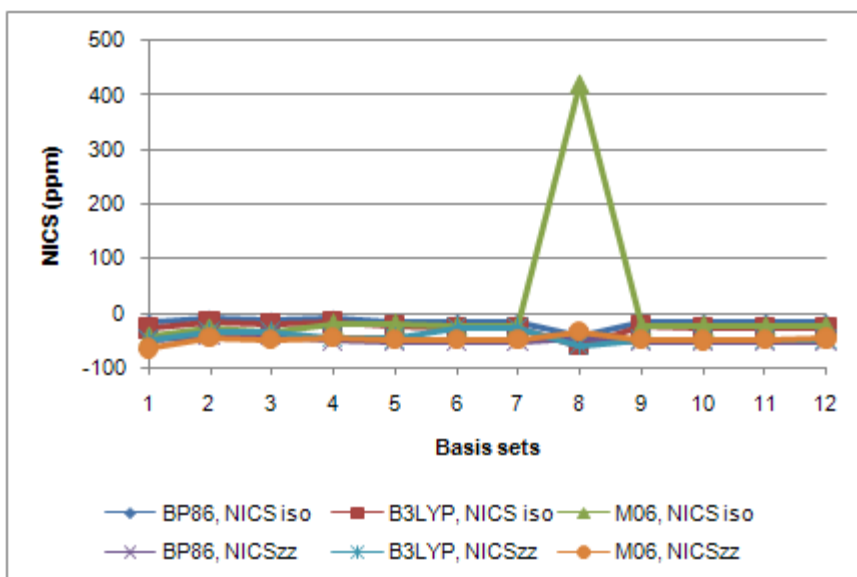


Figure S-51A

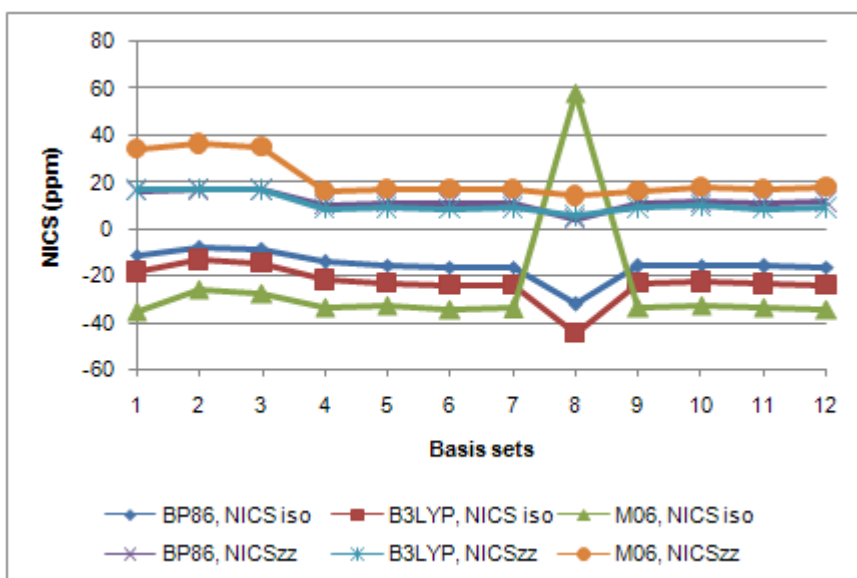


Figure S-51B

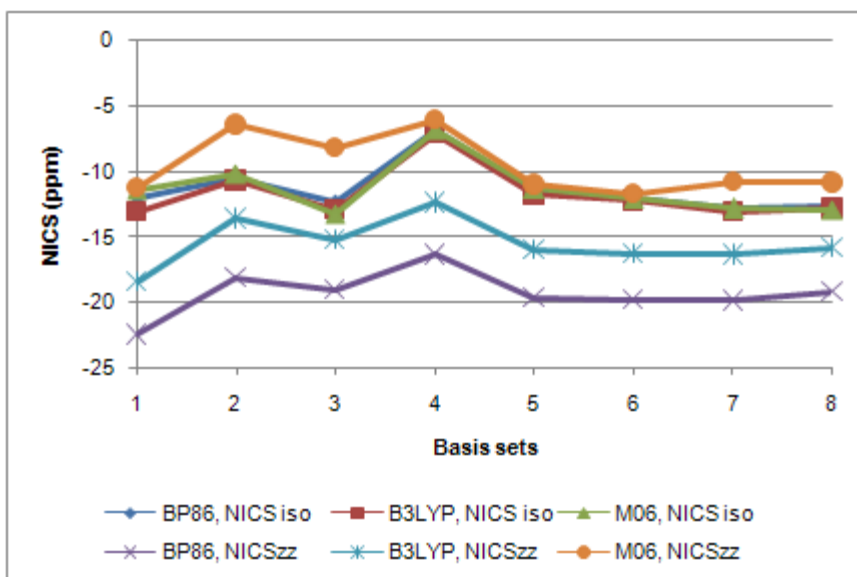


Figure S-52A

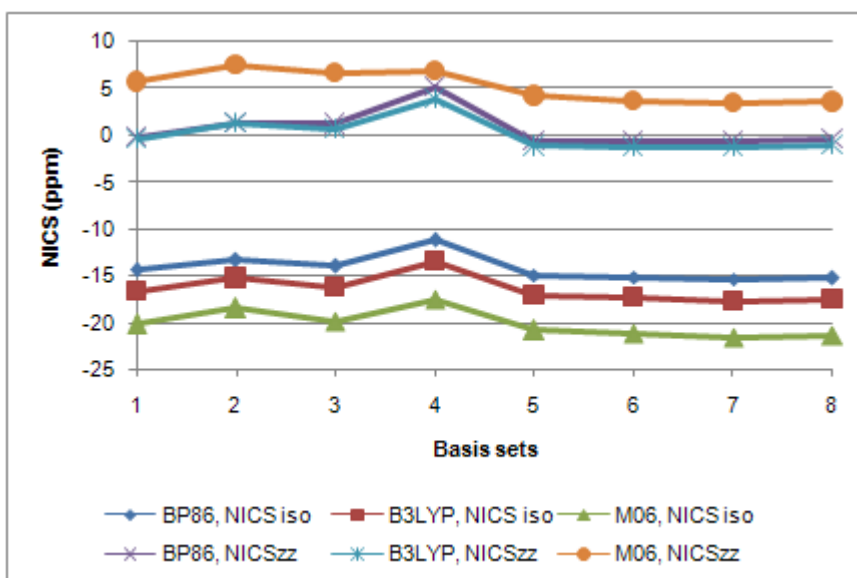


Figure S-52B

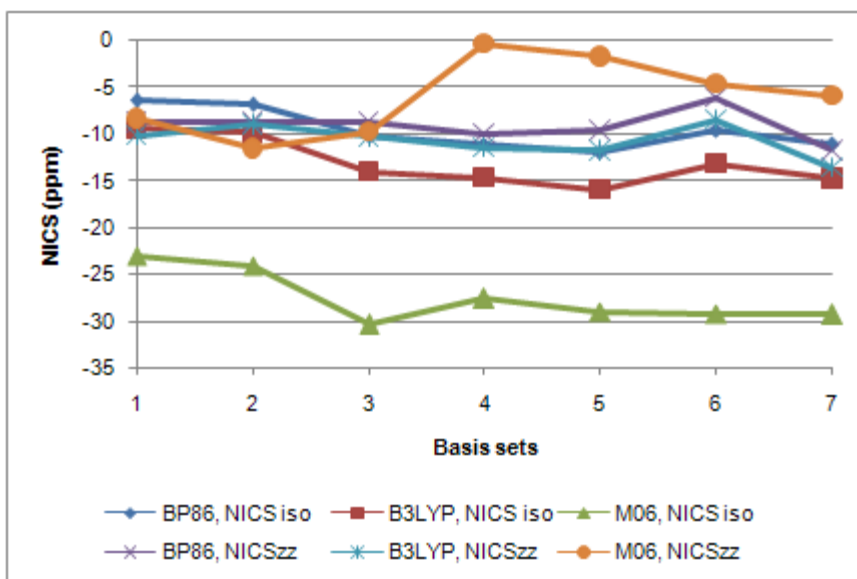


Figure S-53A

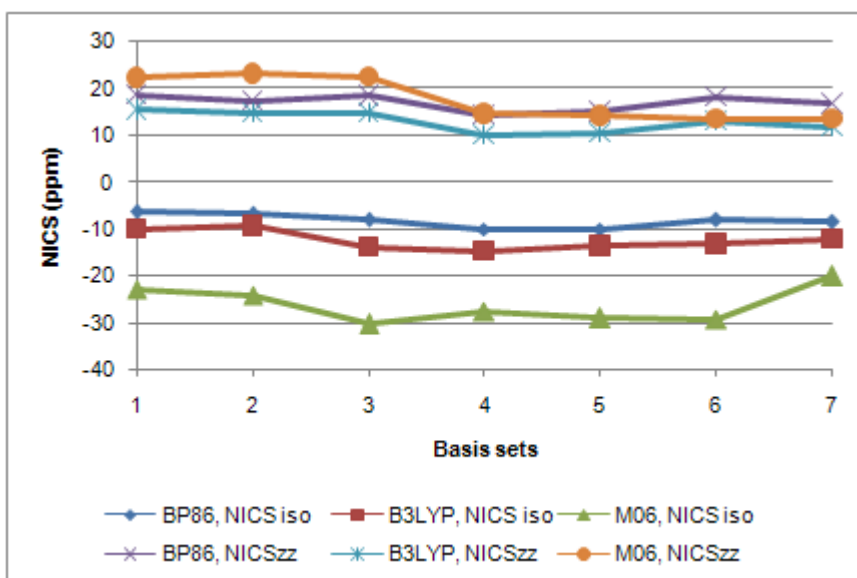


Figure S-53B

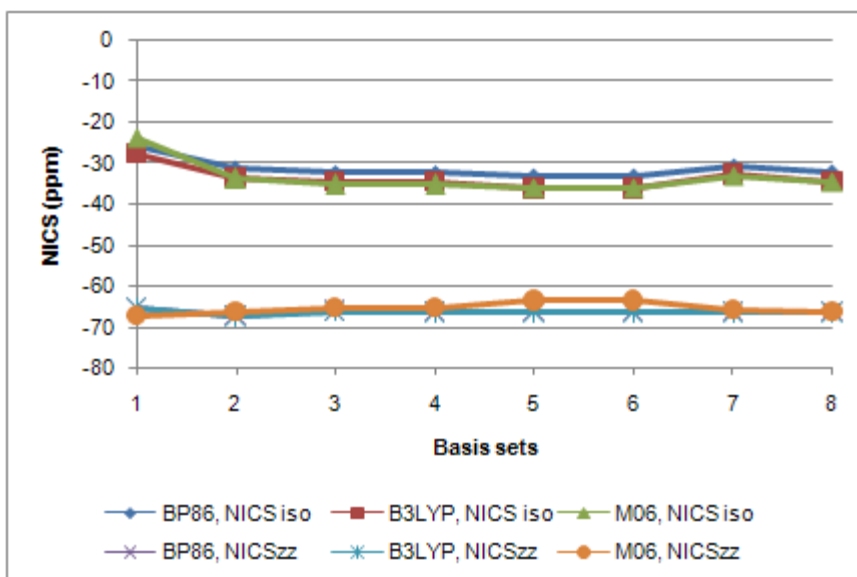


Figure S-54A

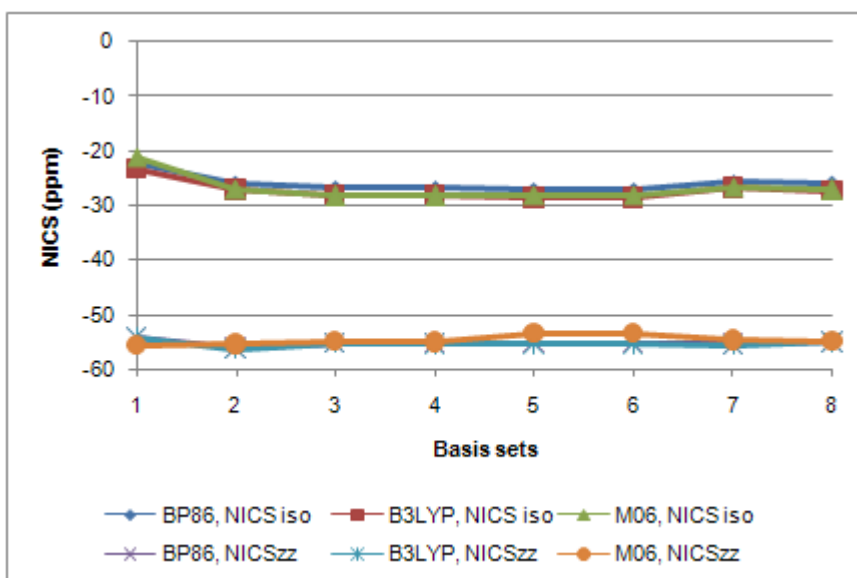


Figure S-54B

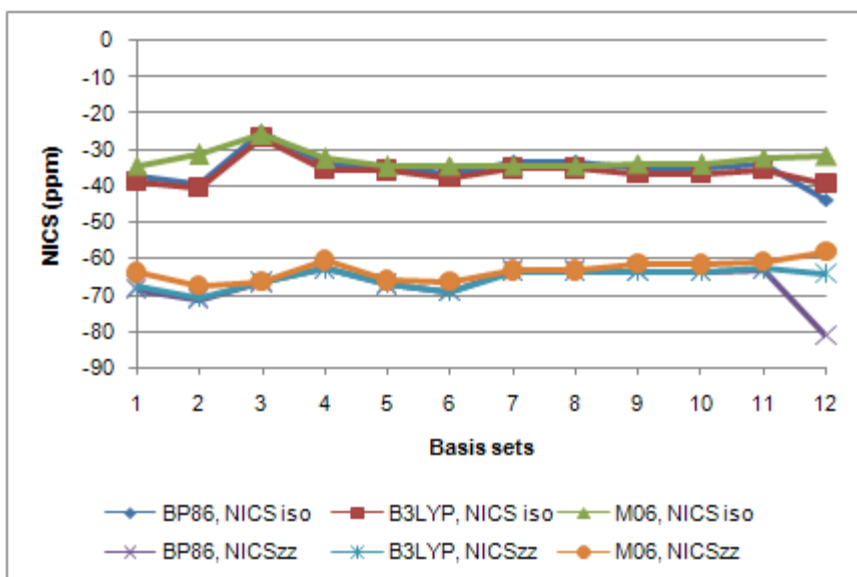


Figure S-55A

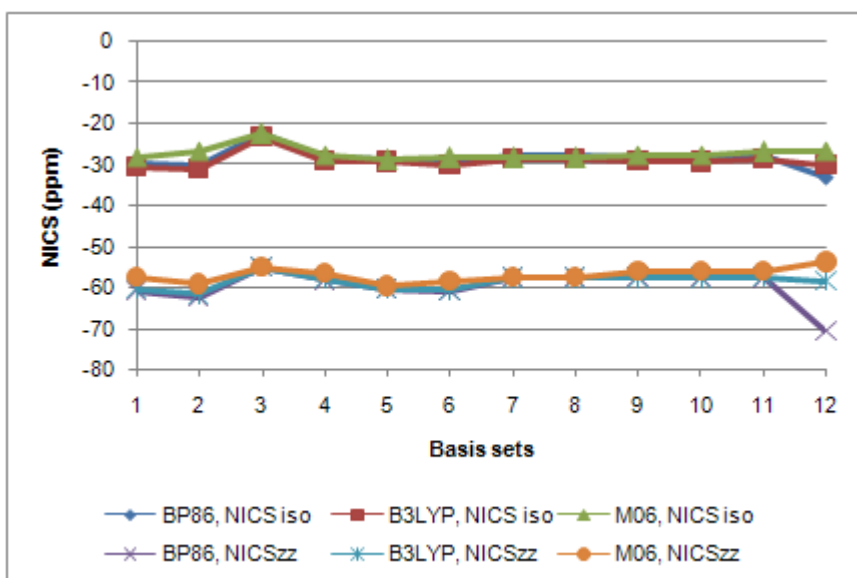


Figure S-55B

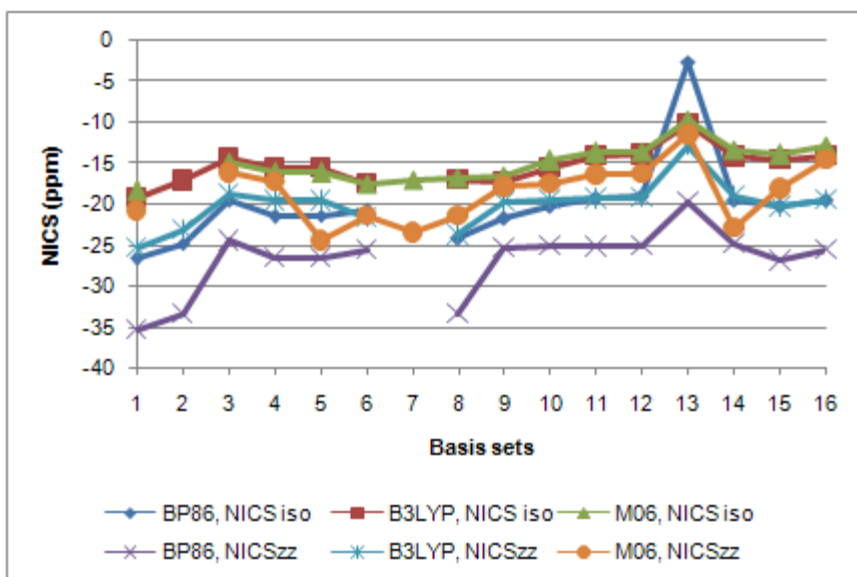


Figure S-56A

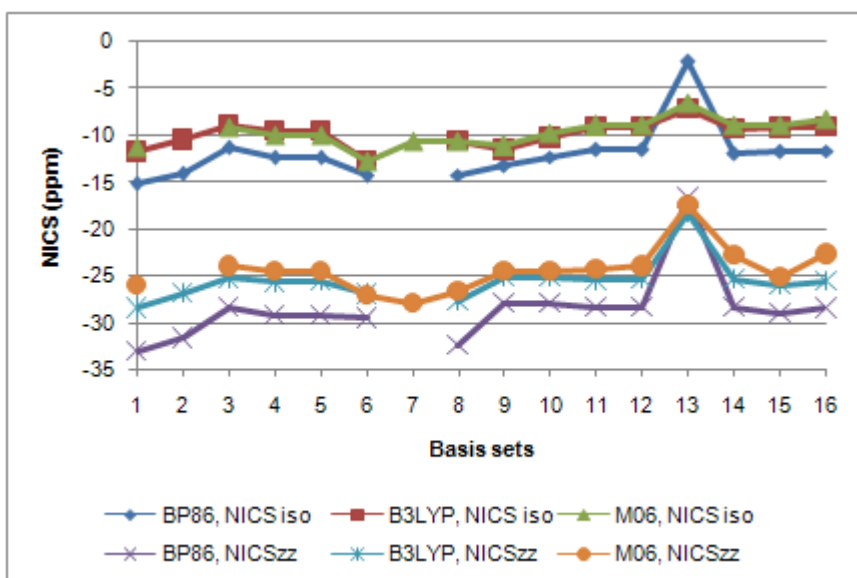


Figure S-56B

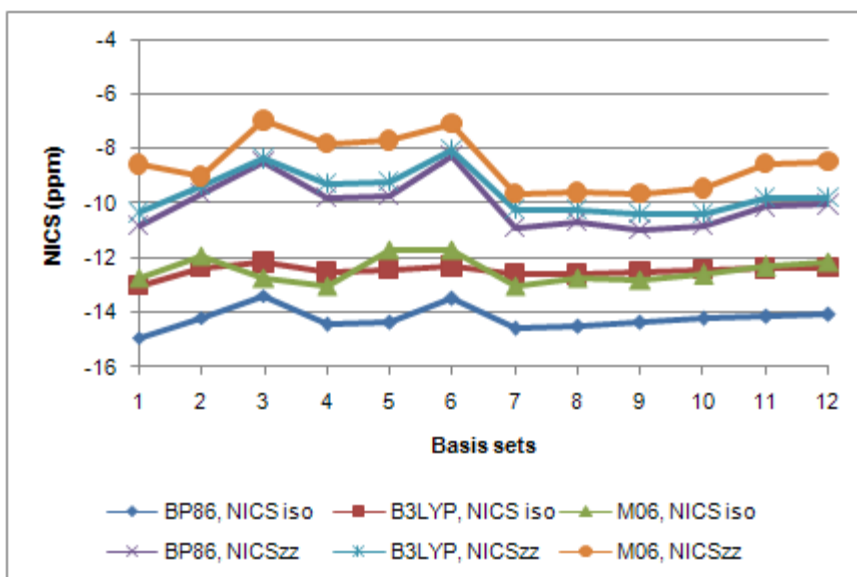


Figure S-57A

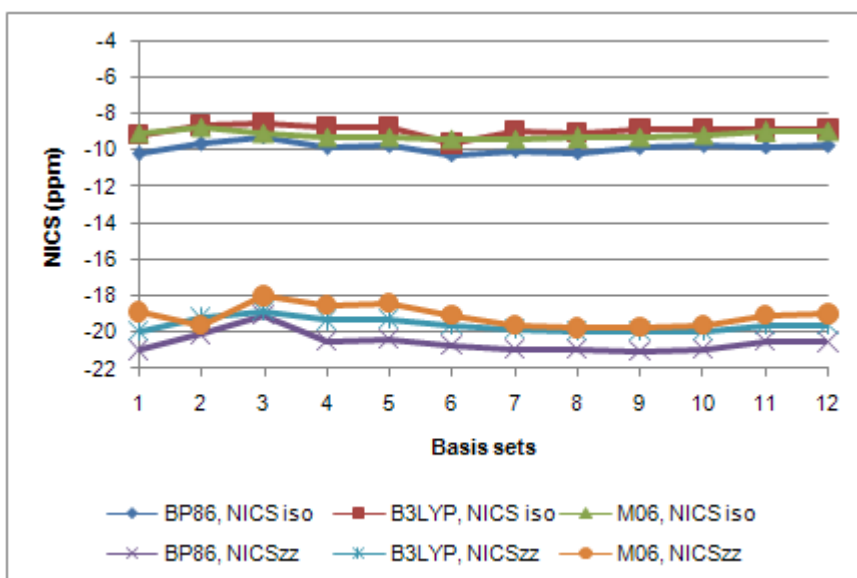


Figure S-57B

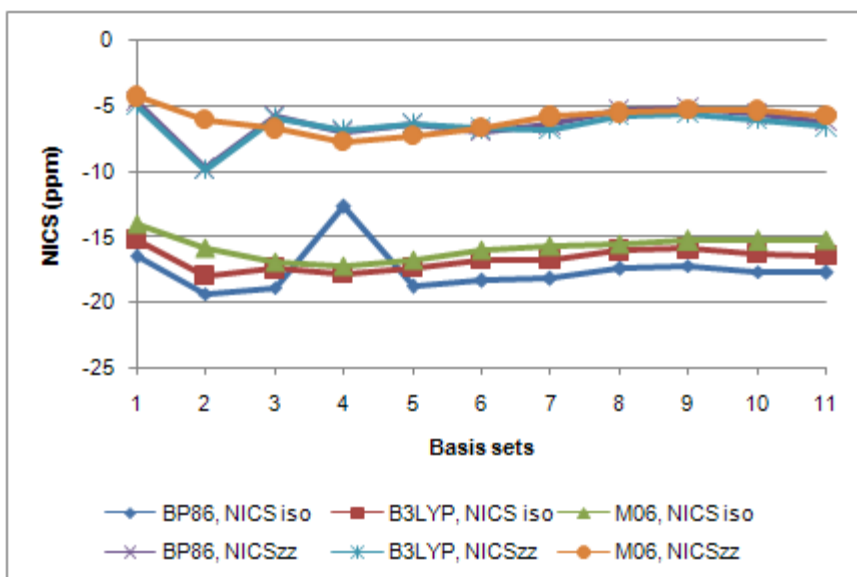


Figure S-58A

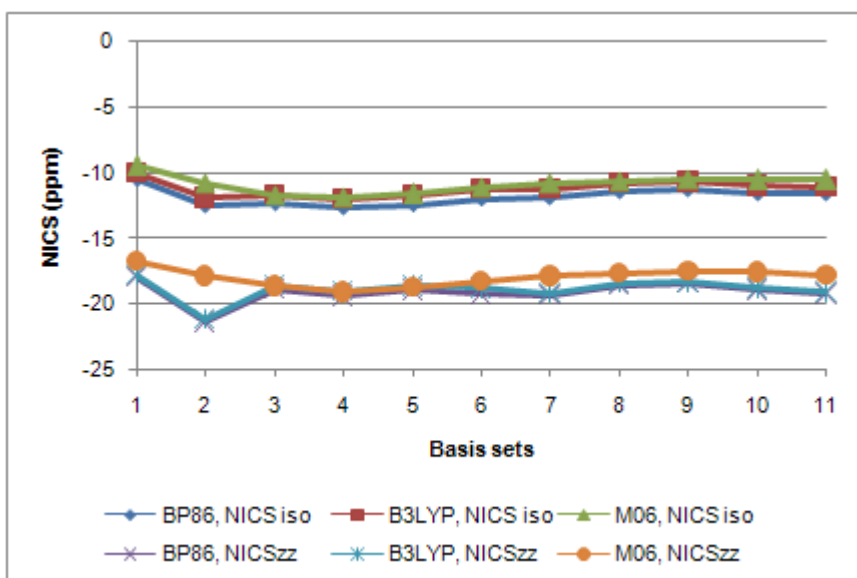


Figure S-58B

References

Aug-cc-pVDZ:

Cu, Ag, Au: Peterson, K.A.; Puzzarini, C. *Theor. Chem. Acc.*, **2005**, *114*, 283.

Ga: Peterson, K.A. *J. Chem. Phys.*, **2003**, *119*, 11099.

Aug-cc-pVTZ:

Cu, Ag, Au: Peterson, K.A.; Puzzarini, C. *Theor. Chem. Acc.*, **2005**, *114*, 283.

Ga: Peterson, K.A. *J. Chem. Phys.*, **2003**, *119*, 11099.

Lan2DZ:

Li: Dunning Jr, T. H.; Hay, P. J. *In Methods of Electronic Structure Theory*, **1977**, Vol. 2, Schaefer III, H. F. ed., PLENUM PRESS.

Al, Sc, Cu, Ga, Y, Ag, La, Au: (a) Hay, P. J.; Wadt, W. R. *J. Chem. Phys.*, **1985**, *82*, 270.

(b) Hay, P. J.; Wadt, W. R. *J. Chem. Phys.*, **1985**, *82*, 284. (c) Hay, P. J.; Wadt, W. R. *J. Chem. Phys.*, **1985**, *82*, 299.

Lan2TZ:

Sc, Cu, Y, Ag, La, Au: (a) Hay, P.J.; Wadt, W.R. *J. Chem. Phys.*, **1985**, *82*, 299. (b) Roy, L.E.; Hay, P.J.; Martin, R.L. *J. Chem. Theory Comput.*, **2008**, *4*, 1029.

Lan2TZ(f):

Sc, Cu, Y, Ag, La, Au: (a) Hay, P.J.; Wadt, W.R. *J. Chem. Phys.*, **1985**, *82*, 299. (b) Roy, L.E.; Hay, P.J.; Martin, R.L. *J. Chem. Theory Comput.*, **2008**, *4*, 1029. (c) Ehlers, A.W.; Bohme, M.; Dapprich, S.; Gobbi, A.; Hollwarth, A.; Jonas, V.; Kohler, K.F.; Stegmann, R.; Veldkamp, A.; Frenking, G. *Chem. Phys. Lett.*, **1993**, *208*, 111.

DZVP(DFT orbital):

Li, Al, Ga, Cu, Y, Ag, : Godbout, N.; Salahub, D. R.; Andzelm, J.; Wimmer, E. *Can. J. Chem.*, **1992**, *70*, 560.

cc-pVDZ-PP:

Cu, Ag, Au: Peterson, K.A.; Puzzarini, C. *Theor. Chem. Acc.*, **2005**, *114*, 283.

Ga: Peterson, K.A.; *J. Chem. Phys.*, **2003**, *119*, 11099.

cc-pVTZ-PP:

Cu, Ag, Au: Peterson, K.A.; Puzzarini, C. *Theor. Chem. Acc.*, **2005**, *114*, 283.

Ga: Peterson, K.A.; *J. Chem. Phys.*, **2003**, *119*, 11099.

Def2-TZVP:

Li, Al, Sc, Cu, Ga, Y, Ag, La, Au: Weigend, F.; Ahlrichs, R.; *Phys. Chem. Chem. Phys.*, **2005**, *7*, 3297.

Def2-TZVPP:

Li, Al, Sc, Cu, Ga, Y, Ag, La, Au: Weigend, F.; Ahlrichs, R.; *Phys. Chem. Chem. Phys.*, **2005**, *7*, 3297.

Def2-QZVP:

Li, Al, Sc, Cu, Ga, Y, Ag, La, Au: Weigend, F.; Ahlrichs, R.; *Phys. Chem. Chem. Phys.*, **2005**, *7*, 3297.

Def2-QZVPP:

Li, Al, Sc, Cu, Ga, Y, Ag, La, Au: Weigend, F.; Ahlrichs, R.; *Phys. Chem. Chem. Phys.*, **2005**, *7*, 3297.

Aug-cc-pVDZ:

Sc, Cu: (a) Balabanov, N.B.; Peterson, K.A. *J. Chem. Phys.*, **2005**, *123*, 064107.

(b) Balabanov, N.B.; Peterson, K.A. *J. Chem. Phys.*, **2006**, *125*, 074110.

Aug-cc-pVTZ:

Sc, Cu: Balabanov, N.B.; Peterson, K.A. *J. Chem. Phys.*, **2005**, *123*, 064107.

Aug-cc-pVQZ:

Sc, Cu: Balabanov, N.B.; Peterson, K.A. *J. Chem. Phys.*, **2005**, *123*, 064107.